Analysis and Characterization of Titan Aerosol Simulants by Mass Spectrometry

Thesis by
Kathleen Upton

In Partial Fulfillment of the Requirements for the degree of
Doctor of Philosophy in Chemistry

CALIFORNIA INSTITUTE OF TECHNOLOGY
Pasadena, California

2018
(Defended September 20th 2017)

Kathleen Upton
ORCID: 0000-0003-4292-7616

ACKNOWLEDGEMENTS

There are so many people I would like to thank for their help and support during my time at Caltech.

I would like to thank my advisor, Jack Beauchamp. He has helped me grow immensely as a researcher. He taught me to “just do it” when it came to experiments, since experience is the best teacher and sometimes crazy ideas lead to new and unexpected avenues of investigation.

A large part of my time at Caltech was funded by the Harriett Jenkins Pre-Doctoral Fellowship, during which I worked with Ella Sciamma-O’Brien and Farid Salama. I would like to thank both of them for working so closely with me, exposing me to new types of experiments, providing different scientific viewpoints, and giving me invaluable collaborative experience.

Nathan Dalleska lent his much appreciated insight and expertise to multiple of my experiments. The access to the EAC combined with his advice was instrumental in the success of a majority of my research. His participation in group meeting always provided levity and useful feedback. I would like to thank him for teaching me so much about instrumentation that I know will be vital for my future success.

My success at Caltech would not have been possible without the wonderful support staff. I would like to thank Priscilla for helping to keep the group running. Jeff in the electronic shop and Rick in the glass shop were able to work magic. Joe always knew how to fix even the most unexpected of problems. Felicia, Amy, and Alison were always willing to help and their assistance allowed me to navigate administrative barriers.

I would like to thank the members of the Beauchamp group over the years for their camaraderie. Daniel was a great mentor, introducing me to new instruments and teaching me the fundamentals of being a graduate student and setting a strong foundation for me. Kevin's friendship and listening ear was so helpful over the years to not only better my research, but also navigate the stresses of graduate school. Josh, Jinshan, and Xinxing, the postdoctoral researchers in the group, all gave me exposure to different pathways to being researcher. Their advice helped me become a better researcher.

My experience at Caltech would have been lacking if not for friends I made during my time. Morgan acted as a wonderful mentor to show me what a successful female researcher could do. She was the first one that encouraged me to apply to Caltech, and her mentoring helped keep me encouraged during the lows of my graduate experience. Kate Schilling provided friendship as well, sharing laughs over Star Trek and helping me remember what matters the most. Laura, Victoria, and I shared awesome lunches where we not only commiserated about graduate school, but also how to balance family.

I must also thank Agnes. She started as the Administrator for Chemistry, but became my close friend, staying so even as she moved to Caltech Y. Her friendship helped keep me together during the stressful times. She helped put me in touch with resources I didn't know about to enable my success. She also taught me to take care of myself and my mental health, something that many graduate students forget about. I know this would not have happened without her.

Lastly I have to thank my family. My father was one of the first to encourage my spark of science, showing me the wonder that the field could have. His encouragement to try my best and never give up helped me maintain my drive throughout graduate school. My mother helped to feed my inquisitive nature, an important factor for any scientist. Shev always encouraged my questions and helped me find answers. She always listened to my difficulties and offered help in any way she could. Both of their support got me to where I am today. I must also give my utmost thanks to my husband, Michael. He has supported me both long distance and at home during my entire graduate career. He always listens and lets me vent my frustrations. I'm sure he has learned more about mass spectrometry than he ever wanted to know. His unfaltering love and support is a major reason I have reached this point. I also have thanks for my cat, Nora, who let me hug her when I was upset; even if she didn't always appreciate it herself, I appreciated it.

ABSTRACT

Saturn's large moon of Titan is unique as the only solid body in the outer solar system to possess a dense atmosphere, which is comprised of mostly nitrogen and methane. Atmospheric chemistry on this moon creates aerosols comprised of carbon, hydrogen, and nitrogen. Laboratory based synthesis of simulated Titan aerosols, also called tholins, led to molecules with rich chemical diversity, functionalities, and molecular weights. While this diversity has intriguing implications for Titan, it complicates the analysis and characterization of these simulants. This thesis discusses three different mass spectrometry methodologies, prioritizing a combination of mission applicability, broad spectrum characterization, and specific functional group identification. Chapters 2 and 3 utilize a home-built Direct Analysis in Real Time (DART) ionization source, termed EZ-DART, to test its suitability for the analysis of these simulants and the source's mission applicability. Chapter 2 focuses on the development and characterization of the EZ-DART source. Chapter 3 presents the analysis of Titan aerosol simulants, produced in a new and unique way, by EZ-DART, allowing for the identification of various compounds of astrobiological significance. Solid phase microextraction gas chromatography mass spectrometry (SPME-GC-MS) is utilized in Chapter 4 with different Titan aerosol simulants, identifying multiple compounds of significance to Titan and astrobiology. The versatility allowed by SPME increases the applicability of GC for future lander missions. While not mission applicable, Chapter 5 shows the breadth of primary amines in Titan aerosol simulants through the use of supramolecular complexation to 18-crown-6 ether. This technique not only enabled the unambiguous identification of primary amines, but also allowed for the structural characterization of some components. The range of methods and identified compounds

discussed within this thesis demonstrates not only the rich chemistry of these Titan aerosol simulants, but also introduces intriguing possibilities for Titan's atmospheric chemistry and presents potential significance to astrobiology.

PUBLISHED CONTENT AND CONTRIBUTIONS

Chapter 2 is reproduced in part from:

Upton, K., Schilling, K, Beauchamp, J. L. Easily Fabricated Ion Source for Characterizing Complex Organic Mixtures by Direct Analysis in Real Time Mass Spectrometry, *Analytical Methods*, 2017, **9**, 5065-5074 DOI: 10.1039/C7AY00971B.

K.T.U. was the lead researcher on this project and main author of the manuscript

Chapter 5 figures 5.2, 5.3, and 5.5 are all reprinted with permission from the copyright holder Robert Hodyss from R. Hodyss, Dissertation (Ph.D.), The California Institute of Technology, 2006.

TABLE OF CONTENTS

LIST OF FIGURES

LIST OF TABLES

NOMENCLATURE

DART. Direct Analysis in Real Time

MS. Mass Spectrometry

Tholin. Same as Simulated Titan Aerosol

PDN. Pulsed Discharge Nozzle

COSmIC. NASA Ames cosmic simulation chamber

RADI. Reagent Assisted Desorption Ionization

CID. Collision Induced Dissociation

ESI. Electrospray Ionization

DC. Direct Current

PPG. Poly(propylene glycol)

SPME. Solid Phase Microextraction

GC. Gas Chromatography

TIC Total Ion Chromatogram

EIC Extracted Ion Chromatogram

EI Electron Impact

Chapter 1

INTRODUCTION

1.1 The Astrochemical Environment of Titan

While there are many chemically interesting environments within the solar system, Saturn's moon of Titan is of continuous intrigue. One of the largest moons in the solar system, Titan is unique as the only solid body in the outer solar system with a dense atmosphere.[1] This icy moon has multiple types of geological features: large lakes around its poles, dry river valleys, and dunes around the equator. [2-4] Gravitational studies have shown that a water and ammonia ocean or slurry likely exists under its crust.[5] While this may sound like a second Earth, Titan deviates greatly. The atmosphere and surface are extremely cold, with minimums of approximately 95K, and the lakes are liquid methane and ethane.[5, 6] As such any water present on the surface would be unreactive and closer to granite than water on Earth.[7] Any chemistry involving water is proposed to involve the subsurface ocean. The geological diversity possible with lakes of methane and ethane does increase the variety of chemical environments, the implications of which have been investigated in other studies.[8-10] These different features present Titan as a frozen early Earth, the study of which provides insights into the chemical evolution of our own planet.[11-13]

Nowhere is this more evident than in the study of Titan's dense atmosphere. This atmosphere is visibly brown-orange in color and optically opaque, requiring techniques such as radar to study the features of the surface.[14, 15] The atmosphere is composed mostly of nitrogen (90-98%), with methane (2-10%) being the second most abundant constituent.[11]

Trace amounts of other gases, such as carbon monoxide and helium, along with small hydrocarbons and hydrogen cyanide round out the other components.[16] The interest in the study of Titan's atmosphere stems from how this composition mirrors that of early Earth.[12] Models of Earth's Archean atmosphere, supported by geochemical data, predict that two stable states existed: with and without a haze layer. These states were driven by the atmospheric methane content, with more methane contributing to increased haze formation.[17] Titan thus presents a frozen version of the stable haze state, allowing for the study of atmospheric processes during this regime of Earth's atmosphere.

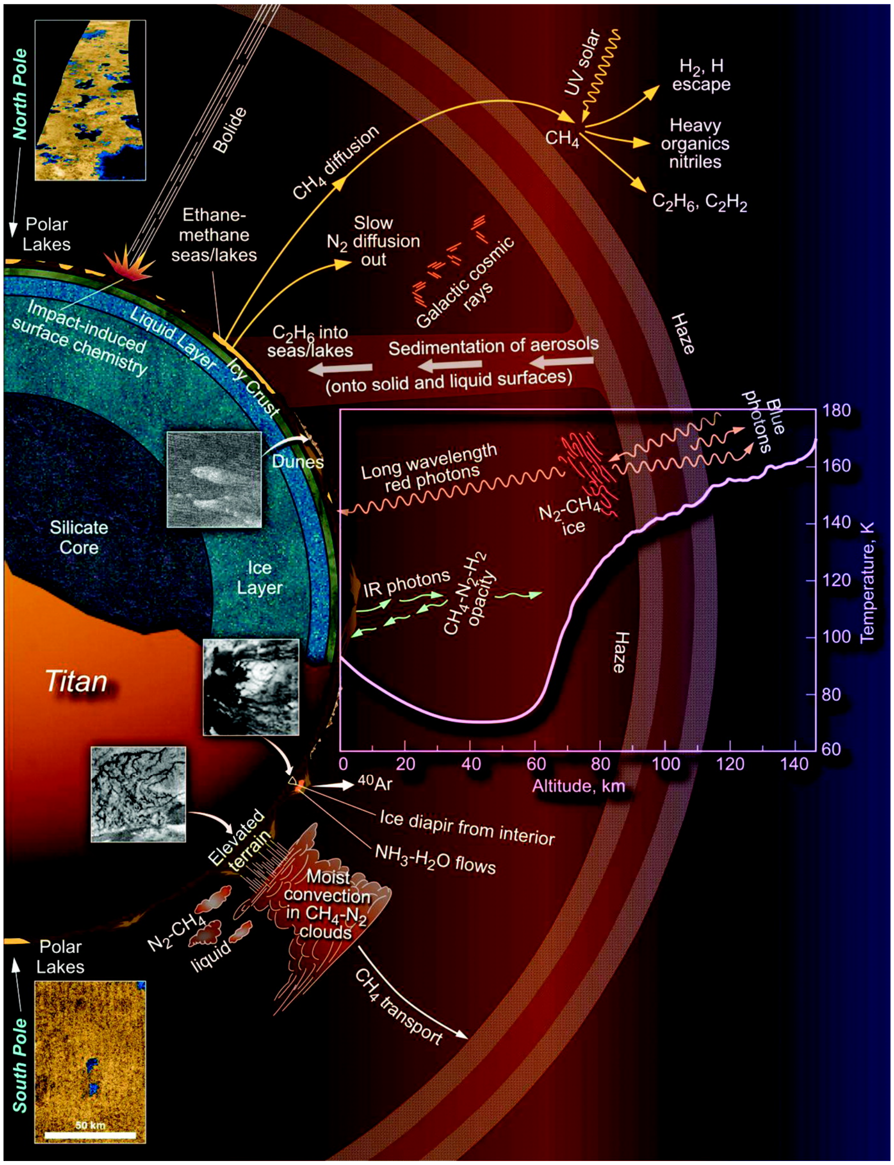

Figure 1.1. A cross section of Titan showing the complex processes at work in the atmosphere along with the various geographical features. Reproduced with permission from Cable et al. 2012[18]

The haze formation on Titan is driven mostly by photochemical processes in the atmosphere. Here nitrogen and methane are photoionized or photodissociated by solar radiation.[12, 19-21] The products of these reactions along with the wavelengths required to induce the chemistry are shown in Table 1 below. These reactions produce ions and radicals that can undergo subsequent chemistry to produce hydrogen cyanide and small hydrocarbons such as acetylene.[22-24] These molecules undergo further photochemistry to produce heavier nitriles and hydrocarbons.[25-27] Photochemical processes dominate in the upper atmosphere at altitudes of 1000 km, but other processes such as meteor impacts, particles from Saturn's magnetosphere, and cosmic rays can drive additional chemistry throughout different atmospheric layers.[28]

Photochemical reaction	Wavelength maximum (nm)
$N_2 + h\nu \rightarrow N^+ + N + e^-$	51[29]
$N_2 + h\nu \rightarrow 2N^\bullet$	80[21]
$CH_4 + h\nu \rightarrow CH_3^+ + H + e^-$	87[29]
$CH_4 + h\nu \rightarrow CH_3^\bullet + H^\bullet$	155[20, 21]

Table 1.1. Example photoionization and photodissociation reactions for methane and nitrogen with required wavelengths. All wavelengths reported are maximums for their respective reaction. Table adapted from Cable et al. 2012[18]

Gas phase molecules produced from the abundant photochemistry in the upper atmosphere condense into aerosols through a variety of mechanisms.[18] These aerosols provide sources for further condensation of other molecules through direct particle surface chemistry, subsequently producing larger aerosols.[30] Since the condensation occurs at different temperatures and pressures stratification of the haze occurs, with a thin haze in the thermosphere and a thicker haze layer in the mesosphere.[31] These aerosols act as condensation sources for other species, increasing their size as they approach the surface.[32] This aerosol rain coats every surface on Titan, sinking to the bottom of methane lakes and composing the dunes, providing rich chemical diversity to the surface.[7, 33] With the possibility of transport to the subsurface ocean, there is the significant probability for the synthesis of prebiotic molecules. This, combined with the chemical variety of the atmosphere, makes Titan a continual target for astrochemical study.

1.2 Simulating Titan's Atmosphere in the Laboratory

Due to the diversity of chemistry possible in Titan's atmosphere, many laboratories have developed methods to simulate the atmosphere of Titan and enable aerosol production.[18] These simulation processes have roots in the original Miller-Urey experiment. In that work a vial with a simulated early Earth ocean and atmosphere was exposed to an electrical discharge to simulate lightning.[34] The products from this discharge chemistry were found to include many prebiotic molecules such as amino acids.[35] Considering the similar chemical possibilities with Titan's atmosphere, replicating the aerosols with a similar apparatus presents an experimental starting point.

When replicating the conditions on Titan to produce aerosols there are many more difficulties compared to the Miller-Urey experiment. These Titan atmospheric simulation experiments take into account the gas mixture on Titan, low temperature, pressure, and possible sources of energy for the chemistry.[18] Since Titan's atmosphere has been well characterized most experiments utilize a 90-95% nitrogen and 5-10% methane gas mixture as a base.[18, 36] Depending on the type of chemistry of interest for a particular experiment other gases may be added that are known to exist in Titan's atmosphere, such as carbon monoxide, hydrogen, or acetylene to name a few.[37-40] The temperature of Titan's atmosphere displays a large variation throughout the different layers, as discussed above, leading to multiple different temperatures being used for the atmospheric simulation experiments. The top of the temperature range, 195K, and the bottom of 95K, are two of the more commonly used temperature points for study, but multiple different cooling methods make temperature control a simpler parameter to account for and adjust.[18] As such the majority of studies take some temperature control into consideration and few simulation experiments are performed outside of Titan's atmospheric temperature range.

Pressure is one area where many of the adjustments made during simulation experiments fall outside of representative Titan conditions.[18] At lower pressures for the photochemically active upper atmosphere, the small number of molecules inhibit aerosol production unless prohibitively long timescales are used.[41, 42] This is due to the mean free path of a representative gas mixture being 0.20 m at Titan conditions and 0.34 m at Earth ambient conditions, as calculated by Cable et al.[18] The majority of apparatuses used for the production of these simulated aerosols are of similar dimensions, making reactions under Titan pressure unfeasible in experimental timescales. When increasing the pressure to overcome this limitation other concerns are introduced. The amount of nitrogen incorporation and aromaticity generation increase with higher pressure, impacted in part by the increasing density of reactive species at these pressures with some apparatuses.[42-46] These deviations from Titan's atmospheric chemistry are balanced against increased aerosol generation depending on experimental goals.

Energy sources to simulate the photochemistry vary considerably between experiments and are often cited as the largest source of chemical variation between simulations. The sources used focus both on the types of energy possible on Titan, and those that enable the dissociation reactions shown above.[18] UV irradiation methods are considered the most representative considering it is the major source of photochemistry on Titan, but photolyzing nitrogen can be difficult with most apparatuses and aerosol yields can be low.[26, 29, 42, 44, 47] Plasma based sources can be used to overcome these low yields. Hot plasma sources typically mimic lighting, similar to the original Miller-Urey experiment. The high aerosol production of these methods have the drawback of decreased relation to actual conditions since lightning has not been recorded on Titan and the high energy can lead to high levels of polymerization.[18, 39, 40, 48, 49] Cold plasma is more representative of chemistry induced by charged particles originating from Saturn and allows for most photochemical reactions discussed above.[37, 38, 50] Although aerosol yields can still be low, cold plasma conditions are a bridge between hot plasma discharges and UV irradiation. Other possible energy sources include gamma-rays,[51] soft x-rays,[52] and proton or electron beams,[18] all of which have their own advantages or disadvantages. Regardless of the energy source used to cause the chemistry, the end result is a brown to orange colored solid, or tholin, which is collected and subjected to further analysis.

In the analyzes presented in this thesis two different tholins are used, both of which have been the subject to prior study. The work discussed in chapters 4 and 5 utilized a hot plasma tholin while chapter 3 concentrates on a cold plasma tholin. While the reasoning behind the selection of these tholins was multifaceted, the selection of the cold plasma tholin in chapter 3 was due to the technique chosen for characterization being well suited to the lower aerosol yield. Additionally this tholin had minimal prior characterization, presenting an ideal initial target.[37, 38] The hot plasma discharge tholin used in the other chapters enabled a large amount of analytical method development due to larger aerosol yields. Prior work utilizing the hot plasma discharge tholins also enables comparison. [45, 49, 53, 54] Overall the selection of each tholin in each chapter was influenced by the overarching analytical goals of this thesis, discussed below.

1.3 Motivation: Analytical Goals

With any study of tholins the primary goal is characterization of the solid. By developing a thorough understanding of the different types of molecules present in the material, one hopes to better understand the atmospheric chemistry of Titan. Prior studies have identified an extraordinary amount of chemical complexity in tholins. For tholins produced from AC discharge, analyses have found a statistical mixture of carbon, hydrogen, and nitrogen.[45, 55] Within each of these possibilities are multiple functional groups, including aromatics, alkynes, amines, and nitriles to name a few. Each chemical functionality is best identified with different analytical methods, and few methods work well for bulk analysis. Spectroscopy is ideal for identifying different functional groups, but cannot characterize a compound's size when used alone. Chromatography is well suited to structural information, but usually depends on choosing a target functionality prior to analysis. Most tholin samples are analyzed by a battery of different methods to overcome this, with a single method used for each analytical goal. Typically a single type of functionality of interest is identified in initial studies of tholins, driving the choices for analytical methods used in subsequent studies. The high complexity consequently mandates a high number of tests and minimalizes the amount of characterization that can reasonably be obtained by any single analysis.

While characterization is a process of applying an increasing number of specific tests to the tholins, the complexity of the material itself leads to a new goal: the identification of mission applicable analytical methods. A major goal during *in-situ* analysis is to identify and characterize as much of the material as possible with minimal sample processing and simple instrumental requirements. The multitude of different analytical methods required to analyze tholins presents complications for missions, since payloads need to be well defined and emphasize the highest amount of data from the fewest possible instruments.[56] Additionally many of the instruments that can provide a high amount of detailed information, such as nuclear magnetic resonance, have requirements making them incompatible with spaceflight. As such, developing techniques well suited to broad tholin characterization is imperative, with mission applicable instrumentation a secondary goal underpinning tholin research.

The work presented in this thesis strives towards both the development of mission applicable analytical methods and the characterization of particular compounds and functionalities within the tholins. To further the mission applicability goal, mass spectrometry is used in all presented methods. Analysis with mass spectrometry is accomplished by desorption of analytes into the gas phase followed by ionization and subsequent detection as a mass to charge ratio. Various mass spectrometers have been included on a multitude of missions, including the original Huygens lander,[16, 57, 58] making it a well suited type of instrumentation for the development of mission applicable analytical methods. Since mass spectrometers detect a mass to charge ratio, it already enables the determination of molecule size and even chemical formula with high enough resolution. Additional structural information can be obtained by either interfacing with a chromatography system, or utilizing a mass spectrometer that allows for tandem mass spectrometry. By obtaining characteristic fragments from a target ion, tandem mass spectrometry allows for the elucidation of important structural information, even if more specific techniques cannot be used.

1.4 Contents of Thesis

While the research discussed in this thesis utilizes mass spectrometry, the research does not always accomplish both tholin characterization and development of a mission applicable method. Chapters two and three focus on the development of an ambient mass spectrometry method and its use in tholin characterization respectively. The chromatography method presented in chapter 4 accomplishes both goals, while the supramolecular chemistry method discussed in chapter 5 allows only for characterization without mission applicability. The research in each of these chapter is discussed in more detail below.

Chapter 2 presents the development of a miniature plasma ionization source based on the technique known as direct analysis in real time (DART). This technique utilizes heated helium metastables to desorb and ionize samples. This ambient mass spectrometry source is shown to be reliable for multiple different types of samples, from pharmaceuticals to vicious liquid asphalt. The source is presented with low power and gas consumption, which combined with the use of helium enable its consideration for Titan mission applications. Being able to analyze multiple different sample types in addition to complex organic mixtures makes this miniaturized source a low technology readiness level presentation of how an ambient plasma source may be utilized.

This mini-DART source is applied to the analysis of cold plasma tholins in chapter 3, further presenting its mission applications while performing an analysis of solid tholin samples unstudied by mass spectrometry. Using the mini-DART for this analysis shows that the source described in chapter 2 can be successfully applied to tholin samples. The use of benzene and acetylene dopants within these tholins enabled a comparative study to characterize the impact these higher molecular weight species have on the different synthetic products observed. The results from this study show that dopants have unexpected effects and bias the products towards certain molecules. While multiple different compounds are identified, some prebiotic molecules are seen. Since the tholins analyzed are proposed to be more representative of the early stage aerosols, the identified molecules present implications for reaction products in different layers of Titan's atmosphere. The mini-DART shows itself to be effective at the analysis of low molecular weight and polar species within the tholin, without analyzing heavier species or hydrocarbons. As such this method allows for the characterization of an important fraction of tholins, enabling necessary insights for other analyzes.

In chapter 4 a solid phase microextraction gas chromatography (SPME-GC) method and its application to a hot plasma tholin is discussed. GC has been applied to tholins extensively and was included as part of the instrumental payload on the Huygens Titan lander of the Cassini mission to the Saturn system.[16, 58] Additionally GC is well suited to the characterization of hydrocarbons and heavier, less polar molecules. These are known constituents of tholins, but difficult to analyze with other methods, making them a well suited target for GC analysis. The application of SPME is where this method differs from prior studies. SPME utilizes an adsorbent fiber to preconcentrate gas phase analytes prior to analysis by GC, targeting specific analytes depending on the fiber media. Multiple different compounds are found, with the identification of multiple nitriles fitting with compounds identified in earlier work. The application of solid phase extraction to mission applications has been discussed and this SPME method demonstrates it is well suited to the characterization of tholins, accomplishing both analytical goals of this thesis.

A hot plasma tholin is also examined in chapter 5, concentrating on the analysis of large primary amines using 18-crown-6 ether complexation. Primary amines are difficult to detect with gas chromatography and larger molecules are difficult to detect with DART, allowing this technique to fill that analytical gap. The 18-crown-6 ether selectively forms a supramolecular complex to the primary amines, which can subsequently be readily identified by electrospray ionization mass spectrometry. Using electrospray excludes this technique from mission applications, but enables specific identification upon which other analytical methods can be developed. There are two different primary amine series identified, and the inclusion of nitrile functionality in one of the series relates to possible prebiotic molecules. The technique thus provides a reliable way of characterizing the primary amines present in tholins that remain unidentified with other methods.

1.5 References

1. A. Coustenis, *Space Science Reviews*, 2005, **116**, 171-184.
2. E. R. Stofan, C. Elachi, J. I. Lunine, R. D. Lorenz, B. Stiles, K. L. Mitchell, S. Ostro, L. Soderblom, C. Wood, H. Zebker, S. Wall, M. Janssen, R. Kirk, R. Lopes, F. Paganelli, J. Radebaugh, L. Wye, Y. Anderson, M. Allison, R. Boehmer, P. Callahan, P. Encrenaz, E. Flamini, G. Francescetti, Y. Gim, G. Hamilton, S. Hensley, W. T. K. Johnson, K.

Kelleher, D. Muhleman, P. Paillou, G. Picardi, F. Posa, L. Roth, R. Seu, S. Shaffer, S. Vetrella and R. West, Nature, 2007, 445, 61-64.

3. N. Lancaster, *Science*, 2006, **312**, 702-703.
4. J. T. Perron, M. P. Lamb, C. D. Koven, I. Y. Fung, E. Yager and M. Ádámkovics, *Journal of Geophysical Research: Planets*, 2006, **111**.
5. R. D. Lorenz, B. W. Stiles, R. L. Kirk, M. D. Allison, P. P. del Marmo, L. Iess, J. I. Lunine, S. J. Ostro and S. Hensley, *Science*, 2008, **319**, 1649-1651.
6. F. M. Flasar, R. K. Achterberg, B. J. Conrath, P. J. Gierasch, V. G. Kunde, C. A. Nixon, G. L. Bjoraker, D. E. Jennings, P. N. Romani, A. A. Simon-Miller, B. Bézard, A. Coustenis, P. G. J. Irwin, N. A. Teanby, J. Brasunas, J. C. Pearl, M. E. Segura, R. C. Carlson, A. Mamoutkine, P. J. Schinder, A. Barucci, R. Courtin, T. Fouchet, D. Gautier, E. Lellouch, A. Marten, R. Prangé, S. Vinatier, D. F. Strobel, S. B. Calcutt, P. L. Read, F. W. Taylor, N. Bowles, R. E. Samuelson, G. S. Orton, L. J. Spilker, T. C. Owen, J. R. Spencer, M. R. Showalter, C. Ferrari, M. M. Abbas, F. Raulin, S. Edgington, P. Ade and E. H. Wishnow, *Science*, 2005, **308**, 975-978.
7. C. A. Griffith, T. Owen, T. R. Geballe, J. Rayner and P. Rannou, *Science*, 2003, **300**, 628-630.
8. M. J. Malaska, R. Hodyss, J. I. Lunine, A. G. Hayes, J. D. Hofgartner, G. Hollyday and R. D. Lorenz, *Icarus*, 2017, **289**, 94-105.
9. J. S. Mendez Harper, G. D. McDonald, J. Dufek, M. J. Malaska, D. M. Burr, A. G. Hayes, J. McAdams and J. J. Wray, *Nature Geosci*, 2017, **10**, 260-265.
10. H. E. Maynard-Casely, R. Hodyss, M. L. Cable, T. H. Vu and M. Rahm, *IUCrJ*, 2016, **3**, 192-199.

11. F. Raulin, C. Brasse, O. Poch and P. Coll, *Chemical Society Reviews*, 2012, **41**, 5380-5393.

12. M. G. Trainer, A. A. Pavlov, H. L. DeWitt, J. L. Jimenez, C. P. McKay, O. B. Toon and M. A. Tolbert, *Proceedings of the National Academy of Sciences*, 2006, **103**, 18035-18042.

13. F. Raulin, *Space Science Reviews*, 2005, **116**, 471-487.

14. J. Radebaugh, R. Lorenz, T. Farr, P. Paillou, C. Savage and C. Spencer, *Geomorphology*, 2010, **121**, 122-132.

15. W. Reid Thompson and C. Sagan, *Icarus*, 1984, **60**, 236-259.

16. H. B. Niemann, S. K. Atreya, S. J. Bauer, G. R. Carignan, J. E. Demick, R. L. Frost, D. Gautier, J. A. Haberman, D. N. Harpold, D. M. Hunten, G. Israel, J. I. Lunine, W. T. Kasprzak, T. C. Owen, M. Paulkovich, F. Raulin, E. Raaen and S. H. Way, *Nature*, 2005, **438**, 779-784.

17. A. L. Zerkle, M. W. Claire, S. D. Domagal-Goldman, J. Farquhar and S. W. Poulton, *Nature Geosci*, 2012, **5**, 359-363.

18. M. L. Cable, S. M. Hörst, R. Hodyss, P. M. Beauchamp, M. A. Smith and P. A. Willis, *Chemical Reviews*, 2012, **112**, 1882-1909.

19. E. H. Wilson and S. K. Atreya, *Planetary and Space Science*, 2003, **51**, 1017-1033.

20. C. Romanzin, E. Arzoumanian, E. Es-sebbar, A. Jolly, S. Perrier, M. C. Gazeau and Y. Bénilan, *Planetary and Space Science*, 2010, **58**, 1748-1757.

21. J. Ferris, B. Tran, J. Joseph, V. Vuitton, R. Briggs and M. Force, *Advances in Space Research*, 2005, **36**, 251-257.

22. M. Cordiner, M. Y Palmer, C. A. Nixon, S. B. Charnley, M. J. Mumma, P. G. J. Irwin, N. A. Teanby, Z. Kisiel and J. Serigano, 2015, *A.A.S, DPS Meeting*
23. W. C. Maguire, R. A. Hanel, D. E. Jennings, V. G. Kunde and R. E. Samuelson, *Nature*, 1981, **292**, 683-686.
24. V. G. Kunde, A. C. Aikin, R. A. Hanel, D. E. Jennings, W. C. Maguire and R. E. Samuelson, *Nature*, 1981, **292**, 686-688.
25. V. Vuitton, R. V. Yelle and J. Cui, *Journal of Geophysical Research: Planets*, 2008, **113**, E05007.
26. H. Imanaka and M. A. Smith, *Geophysical Research Letters*, 2007, **34**, L002204.
27. J. C. Loison, E. Hébrard, M. Dobrijevic, K. M. Hickson, F. Caralp, V. Hue, G. Gronoff, O. Venot and Y. Bénilan, *Icarus*, 2015, **247**, 218-247.
28. V. A. Krasnopolsky, *Icarus*, 2009, **201**, 226-256.
29. H. Imanaka and M. A. Smith, *The Journal of Physical Chemistry A*, 2009, **113**, 11187-11194.
30. P. Lavvas, M. Sander, M. Kraft and H. Imanaka, *The Astrophysical Journal*, 2011, **728**, 80.
31. V. A. Krasnopolsky, *Planetary and Space Science*, 2010, **58**, 1507-1515.
32. P. Lavvas, R. V. Yelle and C. A. Griffith, *Icarus*, 2010, **210**, 832-842.
33. P. Lavvas, C. A. Griffith and R. V. Yelle, *Icarus*, 2011, **215**, 732-750.
34. S. L. Miller and H. C. Urey, *Several questions about the origin of life have been answered, but much remains to be studied*, 1959, **130**, 245-251.
35. S. L. Miller, *Science*, 1953, **117**, 528-529.

36. E. Sciamma-O'Brien, N. Carrasco, C. Szopa, A. Buch and G. Cernogora, *Icarus*, 2010, **209**, 704-714.
37. E. Sciamma-O'Brien, K. T. Upton and F. Salama, *Icarus*, 2017, **289**, 214-226.
38. E. Sciamma-O'Brien, C. L. Ricketts and F. Salama, *Icarus*, 2014, **243**, 325-336.
39. M. Ruiz-Bermejo, C. Menor-Salván, E. Mateo-Martí, S. Osuna-Esteban, J. Á. Martín-Gago and S. Veintemillas-Verdaguer, *Icarus*, 2008, **198**, 232-241.
40. M. Ruiz-Bermejo, C. Menor-Salván, J. L. de la Fuente, E. Mateo-Martí, S. Osuna-Esteban, J. Á. Martín-Gago and S. Veintemillas-Verdaguer, *Icarus*, 2009, **204**, 672-680.
41. B. Cunha de Miranda, G. A. Garcia, F. Gaie-Levrel, A. Mahjoub, T. Gautier, B. Fleury, L. Nahon, P. Pernot and N. Carrasco, *The Journal of Physical Chemistry A*, 2016, **120**, 6529-6540.
42. B. N. Tran, J. C. Joseph, M. Force, R. G. Briggs, V. Vuitton and J. P. Ferris, *Icarus*, 2005, **177**, 106-115.
43. G. Alcouffe, M. Cavarroc, G. Cernogora, F. Ouni, A. Jolly, L. Boufendi and C. Szopa, *Plasma Sources Sci T*, 2010, **19**.
44. H. Imanaka and M. A. Smith, *Proceedings of the National Academy of Sciences*, 2010, **107**, 12423-12428.
45. A. Somogyi, C. H. Oh, M. A. Smith and J. I. Lunine, *Journal of the American Society for Mass Spectrometry*, 2005, **16**, 850-859.
46. C. Szopa, G. Cernogora, L. Boufendi, J. J. Correia and P. Coll, *Planetary and Space Science*, 2006, **54**, 394-404.

47. R. Thissen, V. Vuitton, P. Lavvas, J. Lemaire, C. Dehon, O. Dutuit, M. A. Smith, S. Turchini, D. Catone, R. V. Yelle, P. Pernot, A. Somogyi and M. Coreno, *The Journal of Physical Chemistry A*, 2009, **113**, 11211-11220.
48. A. Somogyi, M. A. Smith, V. Vuitton, R. Thissen and I. Komaromi, *Int J Mass Spectrom*, 2012, **316**, 157-163.
49. C. He, G. Lin, K. T. Upton, H. Imanaka and M. A. Smith, *The Journal of Physical Chemistry A*, 2012, **116**, 4760-4767.
50. H. Imanaka, B. N. Khare, J. E. Elsila, E. L. O. Bakes, C. P. McKay, D. P. Cruikshank, S. Sugita, T. Matsui and R. N. Zare, *Icarus*, 2004, **168**, 344-366.
51. S. I. Ramírez, R. Navarro-González, P. Coll and F. Raulin, *Advances in Space Research*, 2001, **27**, 261-270.
52. T. Penz, H. Lammer, Y. N. Kulikov and H. K. Biernat, *Advances in Space Research*, 2005, **36**, 241-250.
53. S. M. Horst, R. V. Yelle, A. Buch, N. Carrasco, G. Cernogora, O. Dutuit, E. Quirico, E. Sciamma-O'Brien, M. A. Smith, A. Somogyi, C. Szopa, R. Thissen and V. Vuitton, *Astrobiology*, 2012, **12**, 809-817.
54. C. He, G. Lin and M. A. Smith, *Icarus*, 2012, **220**, 627-634.
55. A. Somogyi, R. Thissen, F. R. Orthous-Daunay and V. Vuitton, *Int J Mol Sci*, 2016, **17**.
56. K. P. Hand, A. E. Murray, J. B. Garvin, W. B. Brinckerhoff, B. C. Christner, K. S. Edgett, B. L. Ehlmann, C. R. German, A. G. Hayes, T. M. Hoehler, S. M. Horst, J. I. Lunine, K. H. Nealson, C. Paranicas, B. E. Schmidt, D. E. Smith, A. R. Rhoden, M. J. Russell, A. S. Templeton, P. A. Willis, R. A. Yingst, C. B. Phillips, M. L. Cable, K. L. Craft., A. E.

Hofmann, T. A. Nordheim, R. P. Pappalardo and P. E. T. (2017), *Report of the Europa Lander Science Definition Team*, February, 2017.

57. P. Ehrenfreund, J. J. Boon, J. Commandeur, C. Sagan, W. R. Thompson and B. Khare, *Adv Space Res*, 1994, **15**, 335-342.
58. H. B. Niemann, S. K. Atreya, J. E. Demick, D. Gautier, J. A. Haberman, D. N. Harpold, W. T. Kasprzak, J. I. Lunine, T. C. Owen and F. Raulin, *Journal of Geophysical Research: Planets*, 2010, **115**, E12006.

Chapter 2

EASILY FABRICATED ION SOURCE FOR CHARACTERIZING MIXTURES OF ORGANIC COMPOUNDS BY DIRECT ANALYSIS IN REAL TIME MASS SPECTROMETRY

(Reproduced in part with permission from Upton, K., Schilling, K, Beauchamp, J. L., *Analytical Methods*, 2017, **9**, 5065-5074 DOI: 10.1039/C7AY00971B Copyright 2017 Royal Society of Chemistry)

2.1 Abstract

The increasing use of atmospheric pressure mass spectrometry has led to the development of many ambient ionization sources, for which sampling versatility and low cost are desired features. One such recent ambient ionization method is direct analysis in real time mass spectrometry (DART-MS), which has proven to be well suited to the analysis of native samples of both simple and complex natures. We describe a home-built DART source (EZ-DART) with versatile sampling capabilities, low power requirements, and low assembly cost which can be easily interfaced to mass spectrometers equipped with an atmospheric pressure inlet. The operating temperature range (22-250°C) enables the acquisition of both temperature programmed desorption-based DART mass spectra and the collection of multistep collision-induced dissociation (CID) mass spectra. We present here the validation of the EZ-DART source and a demonstration of its performance in a number

of relevant applications. Additionally, we introduce the new DART application of reagent assisted desorption ionization (RADI) for the targeting of specific chemical functionality in complex organic mixtures through a host-guest chemical system.

2.2 Introduction

Ambient mass spectrometry comprises a range of experimental methodologies by which analyte ions can be produced at atmospheric pressure and then transferred to the vacuum region of a mass spectrometer for analysis. Ambient analysis allows for rapid examination of a variety of samples with minimal to no sample pretreatment, compared to traditional methods requiring more complex procedures to access the analytical information. Recent reviews by Bodzon-Kulakowska and Suder[1] and Ding and Duan,[2] among others,[3, 4] have discussed the multitude of different ambient ionization techniques, likely mechanisms by which they operate, and possible applications. Among the many different techniques for ambient ionization mass spectrometry, a solvent spray or plasma discharge are two of the most common.[5]

Applications for ambient mass spectrometry include, but are not limited to, food science,[6-9] pharmaceutical characterization,[10-15] forensics,[16-24] detection of volatile and semi-volatile organic compounds,[25-29] biological samples,[30-34] and the analysis of complex organics such as aerosols[35-39] and hydrocarbons.[40-42] To be effective, an ambient ionization method must both desorb the target analyte into the gas phase and ionize it, or directly desorb ions from the sample. For the analysis of samples in a native state, the use of spray based methods such as desorption electrospray ionization (DESI),[43, 44] or plasma methods such as direct analysis in real time (DART),[45, 46] have moved to the forefront. DESI uses a solvent spray to desorb and ionize a sample; DART utilizes a plasma discharge to produce metastable gas molecules that are optionally heated to desorb and ionize the sample through a complex mechanism.[45, 47] The mechanism of ionization for DART is proposed to occur either by direct Penning ionization by the helium metastable or proton transfer from protonated water clusters resulting from ion molecule reactions of trace atmospheric species initially ionized by Penning ionization.[45] The formation of various positively and negatively charged gas phase adducts from atmospheric molecules such as ammonia are also commonly observed and assist in ionization processes.[45, 48]

DART analysis has been applied successfully in the majority of applications where other ambient mass spectrometry methods have been utilized.[11, 21, 47 49] The selection of DESI or DART as the ionization source for a particular analytical application requires consideration of the target analyte's solubility in potential DESI spray solvents, and vapor pressure as well as potential reactivity in known DART ionization mechanisms. Prior work has shown that DART analysis can be readily applied to applications with highly complex sample compositions.[42]

For difficult to detect analytes, either due to low ionization efficiencies or low detection limits, ambient mass spectrometry methods such as DART and DESI often employ chemical modification. This process involves the introduction of a chemical reagent that changes the detected analyte ion in a variety of possible ways. When used with DART, prior studies have utilized gas phase reagents such as chloroform, dichloromethane, ammonia, or trifluoroacetic acid to form gas phase adducts.[48, 45] Similar chemical modifications using DESI have also been reported, using the designation "reactive DESI". That method involves host-guest supramolecular chemistry with either the host or guest in the spray to complex with a target functionality present on the analyte in the sample, or derivatization chemistry involving attachment of a fixed charge to the target functionality within the molecule, often with the reagent molecule being delivered in the spray.[50] Many different host-guest supramolecular interactions[51-53] and chemical derivatization methods[50, 54] have been used successfully with reactive DESI. We report in this study a similar method with DART ionization, referred to as reagent assisted desorption ionization (RADI), with which the introduction of host-guest supramolecular chemistry allows for enhanced detection of target species in a complex mixture and simplification of resultant spectra.

In this work, we describe an affordable, versatile, and easily fabricated DART source (which we refer to in this paper by the designation EZ-DART) that has proven effective for a wide variety of samples with varying degrees of complexity. Capabilities of this source are demonstrated in applications including commercial pharmaceutical identification, forensics, and analysis of organic mixtures. By reducing the temperature the sample ion signal persists over a timescale of several seconds. This facilitates the acquisition of multistep CID mass spectra to provide information relating to analyte structure. Systematic variation of the operating temperature over the range of 25-250°C enables the acquisition of temperature programmed desorption-based DART mass spectra. The minimal expense associated with fabrication of the EZ-DART source, which can be used with any mass spectrometric instrument having an atmospheric pressure inlet, offers the potential to expand the applications and user group of this ionization methodology.

2.3 Experimental

2.3.1 EZ-DART Source

The EZ-DART source was fabricated by the Caltech glass shop using borosilicate glass tubing and 1/16" flat ended tungsten wire electrodes. 1/2" glass tubing was used for the body with 1/8" glass tubing for the gas input line. The EZ-DART source design enables the use of helium (99.995% purity used in this study) at a flow a rate of 1.5 L/min. The glass construction enables visual inspection of the electrodes and discharge, the color of which changes if there is an air leak in the helium supply line. Source temperature and helium flow rate both impact sample depletion rates, but only temperature was modified in this study; consistent gas flow and discharge conditions were maintained for all experiments. The operating conditions used for the needle electrode are 1.5-2.5 kV DC with a current of 0.1-0.2 mA limited by a 10 MΩ resistor. The filter electrode is held at ground for most experiments compared to the 110-250 V DC filter voltage commonly used.[11, 21, 45, 49] Filter voltages in this range were applied for the pharmaceutical samples reported below and showed no difference other than decreased overall intensity of the signal. The voltage for both electrodes is controlled by two digital high voltage DC power supplies (Stanford Research Systems, INC. Model PS350, Sunnyvale, CA).

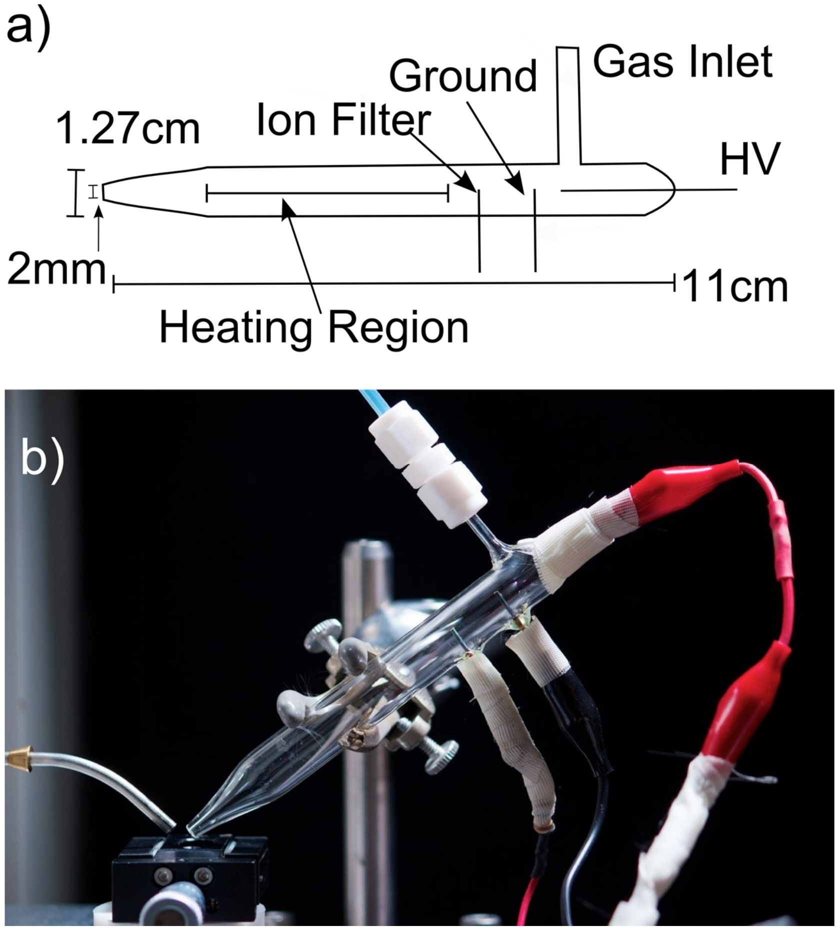

Figure 2.1. a) Scale drawing of EZ-DART source with relevant dimensions. The discharge gap is approximately 4mm b) The actual EZ-DART source in operating configuration without heating tape

In typical operation, the outlet of the EZ-DART is oriented at approximately 45° from normal, with the sample no more than 5 mm from the EZ-DART outlet and ion transfer tube inlet for the angled configuration (shown in figure 2.1b)[55, 56]. The reagent assisted desorption ionization (RADI) experiments were performed with the EZ-DART aligned in a linear configuration with the DART outlet approximately 1 cm from the mass spectrometer inlet. The resultant ions are analyzed by a linear ion trap mass spectrometer (LTQ-XL, Thermo Scientific, San Jose, CA). The inlet capillary for the mass spectrometer was held at 50°C for the angled configuration experiments and 250°C for the linear configuration experiments. A lower temperature was used in the angled configuration to minimize ambient heating of the sample due to conductive heating of the ion transfer tube. This was not a concern in the linear configuration. The capillary (and surrounding font cone) voltage was tuned to allow for highest signal intensity of the target analyte during acquisition. This was a bias of 1.4V for negative ions and 0.2V for positive ions. Sampling occurs by aspiration of ions into the capillary from a nearly field free region. To heat the gas stream for temperature programmed desorption (TPD) analysis, a heating cord (Omega Engineering, Stamford, CT) was wrapped around the EZ-DART between the ion filter and the gas outlet, and then insulated with glass wool and aluminium foil or cloth fiberglass tape. The temperature is controlled with a variable transformer (Variac Co., Cleveland, OH) and measured with a K-type thermocouple placed between the heating tape and the glass (Omega Engineering, Stamford, CT). Reported temperatures are accurate within +/- 3°C. For collision induced dissociation (CID) spectra, a normalized CID energy of 20-25 (arbitrary units) was found to yield nearly 100% dissociation of the selected ion. These spectra are reported in the Supplemental Information, where relevant, with the targeted m/z values for each spectra indicated on the side.

2.3.2 Sample Preparation and Reagents

To show the efficacy and versatility of the EZ-DART source for both positive and negative ion analysis, a variety of representative analytes were chosen in the validation tests. Liquid standard samples were applied with borosilicate glass melting point capillaries (Kimble Chase, 1.5-1.8 x 90 mm) to glass microscope slides (Gold Seal microslides, 25 x 75 mm, 0.97-1.07 mm thickness) and then placed in the sample area for analysis. Maleic acid (Sigma Aldrich, 99%) was dissolved in methanol (Fisher Scientific, HPLC Grade), and then applied to the glass slide and allowed to evaporate into a film. Poly(propylene glycol) (Aldrich, average mass 2,700 amu; containing 120-190 ppm proprietary antioxidant) was applied directly to the glass slide. A reference solution of RDX (Cerilliant, 1 mg/ml in acetonitrile, certified reference material) was diluted to concentrations between 0.25 ng/µl and 1.75 ng/µl in acetonitrile (Omnisolv, HPLC Grade) for application and analyzed immediately.

Pharmaceutical samples were directly analyzed by the EZ-DART source. The coating was removed from ibuprofen, (Walgreens, 200 mg tablet with wax coating) pseudoephedrine (Walgreens, 30 mg tablet with wax coating), and the naproxen sodium tablet (Amneal Pharmaceuticals, 500 mg) before placement on the sampling stage to ensure an exposed surface. A viscous liquid hydrocarbon sample was obtained from the La Brea Tar Pits (the George C. Page Museum, Los Angeles, CA) by collecting a small amount of the surface-exposed tar in a vial. The collected tar was introduced to the EZ-DART source as a film applied directly to a glass slide without solvent. Neurotransmitters dopamine hydrochloride (Sigma Aldrich), norepinephrine hydrochloride (Sigma Aldrich >97%), gamma-aminobutyric acid (Sigma Aldrich >99%), and serotonin hydrogenoxalate (Sigma Aldrich) were tested as neat solids in precision glass capillaries (0.4 mm I.D., Drummond Scientific Co., Broomall, PA) in the linear configuration. The complexation agent 18-crown-6 ether (Sigma Aldrich 99%) was placed in a separate precision glass capillary and held in line either between the EZ-DART outlet and capillary holding a neurotransmitter, or in a reversed configuration between the same capillary and the mass spectrometer inlet.

2.4 Results and Discussion

2.4.1 Pharmaceutical Samples

The examination of pharmaceutical tablets with DART was one of the initial applications proposed by Cody et al., upon which further analyses have been built.[11, 45, 57, 58] While there are other methods by which pharmaceuticals can be characterized, the majority of these methods typically require some amount of sample preparation, which increases the amount of time necessary for analysis.[59, 60] The desire to minimize sample preparation and analysis time makes pharmaceutical identification an ideal application for EZ-DART.

A commercial ibuprofen tablet was chosen as a pharmaceutical sample for positive mode ionization due to its prior analysis by DART and its ease of ionization.[11] The wax-based pill coating was removed and the tablet placed in front of the gas stream in the angled configuration while the EZ-DART was operated at ambient temperature. Figure 2.2a shows the spectrum obtained with this procedure. The protonated species, ammonia adduct, and their associated dimers are detected.[11] The carboxylic acid group in ibuprofen allowed for detection in negative mode as the $[M-H]^-$ species. The same procedure as above produces the spectrum shown in 2.2b when negative ions are detected.

Pseudoephedrine was examined in tablet form for its forensic relevance to the illicit manufacture of methamphetamine. The spectrum, shown in figure 2.2c, exhibits not only protonated pseudoephedrine, but also the ammonium adduct of triacetin and a dimer of triacetin and pseudoephedrine. Triacetin is a known matrix molecule in pharmaceuticals. This observation indicates that some additives included in the pill matrix may be observed during routine DART analysis. The ability of the DART to detect some matrix molecules may be of assistance to the analyst in providing additional points of comparison between questioned samples.

The sodium salt of naproxen was used as a pharmaceutical exemplar for negative mode analysis. The spectrum, shown in figure 2.2d, shows matrix species similar to the pseudoephedrine tablet, but the negative ion dimer is the most abundant species. The observation of the monomer, dimer, and trimer is of interest considering the nature of the starting material as a sodium salt. No sodium-bound species are observed in negative mode, suggesting that ions are not derived directly from the solid, but rather are generated post desorption in the gas phase. Additional negative mode data for maleic acid, also showing formation of the monomer, dimer, and trimer, are presented in the Supplemental Information.

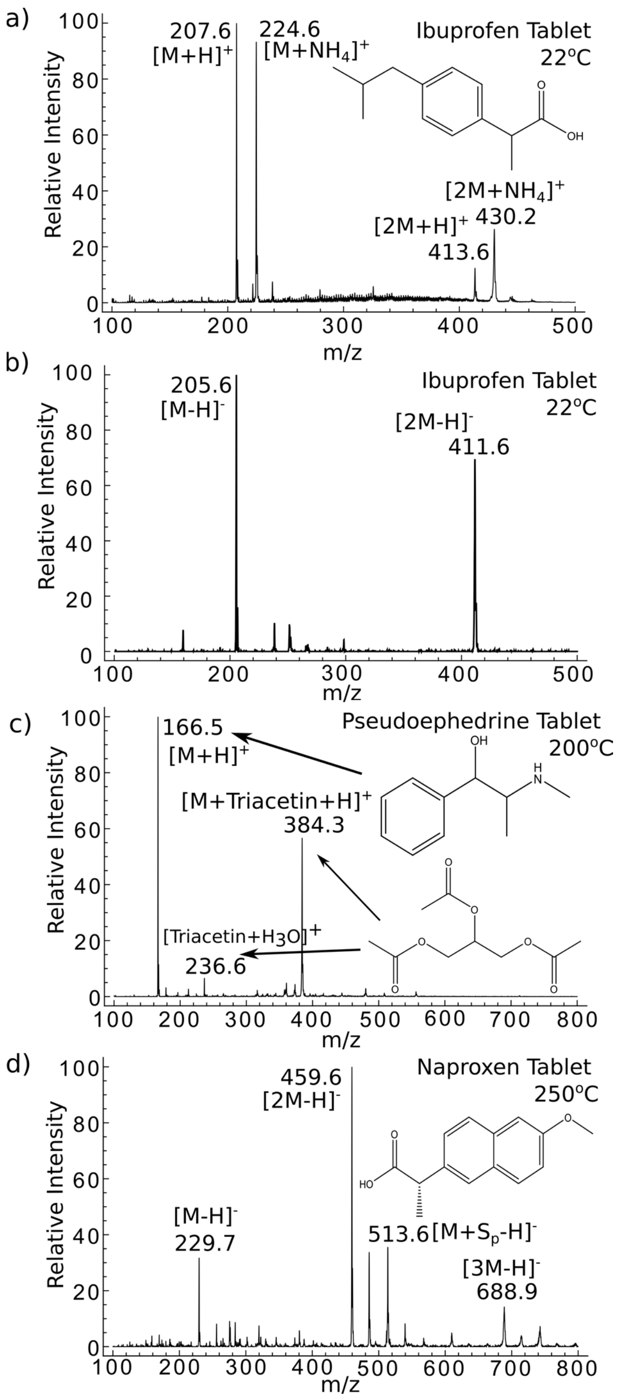

Figure 2.2. a) Positive mode spectrum of an ibuprofen tablet b) Negative mode spectrum of an ibuprofen tablet c) Positive mode spectrum of a pseudoephedrine tablet. d) Negative mode spectrum of a naproxen sodium tablet. The 513 Da adduct peak in the naproxen sodium spectrum is attributed to magnesium stearate present in the tablet. Temperatures shown refer to the heater temperature of the EZ-DART source.

For all the above experiments no changes were made to the settings of the EZ-DART source between the positive and negative mode samplings. These results show that the EZ-DART source can identify a variety of different pharmaceutical tablets with either positive or negative analyte ions without the need for adjustment of operating conditions external to the mass spectrometer. However, the presence of matrix ions indicates that the formation of adducts of the analytes of interest with other sample molecules needs to be taken into consideration for the analysis of complex multi-component organic samples.

2.4.2 Species of Forensic Interest

DART-MS has proven useful for forensic applications, including the analysis of illicit drugs, condom and sexual lubricants, and explosives.[21, 49, 61, 62] Cody et al. analyzed currency to find cocaine by placing a bank note directly into the sampling region.[45] We reproduced that test as shown in figure 2.3. A well-circulated twenty dollar bill was placed in the sample area. The resultant mass spectrum had major peaks corresponding to the $[M+H]^+$ species for cocaine and methamphetamine, with the other species corresponding to a polymer series spaced by 58 Da, all of which are ammonia adducts. These adducts were confirmed by observation of a 17 Da loss in CID, corresponding to the loss of an ammonia adduct. A second twenty dollar bill and a fifty dollar bill showed similar results. Cocaine and methamphetamine were confirmed by CID, similar to the structural confirmation performed in other DART experiments,[63] the data for which are included in the Supplemental Information. Prior analyses of bank notes have given similar results,[64, 65] showing that small amounts of illicit substances can be detected readily with no sample preparation using the

EZ-DART. With the success of this sampling, further testing is warranted for the EZ-DART on forensic samples, such as swabs from buildings contaminated by illicit drug manufacture.[49]

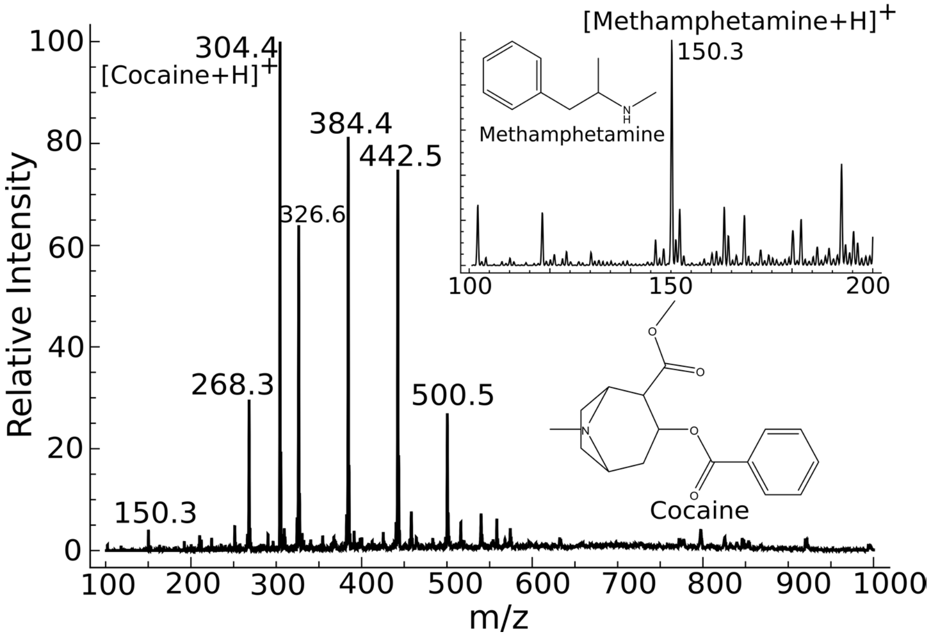

Figure 2.3. Spectrum of a 2009 issue bank note taken at 250°C heater temperature where 304.4 m/z corresponds to protonated cocaine. Inset shows region in which methamphetamine was detected.

The forensic interest in trace analysis of chemicals spreads beyond illicit substances, with explosives detection being one of the earliest experimental targets. DART has been effective at trace detection of different explosives, such as peroxides and nitroaromatics.[20, 21, 45] The ability of DART to determine trace amounts of the majority of these explosives under qualitative screening conditions was found to be comparable to or improved from common determination methodology, with faster analysis times. With the proven success of

DART in this application, the ability of the EZ-DART source to detect comparably trace amounts of explosives was tested using RDX solutions from 0.25 ng/µl to 1.75 ng/µl, examined in triplicate by depositing 2 µl (providing for deposition amounts of 0.5 ng to 3.5ng) onto a glass surface, with a new surface being used after each deposition. A representative spectrum for these data is shown in figure 2.4. Since the $[M\text{-}H]^-$ peak was not seen, the nitrite adduct was monitored for each deposition. This peak was ratioed to the reliable background peak of 255 Da (palmitic acid from fingerprint contamination). A lower limit of detection of 1.1 ng was determined, with a linear range of detection extending to 2.5 ng. Details are given in the Supporting Information. The LOD result is twice the lower limit of detection of 0.5 ng reported previously using a commercial DART source.[20] The result suggests that the EZ-DART source should be able to detect similar levels of explosive residue, even if they are detected only as adducts. While the limited linear range of the source would preclude its use for quantitative assessments, the DART study noted for comparison focused on qualitative screening conditions.[20]

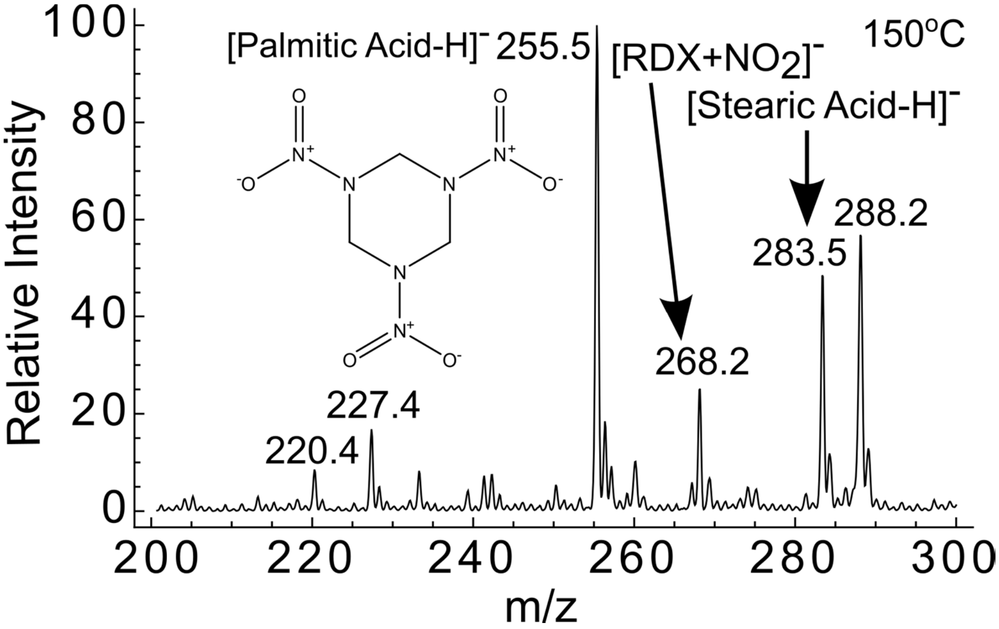

Figure 2.4. Average of three spectra of a drop of acetonitrile containing 1.5 ng of RDX on glass. The RDX is seen as the nitrite adduct. The 255 Da and 283 Da are palmitic and steric acid respectively, and were seen in each spectrum due to fingerprint contamination.

2.4.3 TPD Based Experiments

Complex organic mixtures, comprising compounds of varying molecular weight and structural complexity, can be difficult to analyze with ambient ionization methods and often require extensive sample preparation to obtain a more complete analysis.[59, 64, 66] Applications adjusting the DART gas heater temperature have been used to characterize pyrolysis product evolution,[67-69] complex sample differentiation,[70-72] and to induce fragmentation of known molecules at higher temperatures (150-400°C).[73-75] Additionally, temperature programmed desorption (TPD) has been used in petroleomics studies with success at helping to simplify analysis.[65] Using the EZ-DART source we examined the TPD analysis of a PPG sample (described in the Supplemental Information) and a viscous liquid asphalt, shown here, demonstrating that methods requiring DART heater adjustment can be used with the EZ-DART source.

A viscous liquid asphalt sample from the La Brea Tar Pits was chosen as a representative complex organic mixture relevant to samples of interest in petroleum analysis. The sample was examined at both 100°C and at 250°C (figure 2.5). The spectrum shown in figure 2.5b at 250°C shows peaks from 200-400 Da, a region for which peaks have been observed for other petroleum oil samples examined using DART.[45, 75] Of particular interest is the shifting of mass envelopes noted in comparing the two scans, with many of the low mass species visible at 100°C decreasing at 250°C. An additional envelope of even higher mass was observed at 250°C, accompanied by the change in the calculated average mass from 222 to 400 Da. Peaks in this higher mass envelope are not observed in the lower temperature spectrum. The 100°C spectrum appears to have a single mass envelope centered at around 250 Da. In contrast, the 250°C spectrum has a high mass envelope centered around 550 Da, in addition to two lower intensity mass envelopes, centered around 280 Da and 300 Da, respectively.

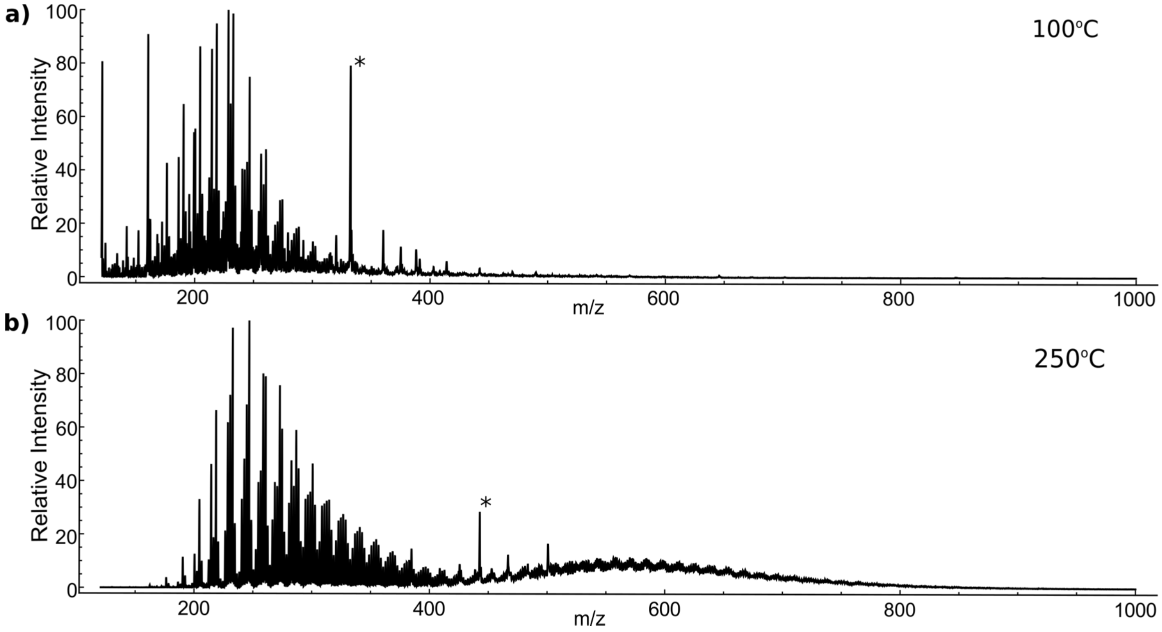

Figure 2.5. EZ-DART mass spectrum of La Brea Tar Pits asphalt taken at a) 100°C b) 250°C. An asterisk indicates background ions.

These EZ-DART spectra were compared to an ESI spectrum of the same sample, the procedure and spectrum for which are provided in the Supplemental Information. Interestingly, the peaks detected in the EZ-DART spectrum were mostly even mass ions, indicating incorporation of an odd number of nitrogen, whereas the ESI peaks were odd masses, possibly indicating the detection of different components or adducts in the sample with each method. The resultant CID spectra for the EZ-DART data did not display losses of 17 or 18 mass units, which would have been indicative of ammonia or water adducts, respectively. This suggests that the detection of species with nitrogen is not related to adduct formation during EZ-DART analysis, but instead a fundamental difference in species detected between ESI and DART.

The difference in the mass envelopes is another indication of deviation between species detected by ESI and EZ-DART. The ESI spectrum shows a more continuous increase in mass over the entire region, with only a few peaks dominating the spectrum. The EZ-DART spectrum shows two distinct envelopes, for which the lower mass envelope at 250°C shows smaller envelopes with Δm/z of 14 or 16 Da, which suggests oxidized species with varying numbers of carbonyl and hydroxyl groups. These factors are suggestive that ESI and EZ-DART combined could provide a much more thorough and complete characterization of a complex organic mixture than either technique alone.

These data show that the EZ-DART allows for the ionization and detection of species with varying volatilities present in complex organic mixtures through TPD analysis. The changes with increasing temperature in the observed mass spectra are consistent with increasingly lower volatility compounds being introduced into the vapor phase, in agreement with previous TPD DART studies.[70] TPD-based DART characterization is a technique readily and effectively utilized with the EZ-DART source.

2.4.4 Reagent Assisted Desorption Ionization

The use of gas phase chemical modification has been a part of DART analyses since the original work by Cody et al in 2005. In these studies dichloromethane and trifluoroacetic acid were used as dopants to enhance the negative ion signal for analytes of interest.[45] Other studies have used chloroform to similar effect.[48] Studies of alcohols by DART utilized an adduct with superoxide produced during sampling.[76] The commonly observed ammonia adduct has been enhanced to advantage by the introduction of ammonia vapor. These types of chemical modification with DART have focused on adducts created through the introduction of gas phase vapors.

The formation of chemically modified analytes during sampling has also been extensively used in the case of reactive DESI. These experiments can differ from those seen with DART with the involvement of either covalent derivatization, such as fixed charge derivatization with betaine aldehyde[50] and ketone modification with hydroxylamine,[54] or non-covalent complexation, such as dicationic pairing[51, 52] and other supramolecular host-guest complexes.[53] DART detection of organometallic compounds have involved some similar experiments by mixing the ligand and metal together prior to sampling,[77, 78] and gas phase chemical reactions have been induced by low temperature plasma,[79, 80] showing the potential for host-guest supramolecular chemistry with DART. Drawing from these experiments, we introduce the concept of using host-guest based supramolecular complexation chemistry directly in the gas phase, termed here reagent assisted desorption ionization (RADI), specifically for the enhanced detection of neurotransmitters.

Several neurotransmitters were chosen for the initial testing of RADI, all of which contain a primary amine functionality along with considerable interest in detecting these molecules in neurological and other tissues. These include serotonin, norepinephrine, dopamine, and gamma-aminobutyric acid (GABA). These small molecules are usually detected through covalent derivatization in MALDI analysis of tissues[81] and chromatographic separation techniques[82, 83]. A host-guest chemical system was chosen to examine the detection of all four neurotransmitters alone as well as simultaneously from the same sample.

All four neurotransmitters have a primary amine group that is sterically available, making an ideal target for complexation. 18-crown-6 ether is a proven host for primary amines,[83-85] with three of the oxygen atoms forming strong hydrogen bonds to a protonated amine group, which would stabilize the charge and increase the ease of detection with mass spectrometry. Additionally this interaction is known to be much stronger in the gas phase compared to the solution phase, making it an ideal host to test RADI.[86]

This stronger gas phase interaction is key to the mechanism of RADI. The 18-crown-6 ether and neurotransmitter position in the EZ-DART gas stream were interchangeable; either could be ionized first. This is suggestive that the assistance provided by the 18-crown-6 ether does not occur in the solid phase. The neurotransmitter and the 18-crown-6 ether are most likely both desorbed from the solid into the gas phase. At this point ionization occurs by the typical proposed proton transfer mechanism. Since ionization is occurring in ambient conditions, molecules with higher proton affinity can scavenge protons from the neurotransmitter under typical conditions. The 18-crown-6 ether prevents this behavior by forming a strong complex to the protonated primary amine directly in the gas phase, protecting it from any proton scavengers prior to detection. As such, RADI can expand the applicability of the EZ-DART source for what may otherwise be difficult analyses

Initially all four neurotransmitters were tested individually and together to determine their respective spectra and relative intensity without the 18-crown-6 ether. These are shown in figure 2.6a-e. The spectra for the serotonin and norepinephrine samples have a high background signal, with a few background peaks observed for the dopamine sample and none for the GABA sample. The protonated species is identifiable above background in all individual neurotransmitters except for norepinephrine, which shows a water loss as the major peak. Products of dehydration and ammonia elimination reactions are observed with the DART analysis of neurotransmitters; this supports the analogy to APCI ionization mechanisms. While these losses are understood, they would complicate the analysis of neurotransmitters in a biological matrix.

The testing of the four neurotransmitters mixed as a solid, shown in figure 2.6e, shows that the sampling of multiple neurotransmitters simultaneously also presents problems. Protonated GABA appears to be the most intense species, likely due to its small size and simple functionality relative to the other neurotransmitters. While background ions and an extremely small intensity signal for dopamine are seen, there is no evidence of serotonin or norepinephrine in the sample. The competition from both protonated and dehydrated GABA when examining the mixture shows that DART alone is not sufficient to perform a complete analysis. Discrimination may be a serious problem when comparing analytes with slightly varying volatilities and proton affinities.

Next the 18-crown-6 ether host-guest interaction was tested with the four neurotransmitters individually and in a solid mixture, shown in figure 2.6f-j. The introduction of the 18-crown-6 ether separately from the neurotransmitter allowed for the confirmation of the complex formation in the gas phase. The abundance of ammonia seen in gas phase DART spectra combined with its affinity for complexation with 18-crown-6 ether makes it a competitive guest for the crown ether relative to the neurotransmitter. This competition could decrease formation of the complex of interest. While ammonia adduction was observed in each case, adduction of the 18-crown-6 ether to the neurotransmitters was still seen. Since both the neurotransmitter and 18-crown-6 ether are desorbed as neutrals, the formation of the complex would require the neurotransmitter to become ionized through the typical proton transfer mechanisms. While that process is occurring, ambient ammonia is also being protonated, with which the 18-crown-6 ether forms an extremely stable complex. The concurrent nature of the ionization helps to explain the prevalence of the ammonia complex compared to the analyte.

The protonated and ammoniated 18-crown-6 ether was the most abundant species for serotonin, norepinephrine and dopamine, while the adducted neurotransmitter was most abundant for GABA. Complexation was seen exclusively to the protonated ion, with no water or ammonia losses observed for any of the adducted neurotransmitters. The mechanisms impacting the relative abundance for each species is likely related to their overall structure. While all four neurotransmitters contain a primary amine, the steric hindrance around that primary amine differs for each molecule. GABA contains the most accessible primary amine, with dopamine being the next most accessible, and norepinephrine being the least with the hydroxyl group in close proximity. While this explains the relative abundance trend for these three neurotransmitters, serotonin displays a different behavior even though the primary amine has similar accessibility to dopamine. The presence of a secondary amine in the ring for serotonin presents an additional protonation site less likely to complex to the 18-crown-6 ether, decreasing the chance for complex formation.

All four neurotransmitters also display a signal enhancement when compared to the unfragmented and uncomplexed ion. This enhancement trends differently than the overall intensities. GABA and serotonin both only display an increase of one order of magnitude in the signal/noise ratio from the uncomplexed spectrum. Dopamine shows an increase of three orders of magnitude and norepinephrine an increase of two orders of magnitude. While not all of these increases are significant, the increase in the mixed sample is incredibly pronounced, where both serotonin and norepinephrine are indistinguishable from the noise without the 18-crown-6 ether complexation. Thus we can see that RADI using 18-crown-6 ether increases detection relative to background, simplifies the spectra, and allows for the simultaneous detection of all four transmitters from the same sample.

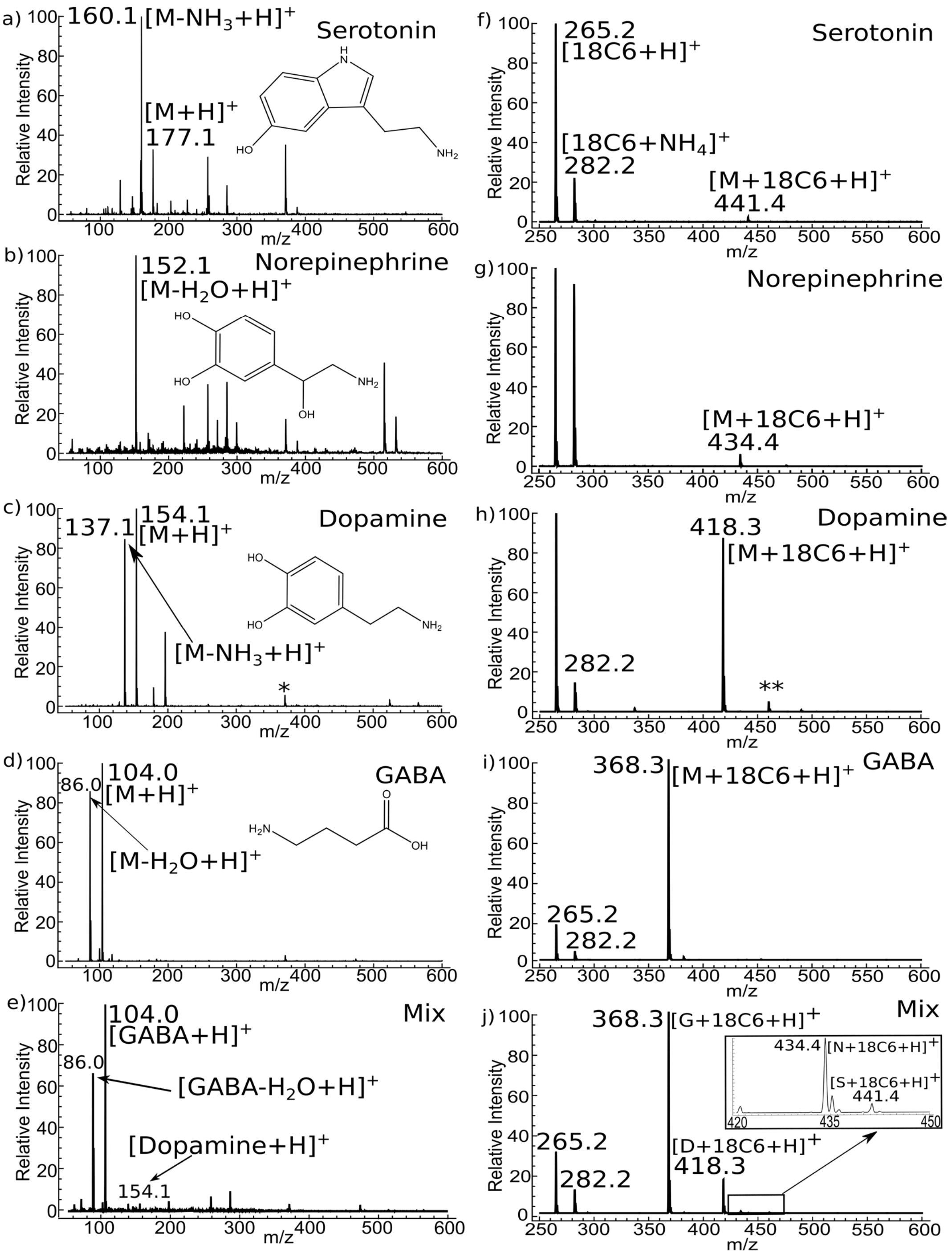

Figure 2.6. a-e: Spectra of each neurotransmitter and mixture of all four neurotransmitters. A single asterisk refers to background ions while a double asterisk refers to sample impurities. f-j: Spectra of each neurotransmitter and mixture of all four with 18-crown-6 ether sampled separately in the EZ-DART gas stream. All spectra were taken at 250°C EZ-DART gas temperature.

More host-guest systems will need to be tested for the application of RADI to the detection of other functional groups. The current method using 18-crown-6 ether could be applied to the detection of neurotransmitters and other difficult to detect analytes with primary amines in a multitude of different samples of biological relevance. Since the 18-crown-6 ether host guest system simplifies the spectra and enhances the detection of targeted samples, it is reasonable to think that this method could be applied to imaging applications, considering that reactive DESI has been successfully applied in this way before.[87]

2.5 Conclusions

An inexpensive and versatile home-built DART source has been developed as an easily assembled device enabling versatile capabilities. The ability to interface the EZ-DART to mass spectrometers equipped with an atmospheric pressure inlet and the enhanced analytical possibilities from CID allow for its application to multiple relevant applications by a variety of user groups. Additionally the use of reagent assisted desorption ionization (RADI) opens up the use of DART sampling to other complex organic mixtures and new analytical applications.

2.6 Acknowledgements

The research was funded by NSF award number CHE-1508825. The early part of this work was funded by NASA Astrobiology Institute, Titan as a Prebiotic Chemical System and the Keck Institute for Space Studies, Future Missions to Titan: Scientific and Engineering Challenges. K.T.U. acknowledges financial support from the Harriett Jenkins

Pre-Doctoral Fellowship Program. The authors would like to thank Mike Uribe Productions for the EZ-DART photographs and the Caltech Glass Shop for assistance with manufacture of the EZ-DART source.

2.7 References

1. A. Bodzon-Kulakowska and P. Suder, *Mass Spectrometry Reviews*, 2016, **35**, 147-169.
2. X. Ding and Y. Duan, *Mass Spectrometry Reviews*, 2015, **34**, 449-473.
3. M. E. Monge, G. A. Harris, P. Dwivedi and F. M. Fernández, *Chem. Rev.*, 2013, **113**, 2269-2308 DOI: 10.1021/cr300309q
4. C. Wu, A. L. Dill, L. S. Eberlin, R. G. Cooks and D. R. Ifa, *Mass Spectrometry Reviews*, 2013, **32**, 218-243.
5. G. A. Harris, A. S. Galhena and F. M. Fernández, *Analytical Chemistry*, 2011, **83**, 4508-4538.
6. L. Zhang, W. Yong, J. Liu, S. Wang, Q. Chen, T. Guo, J. Zhang, T. Tan, H. Su and Y. Dong, *J Am Soc Mass Spectrom*, 2015, **26**, 1414-1422.
7. E. S. Roberts, B. A. Boudreau, D. W. Brown, K. L. McQuade and E. E. Remsen, *Analytical Methods*, 2016, **8**, 673-681.
8. M. J. Pavlovich, E. E. Dunn and A. B. Hall, *Rapid Communications in Mass Spectrometry*, 2016, **30**, 1123-1130.
9. Z. Li, Y.-W. Zhang, Y.-D. Zhang, Y. Bai and H.-W. Liu, *Analytical Methods*, 2015, **7**, 86-90.

10. O. S. Ovchinnikova and G. J. Van Berkel, *Rapid Communications in Mass Spectrometry*, 2010, **24**, 1721-1729.
11. J. P. Williams, V. J. Patel, R. Holland and J. H. Scrivens, *Rapid Communications in Mass Spectrometry*, 2006, **20**, 1447-1456.
12. M. E. Monge, P. Dwivedi, M. Zhou, M. Payne, C. Harris, B. House, Y. Juggins, P. Cizmarik, P. N. Newton, F. M. Fernández and D. Jenkins, *PloS one*, 2014, **9**, e95353.
13. J. L. Easter and R. R. Steiner, *Forensic Science International*, 2014, **240**, 9-20.
14. E. A. Prokudina, J. Prchalová, E. Vyšatová, M. Kuchař, A. Rajchl and O. Lapčík, *International Journal of Mass Spectrometry*, 2015, **392**, 28-33.
15. S. Kumar, V. Bajpai, A. Singh, S. Bindu, M. Srivastava, K. B. Rameshkumar and B. Kumar, *Analytical Methods*, 2015, **7**, 6021-6026.
16. L. S. Eberlin, R. Haddad, R. C. Sarabia Neto, R. G. Cosso, D. R. J. Maia, A. O. Maldaner, J. J. Zacca, G. B. Sanvido, W. Romao, B. G. Vaz, D. R. Ifa, A. Dill, R. G. Cooks and M. N. Eberlin, *Analyst*, 2010, **135**, 2533-2539.
17. J. H. Kennedy, C. Aurand, R. Shirey, B. C. Laughlin and J. M. Wiseman, *Analytical Chemistry*, 2010, **82**, 7502-7508.
18. E. Sisco and T.P. Forbes, *Analyst*, 2015. **140**, 2785-2796.
19. T. P. Forbes and E. Sisco, *Analytical Methods*, 2015, **7**, 3632-3636.
20. E. Sisco, J. Dake and C. Bridge, *Forensic Science International*, 2013, **232**, 160-168.
21. J. M. Nilles, T. R. Connell, S. T. Stokes and H. Dupont Durst, *Propellants, Explosives, Pyrotechnics*, 2010, **35**, 446-451.
22. M. A. Marino, B. Voyer, R. B. Cody, A. J. Dane, M. Veltri and L. Huang, *Journal of Forensic Sciences*, 2016, **61**, S82-S91.

23. R. Williamson, A. Raeva and J. R. Almirall, *Journal of Forensic Sciences*, 2016, **61**, 706-714.

24. J. LaPointe, B. Musselman, T. O’Neill and J. R. E. Shepard, *Journal of The American Society for Mass Spectrometry*, 2015, **26**, 159-165.

25. R. A. Musah, A. D. Lesiak, M. J. Maron, R. B. Cody, D. Edwards, K. L. Fowble, A. J. Dane and M. C. Long, *Plant physiology*, 2016, **170**, 1075-1089.

26. E. Sisco and J. Dake, *Analytical Methods*, 2016, **8**, 2971-2978.

27. T. T. Häbe and G. E. Morlock, *Journal of Chromatography A*, 2015, **1413**, 127-134.

28. Á. Kuki, L. Nagy, T. Nagy, M. Zsuga and S. Kéki, *Atmospheric Environment*, 2015, **100**, 74-77.

29. J. H. Gross, *J Am Soc Mass Spectrom*, 2015, **26**, 511-521.

30. Á. M. Móricz, T. T. Häbe, A. Böszörményi, P. G. Ott and G. E. Morlock, *Journal of Chromatography A*, 2015, **1422**, 310-317.

31. A. D. Lesiak, R. B. Cody, A. J. Dane and R. A. Musah, *Analytical Chemistry*, 2015, **87**, 8748-8757.

32. Y.-q. Song, J. Liao, C. Zha, B. Wang and C. C. Liu, *Analytical Methods*, 2015, **7**, 1600-1605.

33. Y. Wang, S. Liu, Y. Hu, P. Li and J.-B. Wan, *RSC Advances*, 2015, **5**, 78728-78737.

34. M. F. Mirabelli, G. Coviello and D. A. Volmer, *Analytical and bioanalytical chemistry*, 2015, **407**, 4513-4522.

35. M. Li, H. Chen, B.-F. Wang, X. Yang, J.-J. Lian and J.-M. Chen, *International Journal of Mass Spectrometry*, 2009, **281**, 31-36.

36. M. N. Chan, T. Nah and K. R. Wilson, *Analyst*, 2013, **138**, 3749-3757.

37. Y. Zhao, L. M. Wingen, V. Perraud and B. J. Finlayson-Pitts, *Atmos. Chem. Phys.*, 2016, **16**, 3245-3264.

38. S. M. Jones, M. S. Anderson, A. G. Davies, J. P. Kirby, M. J. Burchell and M. J. Cole, *Icarus*, 2015, **247**, 71-76.

39. S. Zhou, M. W. Forbes and J. P. D. Abbatt, *Analytical Chemistry*, 2015, **87**, 4733-4740.

40. K. Qian, K. E. Edwards, J. H. Diehl and L. A. Green, *Energy & Fuels*, 2004, **18**, 1784-1791.

41. W. Romao, L. V. Tose, B. G. Vaz, S. G. Sama, R. Lobinski, P. Giusti, H. Carrier and B. Bouyssiere, *J Am Soc Mass Spectrom*, 2016, **27**, 182-185.

42. V. V. Lobodin, L. Nyadong, B. M. Ruddy, M. Curtis, P. R. Jones, R. P. Rodgers and A. G. Marshall, *International Journal of Mass Spectrometry*, 2015, **378**, 186-192.

43. Z. Takáts, J. M. Wiseman, B. Gologan and R. G. Cooks, *Science*, 2004, **306**, 471-473.

44. M. C. Wood, D. K. Busby and P. B. Farnsworth, *Analytical Chemistry*, 2009, **81**, 6407-6415.

45. R. B. Cody, J. A. Laramée and H. D. Durst, *Analytical Chemistry*, 2005, **77**, 2297-2302.

46. M. Smoluch, P. Mielczarek and J. Silberring, *Mass Spectrometry Reviews*, 2016, **35**, 22-34.

47. G. A. Harris, D. M. Hostetler, C. Y. Hampton and F. M. Fernández, *Journal of the American Society for Mass Spectrometry*, 2010, **21**, 855-863.

48. M. C. Bridoux, A. Schwarzenberg, S. Schramm and R. B. Cole, *Analytical and Bioanalytical Chemistry*, 2016, **408**, 5677-5687.

49. A. H. Grange and G. W. Sovocool, *Rapid Communications in Mass Spectrometry*, 2011, **25**, 1271-1281.

50. C. Wu, D. R. Ifa, N. E. Manicke and R. G. Cooks, *Analytical Chemistry*, 2009, **81**, 7618-7624.
51. D. Lostun, C. J. Perez, P. Licence, D. A. Barrett and D. R. Ifa, *Analytical Chemistry*, 2015, **87**, 3286-3293.
52. W. Rao, D. Mitchell, P. Licence and D. A. Barrett, *Rapid Communications in Mass Spectrometry*, 2014, **28**, 616-624.
53. J. E. Barbara, J. R. Eyler and D. H. Powell, *Rapid Communications in Mass Spectrometry*, 2008, **22**, 4121-4128.
54. G. Xu, B. Chen, G. Liu and S. Yao, *Analyst*, 2010, **135**, 2415-2419.
55. T. T. Häbe and G. E. Morlock, *Rapid Communications in Mass Spectrometry*, 2016, **30**, 321-332.
56. E. S. Chernetsova and G. E. Morlock, *Rapid Communications in Mass Spectrometry*, 2015, **29**, 1242-1252.
57. F. M. Fernández, R. B. Cody, M. D. Green, C. Y. Hampton, R. McGready, S. Sengaloundeth, N. J. White and P. N. Newton, *ChemMedChem*, 2006, **1**, 702-705.
58. P. N. Newton, M. D. Green, D. C. Mildenhall, A. Plançon, H. Nettey, L. Nyadong, D. M. Hostetler, I. Swamidoss, G. A. Harris, K. Powell, A. E. Timmermans, A. A. Amin, S. K. Opuni, S. Barbereau, C. Faurant, R. C. W. Soong, K. Faure, J. Thevanayagam, P. Fernandes, H. Kaur, B. Angus, K. Stepniewska, P. J. Guerin and F. M. Fernández, *Malaria Journal*, 2011, **10**, 352-352.
59. B. Kasprzyk-Hordern, R. M. Dinsdale and A. J. Guwy, *Journal of Chromatography A*, 2007, **1161**, 132-145.

60. T. Ternes, M. Bonerz and T. Schmidt, *Journal of Chromatography A*, 2001, **938**, 175-185.
61. R. A. Musah, R. B. Cody, A. J. Dane, A. L. Vuong and J. R. E. Shepard, *Rapid Communications in Mass Spectrometry*, 2012, **26**, 1039-1046.
62. R. R. Steiner and R. L. Larson, *Journal of Forensic Sciences*, 2009, **54**, 617-622.
63. B. Antal, Á. Kuki, L. Nagy, T. Nagy, M. Zsuga and S. Kéki, *Analytical and bioanalytical chemistry*, 2016, **408**, 5189-5198.
64. R. Sleeman, F. Burton, J. Carter, D. Roberts and P. Hulmston, *Analytical Chemistry*, 2000, **72**, 397 A-403 A.
65. A. J. Jenkins, *Forensic Science International*, 2001, **121**, 189-193.
66. K. A. S. Fahnestock, L. D. Yee, C. L. Loza, M. M. Coggon, R. Schwantes, X. Zhang, N. F. Dalleska and J. H. Seinfeld, *J. Phys. Chem. A*, 2015, **119**, 4281-4297, DOI: 10.1021/jp501779w
67. J. Adams, International Journal of Mass Spectrometry, 2011, **301**, 109-126.
68. E. O. Espinoza, C. A. Lancaster, N. M. Kreitals, M. Hata, R. B. Cody and R. A. Blanchette, *Rapid Communications in Mass Spectrometry*, 2014, **28**, 281-289.
69. R. B. Cody, A. J. Dane, B. Dawson-Andoh, E. O. Adedipe and K. Nkansah, *Journal of Analytical and Applied Pyrolysis*, 2012, **95**, 134-137.
70. J. M. Nilles, T. R. Connell and H. D. Durst, *Analyst*, 2010, **135**, 883-886.
71. Y.-H. Liu, S. Takeda, I. Kaneko, H. Yoshitake, M. Yanagida, Y. Saito and T. Sakai, *Electrochemistry Communications*, 2015, **61**, 70-73.
72. E. Sisco, T. P. Forbes, M. E. Staymates and G. Gillen, *Analytical Methods*, 2016, **8**, 6494-6499.

73. H. Yang, L. Shi, W. Yao, Y. Wang, L. Huang, D. Wan and S. Liu, *Journal of The American Society for Mass Spectrometry*, 2015, **26**, 1599-1605.
74. T. Nah, M. Chan, S. R. Leone and K. R. Wilson, *Analytical Chemistry*, 2013, **85**, 2087-2095.
75. J. L. Rummel, A. M. McKenna, A. G. Marshall, J. R. Eyler and D. H. Powell, *Rapid Communications in Mass Spectrometry*, 2010, **24**, 784-790.
76. J. A. Laramee, H. D. Durst, J. M. Nilles and T. R. Connell, *Am. Lab.*, 2009, **41**, 24–27.
77. Q. Zhang, J. Bethke and M. Patek, *International Journal of Mass Spectrometry*, 2014, **374**, 39-43.
78. M. G. Mazzotta, J. O. E. Young, J. W. Evans, L. A. Dopierala, Z. A. Claytor, A. C. Smith, C. Snyder, N. C. Tice and D. L. Smith, *Analytical Methods*, 2015, **7**, 4003-4007.
79. W. Zhang and G. Huang, *Rapid Communications in Mass Spectrometry*, 2015, **29**, 1947-1953.
80. M. Benassi, J. F. Garcia-Reyes and B. Spengler, *Rapid Communications in Mass Spectrometry*, 2013, **27**, 795-804.
81. M. L. Manier, J. M. Spraggins, M. L. Reyzer, J. L. Norris and R. M. Caprioli, *Journal of Mass Spectrometry*, 2014, **49**, 665-673.
82. A. Zapata, V. I. Chefer, T. S. Shippenberg and L. Denoroy, *Curr Protoc Neurosci*, 2009, **Chapter 7**, Unit 7 4 1-30.
83. M. Moini, C. L. Schultz and H. Mahmood, *Analytical Chemistry*, 2003, **75**, 6282-6287.
84. B. L. Williamson and C. S. Creaser, *International Journal of Mass Spectrometry*, 1999, **188**, 53-61.
85. A. Spath and B. Konig, *Beilstein journal of organic chemistry*, 2010, **6**, 32.

86. R. R. Julian and J. L. Beauchamp, *International Journal of Mass Spectrometry*, 2001, **210–211**, 613-623.

87. J. M. Wiseman, D. R. Ifa, Y. Zhu, C. B. Kissinger, N. E. Manicke, P. T. Kissinger, R. G. Cooks, *Proceedings of the National Academy of Sciences*, 2008, **105**, 18120-18125.

2.8 Supplemental Information

2.8.1 Maleic Acid Data

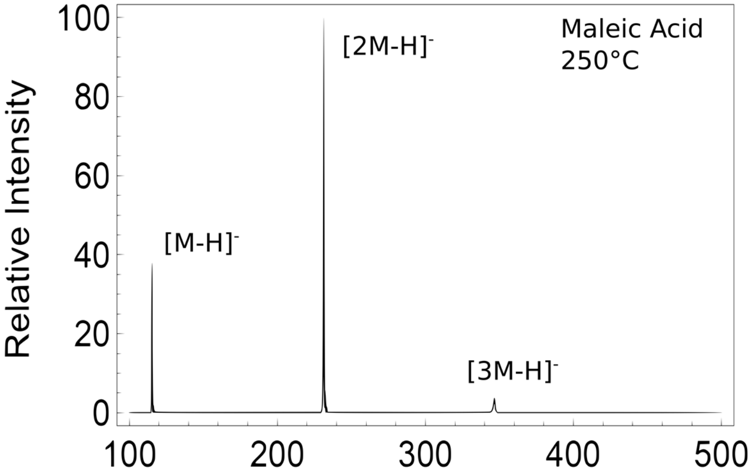

Figure 2.7 Spectrum of maleic acid in negative mode showing the deprotonated monomer, dimer, and trimer. The temperature refers to the measured heating tape temperature.

2.8.2 CID Data for Currency

An EZ-DART spectrum was taken for both fifty (figure 2.8a) and twenty (figure 2.3 and figure 2.8c) dollar notes, both of which had been in circulation prior to testing. The methamphetamine identification was supported by the CID data for the 150.1 m/z peak,[1] shown in figure 2.8b, from the fifty dollar note. The cocaine identification was supported by the CID data for the 304.4 m/z peak,[2] shown in figure 2.8d, from the 20 dollar note. Structures for both are shown in figure 2.8c and their respective CID spectra. While the both notes displayed each peak, identification required separate CID spectra due to the relative intensities being insufficient to obtain CID data from a single currency note. Due to the large number of peaks and high amount of background signal observed from the 50 dollar note, additional identifications were not pursued.

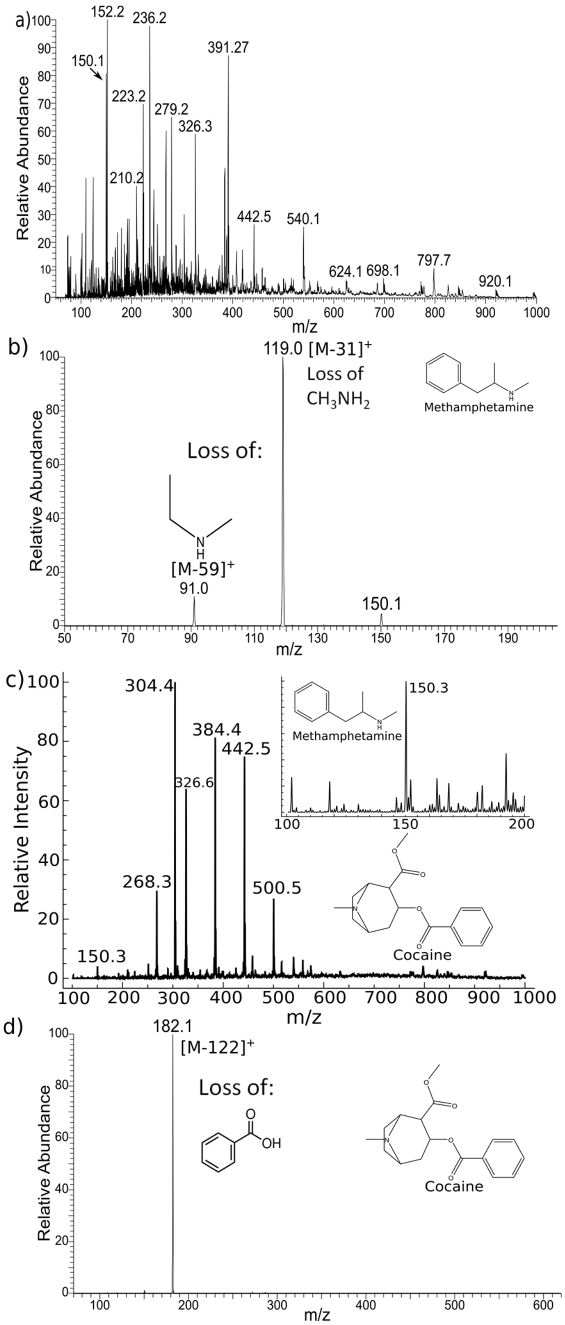

Figure 2.8 a) The overall spectrum of the 50 dollar bill. b) CID spectrum for protonated methamphetamine from a 50 dollar bill. The loss of 31 corresponds to a loss of CH_3NH_2 and the loss of 59 to a loss of C_3H_8NH c) The overall spectrum for the 20 dollar bill as shown in figure 2.3. d) CID spectrum for protonated cocaine from the 20 dollar bill. The loss of 122 corresponds to a loss of benzoic acid. The targeted m/z values for each CID spectra are indicated on the side.

2.8.3 LOD Determination for RDX

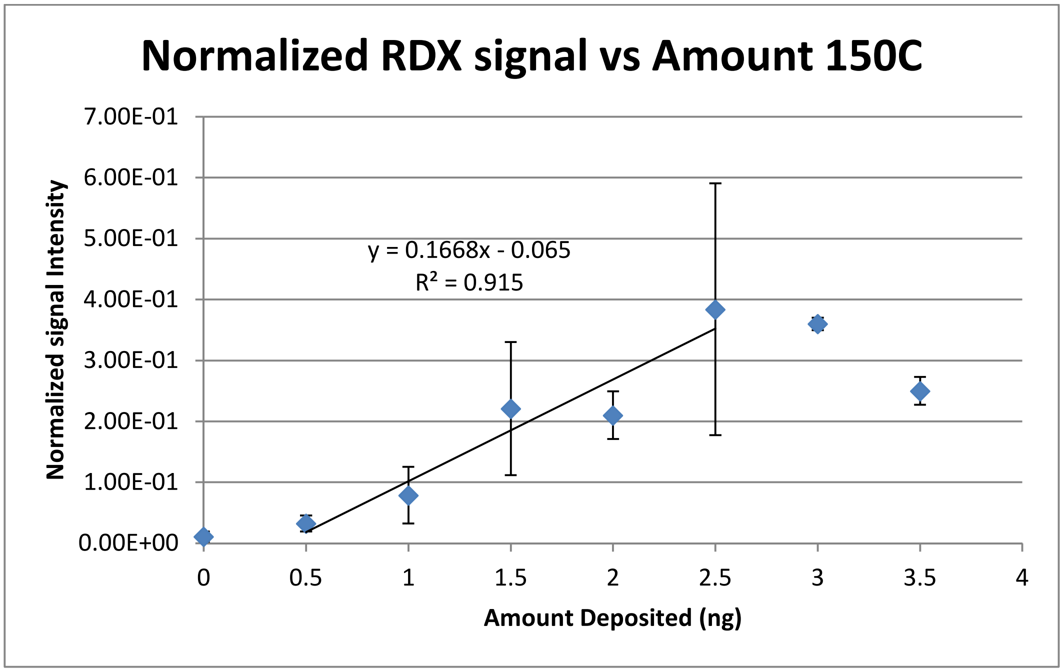

Figure 2.9 Calibration curve of RDX used for the determination of the LOD for RDX. Signal response was normalized to the background peak for palmitic acid.

The lower limit of detection calculation for RDX with an R2 of 0.915. The LOD of 1.1ng was calculated using linear regression analysis.[3] 2.5ng was found to be the limit of linearity for the calibration curve.

The calibration's linearity is observed to drop at higher concentrations, possibly due to the signal for the RDX in these data being normalized to the highest background signal. The drop in linearity may be related to increasing ionization of the background normalization ion with the higher concentrations due to increasing amounts of solvent during standard deposition, as well as the overlap between the sample and the DART region of desorption and ionization. A combination of these two effects could account for the observed loss of linearity. While cluster ion formation has been observed with RDX, such clusters were not observed at higher mass for any amount of RDX used in our experiments.

2.8.4 PPG Data and Discussion

In addition to the La Brea Tar Pit hydrocarbon sample described in the text, Poly(propylene glycol) (PPG) was used for a TPD study, due to the high number of possible ion species which follow an easily interpreted pattern. The average mass of desorbed and ionized PPG molecules detected in the EZ-DART spectrum was calculated for a temperature ramped from 60°C to 250°C, showing an overall linear relationship. Since there were few noticeable changes in average mass at and below 60°C, the lower temperatures were not examined in detail. The mass spectra of PPG at 60°C, 150°C, and 250°C are shown in Figure 2.10, highlighting the temperature-dependent shifting of the mass envelope. Identification of the observed ion species was performed using MS3, shown below.

The stability of the ion current during the temperature ramp suggests that the overall ionization efficiency is not significantly impacted by temperature for a more complex sample. Additionally, these data show that even at elevated temperatures, the only observed species are of mass less than 1000 Da. For this PPG sample, where the average mass is 2700 amu, analysis by EZ-DART does not seem to be appropriate for characterization of the entire polymer, but does provide characterization for the lower molecular weight components in the distribution. The effect of temperature on the detected average mass for PPG has implications for the analysis of other complex organic mixtures with varying volatility. The near complete loss of species under 200 Da at a typical DART operating temperature of 250°C indicates that when performing analysis with the EZ-DART on a complex organic mixture, the temperature must carefully be considered if characterization of both low and mid mass species is desired. From these results, it appears that having the ability to perform TPD analysis enables the possible targeting of compounds with variable volatility when performing the analysis of a complex organic mixture with the EZ-DART.

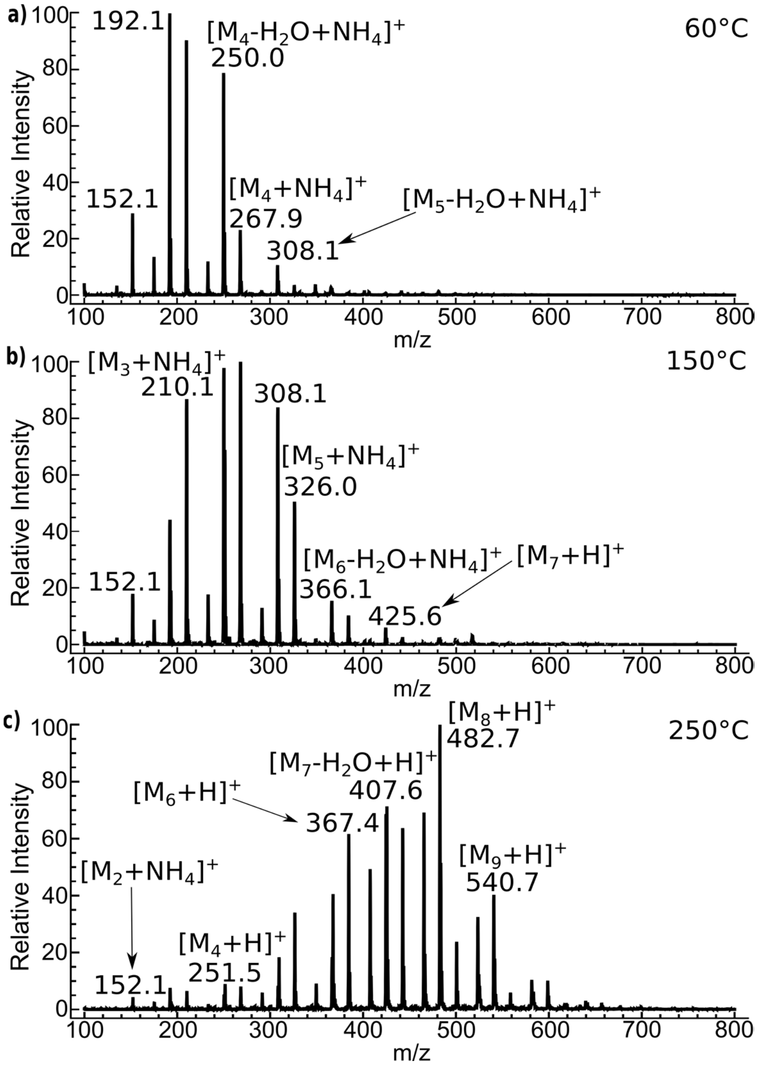

Figure 2.10. Spectrum of PPG with subunit count labeled as M_X and relevant adducts labeled.

The identification of each species present in the PPG spectra was further supported by the presence of adduct species. The additional possible in-source dehydration reactions and heterogeneous dimerization can make the identification of the specific monomer involved in a peak difficult, especially with unit-mass resolution mass spectral data. To assist with data interpretation the most abundant species in the spectra were targeted for CID analysis. An automated multistep CID program was used, targeting the most abundant species for CID. Initial CID removed the adducting molecule or separated a dimer, and subsequent CID allowed for the confirmation of the species involved, sample spectra for which are shown below. The use of the software based CID procedure allowed for simple identification of each species with changes in temperature.

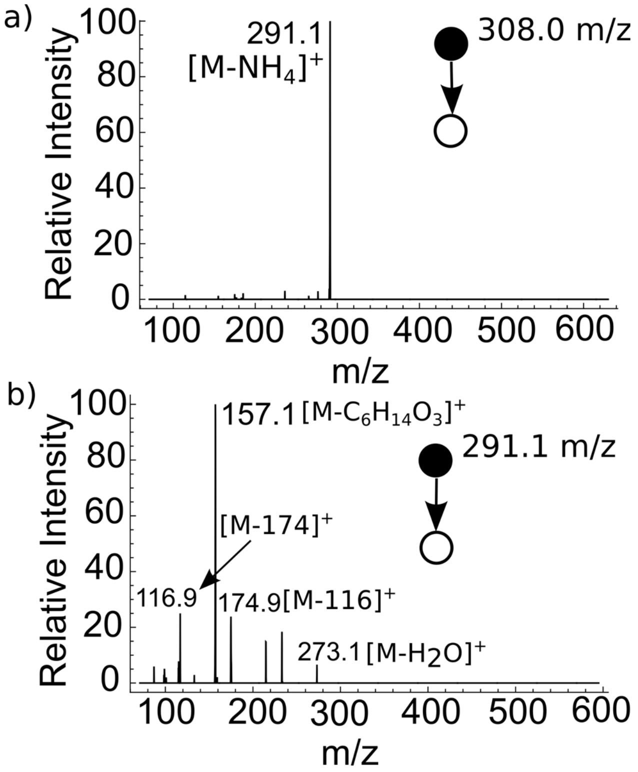

Figure 2.11 a) The CID spectrum of 308 m/z at 150°C showing only the loss of ammonia b) The subsequent CID of 291.1 from a, showing multiple losses. These losses correspond to the losses of different monomer units. The targeted m/z values for each CID spectra are indicated on the side.

2.8.5 ESI Spectrum and Method Discussion for La Brea Tar Pits Sample

Approximately 2 grams of tar was mostly dissolved in 20 mL of 50/50 methanol/toluene solution. The solubilized fraction was then diluted by 1:10 in 100% methanol twice serially. This solution was then electrosprayed, providing the spectrum observed below.

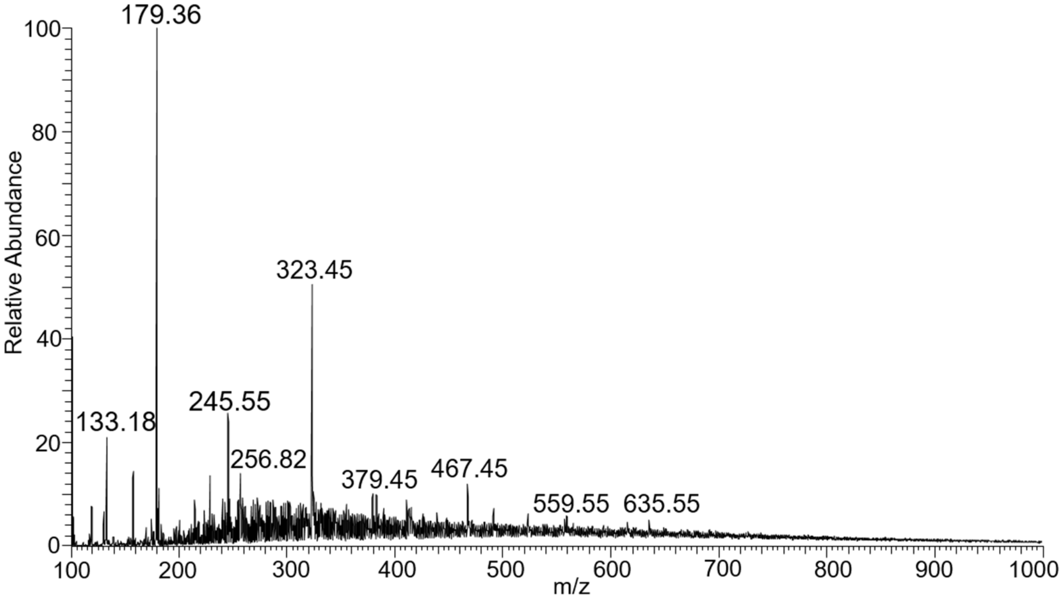

Figure 2.12 The electrospray mass spectrum for dissolved tar.

2.8.6 Supplemental Information References

1. H. P. Hendrickson, A. Milesi-Hallé, E. M. Laurenzana and S. M. Owens, Journal of Chromatography B, 2004, 806, 81-87.
2. B. Hu, X. Peng, S. Yang, H. Gu, H. Chen, Y. Huan, T. Zhang and X. Qiao, Journal of the American Society for Mass Spectrometry, 2010, 21, 290-293.
3. M. M. Sanagi, S. L. Ling, Z. Nasir, D. Hermawan, W. A. W. Ibrahim and A. Abu Naim, Journal Of AOAC International, 2009, 92, 1833-1838.

Chapter 3

THE TITAN HAZE SIMULATION (THS) EXPERIMENT ON COSMIC PART III: EX-SITU ANALYSIS OF AEROSOLS USING DIRECT ANALYSIS IN REAL TIME MASS SPECTROMETRY (DART-MS)

3.1 Abstract

In this work, we present the results of a new ex situ diagnostic, Direct Analysis in Real Time Mass Spectrometry (DART-MS), on the solid phase samples produced in the Titan Haze Simulation (THS) experiment. This study is the next step in the analysis of the THS Titan aerosol simulants, complementing and following up on the gas phase study introducing the THS experiment (Part I) and the initial solid phase analysis by infrared (IR) spectroscopy and Scanning Electron Microscopy (SEM) (Part II). The THS experiment provides a unique simulation of Titan's atmosphere by inducing chemical reactions in N_2-CH_4-based gas mixtures over short timescales, using a pulsed plasma discharge in the stream of a jet-cooled expansion. By generating a pulsed plasma in an expanded gas, the chemistry occurs at Titan-like temperatures (~150-200K) and is truncated. The THS experiment can be tested with a range of mixtures, from N_2 and CH_4 to mixtures containing heavier molecules detected in Titan's atmosphere. The results of this study show, as expected from Part I and Part II, that the chemistry induced in the THS experiment can be considered a good analog of Titan's early and intermediate atmospheric chemistry, and allows one to study specific chemical pathways. This analysis is the first study of Titan aerosol simulants

utilizing DART-MS, and as such also allowed to demonstrate the interest of the DART technique for future analyses and preparation of future missions. This analytical technique enables the study of samples with minimal preparation or pre-processing, making it advantageous for the analysis of complex organic mixtures. The results presented here provide insight into the effects different dopant molecules, in this case benzene and acetylene, have on the aerosol products. By reviewing these effects, we can obtain a better understanding of the mechanisms that are at play within the THS experiment and possibly Titan's atmosphere.

3.2 Introduction

Since the discovery of complex organic molecules on Titan by Cassini and other missions, the synthesis and characterization of atmospheric aerosols representative of Titan has become a key research target for the astrobiology community [1-7]. Various laboratory simulation experiments have been developed to better understand Titan's atmospheric chemistry. There are four major parameters of Titan's atmosphere that need to be taken into account when simulating the chemistry: a representative gas mixture of nitrogen (90-98%) and methane (2-10%), an energy source representative of solar radiation, low pressures (in Titan's atmospheric region where photochemistry is expected to occur, the pressure can be as low as of 10^{-6}-10^{-7} mbar), and a low temperature of approximately 160-180K.[8-12] Replication of these conditions in laboratory environments is of varying difficulty, with adjustments being typical for experimental optimization. The gas mixture is the simplest factor to modify. The effect of changes on the methane/nitrogen ratio in particular have been well characterized in prior studies.[13, 14] Pressure is the most difficult parameter to simulate accurately in the laboratory, since low pressures extend experimental time scales due to limited collisions, reduced chemistry, and slow accumulation of the aerosol, thus complicating the testing of various characterization methods. As a consequence, pressure used in laboratory experiment is often increased to higher range than Titan's atmosphere.[9, 15, 16]

The energy source used to induce chemistry is the primary origin of variability with laboratory production of Titan aerosol simulants. UV light sources are considered to be the most representative of the photochemical energy sources on Titan, but very few such sources are able to dissociate nitrogen, a key step for chemistry in Titan's atmosphere.[9] Synchrotron experiments can produce high enough energies to dissociate nitrogen but they often use a narrow bandwidth, not representative of the solar energy distribution.[17-19] The SOLEIL synchrotron experiments can generate a radiation distribution representative of the solar spectrum, but these experiments are typically performed at room temperature and have undergone limited solid phase analysis at this point.[17-20] Plasma discharge sources are used to overcome the limitations of nitrogen dissociation with UV,[15, 16, 21, 22] but introduce their own issues. The most common concern with plasma sources is the continuous reaction of the gaseous species and aerosols within the discharge region which could result in over processing of the material, since aerosol accumulation in the majority of these experiments occurs in, or close to, the plasma discharge region.[23]

The Titan Haze Simulation (THS) experiment using the COSmIC facility at the NASA Ames Research Center has previously been shown to overcome many of these concerns.[24, 25] The experiment utilizes a pulsed cold plasma discharge in a gas expansion to generate aerosol simulants, with the ability to add other heavy molecules as desired. There are two factors that make this experimental setup unique: the use of a supersonic expansion to cool the gas mixture down to ~150 K (i.e., representative of Titan) prior to inducing the chemistry by plasma discharge, and the pulsed nature of the plasma, which limits the amount of chemical reactions occurring in the active region of the plasma discharge. This enables the analysis of the first and intermediate steps of the chemistry, as well as the examination of specific chemical pathways. Aerosols are produced in the plasma expansion and then deposited on a substrate placed further down in the stream of the jet-cooled expansion for further ex situ analysis. The products of this experiment have been analyzed in the gas phase for nascent ions through time-of-flight mass spectrometry (TOF-MS), [24] and in the solid phase by scanning electron microcopy (SEM) for characterization of aerosol morphology, and infrared (IR) spectroscopy for identification of functional groups.[25]

Mass spectrometry is complementary to IR spectroscopy for the analysis of complex mixtures with unknown constituents, allowing for the exact identification of some species. In this work, we prioritized the detection of small (< 200 Da), polar, and volatile compounds, due to the expectation of simpler products resulting from the truncated THS chemistry, nitrogen containing molecules being astrobiologically significant, and volatiles being trapped in the solid grain matrix during slow deposition, respectively. The small molecule criteria excluded the use of methods typically well suited for complex organic mixtures, such as Matrix Assisted Laser Desorption Ionization (MALDI), due to their higher molecular weight requirements.[26-28] Gas Chromatography Mass Spectrometry (GC-MS) was not chosen as it is usually employed for non-polar compounds, although a future analysis for hydrocarbon constituents could benefit from this method.[29, 30] A pyrolysis mass spectrometry method has recently been applied to Titan aerosol simulants produced at SOLEIL using Photoelectron Spectroscopy (PES).[20] However, while isomers were readily identified for many compounds, there are limitations to this technique from the lack of reference spectra and increased structural isomers for molecules of masses greater than 70 Da. These considerations have led to the investigation of ambient mass spectrometry techniques for the analysis of the THS samples.

Ambient mass spectrometry comprises a wide range of analytical methodologies by which analyte ions can be produced at atmospheric pressure and then transferred to the vacuum region of a mass spectrometer for subsequent analysis.[31, 32] Ionization methods utilizing ambient mass spectrometry have the benefits of preserving more volatile compounds and being well suited for the analysis of polar molecules. The most common ambient ionization method is electrospray ionization (ESI), a solvent based method. ESI has been used for the analysis of Titan aerosol simulants produced in prior work and allows for the analysis of species up to 2000 Da.[14, 27] The use of solvent based methods for Titan simulant analysis is complicated due to incomplete solvation of the sample in solvents suitable for ESI.[26] Additionally, the preparation of the sample can lead to the loss of volatile constituents of interest. Plasma based ambient mass spectrometry has been developed more recently and has been utilized for a wide variety of samples.[33] One particular method, direct analysis in real time (DART), has been successful in the analysis of petroleum samples and simulated organic aerosol.[34-36] For that reason, DART was selected as the ambient ionization method for this study. It is the first time a Titan aerosol simulant has been analyzed with this technique.

As with many ambient mass spectrometric ionization methods, DART performs both desorption of the sample into the gas phase and ionization of the analytes.[37] DART utilizes a corona discharge to produce helium metastables. Upon collision with atmospheric water these metastables create protonated water clusters through Penning ionization. These water clusters then undergo proton transfer with gaseous analyte molecules, desorbed as neutrals by the helium gas, before entering the mass spectrometer.[38] While this proton transfer mechanism is typically dominant, adduct formation with water and ammonia can also be observed, along with the formation of radical cations through direct Penning ionization.[39] In all DART ionization mechanisms, very little fragmentation of the analyte is observed. Additionally, gas temperature can be increased with a heater to amplify the detection of lower volatility molecules.

Detection with DART is dependent on volatility and proton affinity. This has been demonstrated by the difficulty of applying DART ionization to hydrocarbon compounds 40. Even without taking non-polar compounds into account, complex organic mixtures typically contain a variety of DART ionizable molecules. This variety of species introduces competitive ionization, previously observed with DART [41] analyses, where easily ionized molecules suppress the detection of other molecules within a mixture and consequently impact the detection of compounds with low volatilities or proton affinities. Prior studies of Titan aerosol simulants show a similar diversity of compounds with a range of volatilities and proton affinities.[35] This wide assortment of molecules could introduce similar competitive ionization concerns, impacting the detection of molecules within the simulants. However, taking into consideration the similarity between the THS simulants, Earth aerosol simulants, and petroleum samples, as well as prior successful application of DART analysis to the latter two types of samples, the impact of competitive ionization on the analysis should be minimal for the identification of the small, volatile, and polar compounds of interest in this work.

The analysis of THS simulants by DART serves another purpose: a test of the technique's feasibility for future missions. DART is known for its ability to perform an analysis of samples without solvation or other sample processing such as pyrolysis. This implies that DART could be considered as a possible ionization method for future lander missions. To confirm this possibility, a representative Titan aerosol simulant would need to be tested. The SEM study performed on the THS aerosols[25] has shown that the THS aerosol grains are produced in the gas phase and can be jet-deposited onto a substrate for ex situ analysis, and are therefore good analogs of how Titan aerosols would be collected at high speed by a lander during atmospheric descent. This DART study of THS aerosols consequently allows not only for the testing of the DART technique on Titan aerosol simulants for characterization purposes, but also serves as a test feasibility for future missions.

We present here the EZ-DART-MS analysis of THS simulants produced from four gas mixtures, previously analyzed by SEM and IR. The EZ-DART is a home built DART source successfully used in the past in the analysis of other complex organic mixtures.[41] The DART-MS analysis presented here focuses on identifying species present in the samples, and comparing the results to both the THS IR experiments[25] and other Titan simulant studies. The possible implications of the observed compounds for Titan's atmospheric chemistry are also discussed.

3.3 Experimental

3.3.1 COSmIC THS experiment and production of Titan aerosol simulants

The THS experimental setup and the characterization by time-of-flight mass spectrometry of the gas phase chemistry occurring in the plasma have been described in detail in Part I.[24] The description of the production of solid phase samples and their analysis by IR absorption spectroscopy and SEM have been provided in Part II.[25] Here, we present a brief description of the system. The THS experiment utilizes a pulsed plasma expansion, which causes chemical reactions in a jet-cooled gas mixture. This pulsed plasma expansion is generated by a pulsed discharge nozzle (PDN), a representation of which is shown in figure 3.1. In operation, a gas mixture is continuously injected into a copper reservoir where it equilibrates before being released in 1.28ms long pulses through a 127 µm-tall by 100 mm-long slit, cut in a 4.6 mm-thick copper plate (labeled “a” in figure 3.1). This produces a planar supersonic jet expansion with adiabatic gas temperature and pressure drops, enabling cooling of the gas mixture prior to plasma chemistry without the need for other cooling methods. In the subsequent 400 µm x 100 mm slit area (labeled “b” in figure 3.1), cut in a 1.5 mm-thick alumina plate that serves as a dielectric, the pressure and temperature drop to 30 mbar and 150 K, respectively. The plasma discharge that induces the chemistry is generated within this 1.5 mm plasma cavity by applying a pulsed negative voltage (300 µs, 600 V to 1000 V) onto a set of Elkonite (90% tungsten, 10% copper) cathodes placed 400 µm apart, along the slit, on the other side of the alumina plate.

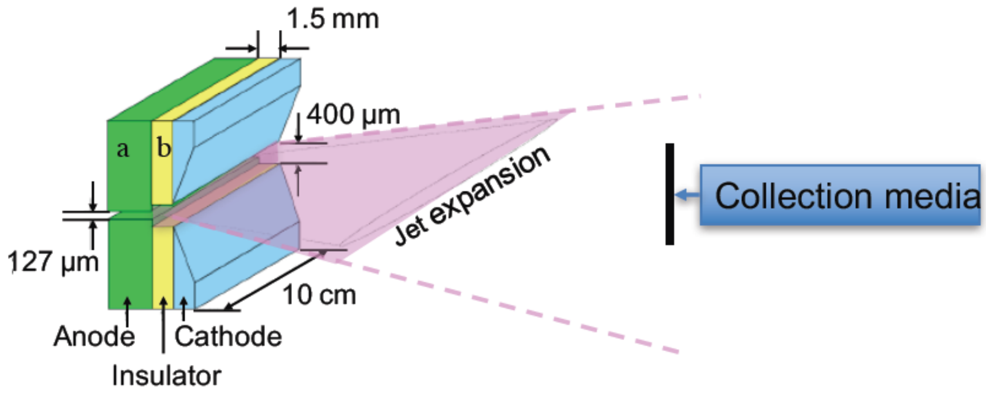

Figure 3.1. Schematics of the THS Pulsed Discharge Nozzle (PDN) and the setup for collection of solid phase samples, 5 cm away from the slit downstream of the PDN. (Schematics of the PDN adapted from Broks et al., 2005)

The characteristics of the cold plasma expansion have been evaluated both computationally and experimentally in prior studies.[25, 42, 43] These investigations have confirmed that the temperature in the plasma cavity is 150 K, without plasma activation, and around 200 K when the plasma is turned on, and remains so even with the addition of methane to the nitrogen gas mixture. In addition, because the gas is accelerated to supersonic speed in the PDN expansion, the residence time of the gas in the active region of the pulsed plasma discharge is on the order of 3 µs, allowing us to control how far the chain of chemical reactions progresses, depending on the precursors present in the initial gas mixture. This controlled or truncated chemistry minimizes concerns of over processing of the aerosols inherent to many other systems using plasma to simulate Titan's chemistry. The cold temperature and truncated chemistry facilitated by the THS experimental setup enable the study of chemical products representative of the early and intermediate stages of Titan's atmospheric chemistry. The addition of larger molecules, detected as trace elements in

Titan's atmosphere, into the initial N_2-CH_4 gas mixture allows for characterization of the effects these molecules have on the aerosol production and composition.

The gas phase experimental results, previously reported in Part I, were measured using an orthogonal reflectron time of flight mass spectrometer (reTOF-MS). For the solid phase studies presented here and in Part II, the reTOF-MS was capped off and rotated out of the chamber, and the chamber was sealed with a flange door. The deposition of the simulants onto substrates and their collection are described below. For the solid phase experiments, four gas mixtures, similar to those studied in Part I, were used to simulate different potential chemical pathways in Titan's atmospheric chemistry: N_2-CH_4 (95-5), N_2-CH_4-C_2H_2 (91-5-4, acetylene), N_2-CH_4-C_6H_6 (90-5-5, benzene), and N_2-CH_4-C_2H_2-C_6H_6 (86-5-4-5, acetylene and benzene). For each run, a ultra-high-purity (UHP, 99.9998%) N_2 gas cylinder and a UHP gas cylinder containing a N_2-CH_4 mixture with 10% + 0.2% CH_4 were used. A methane ratio of 5% was chosen for the solid phase studies (Part II and this study) instead of the 10% used in the gas phase study (Part I), in order to be more representative of Titan's atmosphere, and because the production yield is higher in the THS with 5% CH_4 than 10% CH_4. The protocols for the addition of benzene and acetylene into the N_2-CH_4-based mixtures have been fully explained in Part I. The chosen C_2H_2 and C_6H_6 concentrations are higher than the actual concentrations on Titan. This is done on purpose, in order to enhance and accelerate the chemistry and ensure that the effects of their presence on the solid phase composition are detectable, knowing that only the first and intermediate steps of the chemistry have time to occur in the THS experimental setup due to the short residence time in the plasma discharge. The goal of these experiments is to try and better understand how differences in atmospheric concentration could impact Titan's chemistry.

3.3.2 Collection of THS solid Titan aerosol simulants

The means of deposition and collection of the solid phase products have been described previously in Part II.[25] A summary is presented here. The solid samples collected from the THS experiment for analysis consist of solid grains that are produced in the plasma cavity and then jet-deposited onto a substrate placed within the expansion region approximately 5 cm downstream from the PDN. Figure 3.2c shows an example of THS deposition on aluminum foil. The interference fringes observed can be attributed to variations in deposition thickness.

The THS solid aerosols can be deposited onto different types of substrates. For this study, the THS solid samples were deposited on high vacuum aluminum foil (hv-Al). This substrate was chosen due to a large surface area and its lack of porosity, which allowed for maximum accumulation of grains. Because of the very short residence time of the gas in the plasma cavity and the resulting truncated chemistry, very small amounts of aerosols are produced in the THS experiment, even when adding larger molecules to the initial mixture.[25] As a result, it is necessary to run the experiment for several hours in order to accumulate sufficient material on the substrate for a successful ex-situ analysis. The accumulation time varies depending on the gas mixture, with the more complex mixtures producing material faster.[25] The timescales used for the present analysis were the same as the ones used for the IR ex situ analysis presented in Part II, enabling a comparison between the two studies: 10 hours of deposition were sufficient for complex mixtures containing acetylene and/or benzene, while 40 hours were necessary for the N_2-CH_4 (95-5) mixture. To ensure that the choice of aluminum foil as a substrate did not lead to thermally induced chemical changes, temperature was monitored in blank runs using a K-type thermocouple and no significant increases in temperature (6°C in 40 hours) were observed over the timescale of the experimental runs.

After deposition, the plasma is turned off and the COSmIC chamber is pumped down to base pressure, then returned to atmospheric pressure with pure nitrogen to minimize undesired oxygen induced chemistry. The samples are then removed from the chamber through a custom-designed glove box, as discussed in Part II. The glove box is pumped down and purged with argon three times while the oxygen content is monitored with an oxygen detector to insure it is below 0.1% prior to opening the chamber. Once the samples are removed from the chamber, they are quickly stored in hv-Al foil coated plastic petri dishes and sealed with parafilm for storage. After confirming the integrity of the seal, the samples are taken to a freezer for longer term storage and kept frozen until the chosen ex-situ analysis can be performed. For the study presented here, the samples were analyzed with DART-MS within 30 minutes of their removal from the freezer.

3.3.3 EZ-DART Source

The custom-designed EZ-DART system was developed at Caltech and has been utilized for the characterization of secondary organic aerosols and viscous asphalt samples, making it well suited to this work. Figure 3.2 shows a schematic as well as two pictures of the experimental setup for the EZ-DART system. Helium is used as the flow gas (99.995% purity) at a flow rate of 1.5 L min^{-1}. A corona discharge is used to produce helium metastables, and is generated by applying 1.5-2 kV DC with a current of 0.1-0.2 mA onto a high voltage electrode. While an ion filter is used in typical DART studies, its use was found to negatively impact CID analyses. As such, the ion filter was not used and held at ground to prevent charge buildup. The outlet of the EZ-DART is oriented at a 45° angle from the sample with the outlet no farther than 5 mm from the sample surface, as shown in figure 3.2c. An ion transfer tube is then used to guide the analyte ions into an ion trap mass spectrometer (LTQ-XL, Thermo Scientific, San Jose, CA) for detection and analysis. If desired, the temperature of the helium gas can be increased using a variable transformer controlled (Variac Co., Cleveland, OH) heating cord (Omega Engineering, Stamford, CT) wrapped around the heating region of the EZ-DART. High temperature experiments were performed for comparison to room temperature data. In all cases the temperature was measured with a K-Type thermocouple placed between the heater and glass, with all temperatures reported within + 3°C.[41]

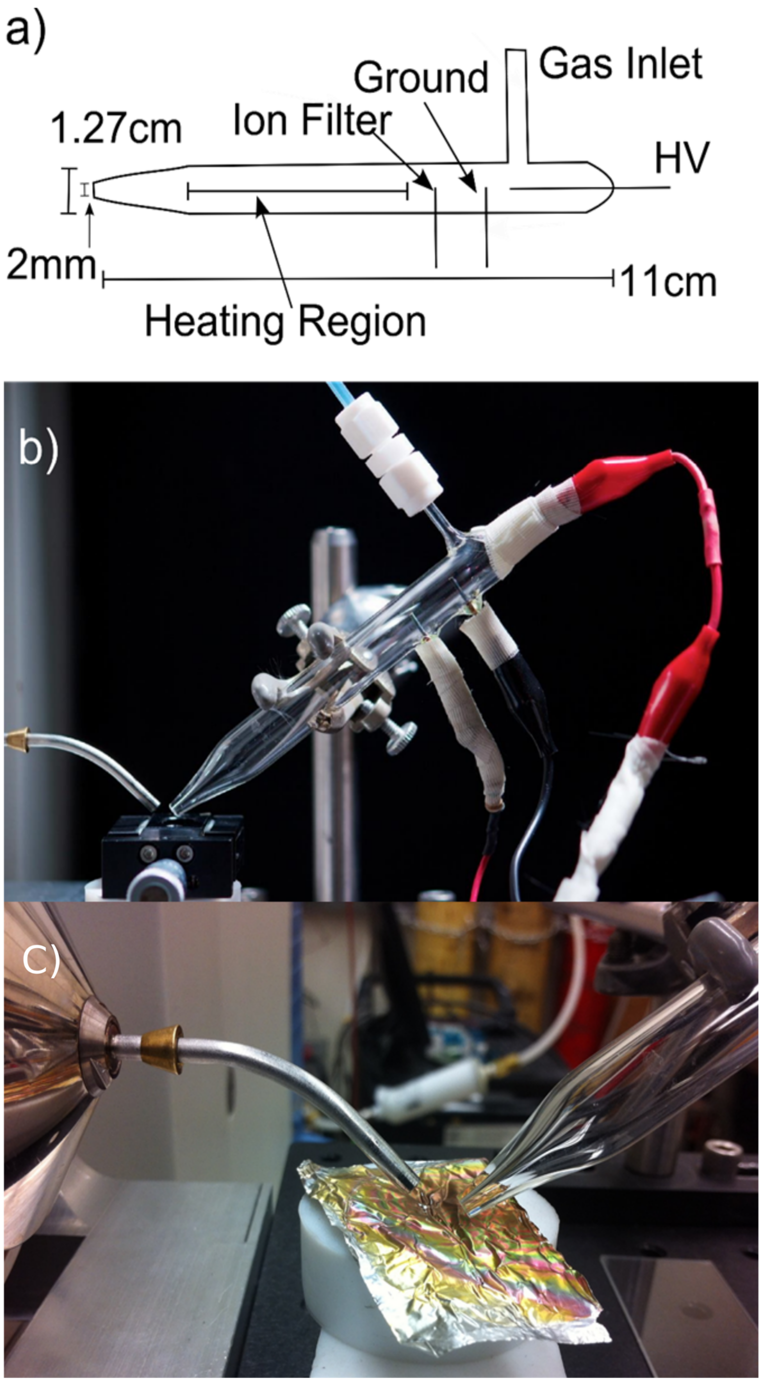

Figure 3.2. a) Schematic of the EZ-DART source, photographs of the b) EZ-DART source experimental setup and c) EZ-DART during sampling of THS aerosols. (Figure adapted from Upton et. al. 2017)

3.3.4 Sample Analysis by EZ-DART

In the study presented here, EZ-DART mass spectra of THS aerosols produced from the four gas mixtures and deposited on hv-Al foil were acquired at Caltech. To ensure sample preservation and reproducibility, the following systematic protocol was adopted: (1) DART mass spectra of a blank hv-Al substrate were acquired at the same temperature as the planned THS sample acquisition prior to each analysis; (2) The THS samples were removed from the freezer and analyzed with the EZ-DART within 5 minutes for room temperature spectra, and within 30 minutes for elevated temperatures. For elevated temperatures, spectra were accumulated while slowly increasing the heater temperature using manual temperature control (5-10°C/min with a maximum of 250°C), allowing for the monitoring of any temperature dependent changes in signal.

In order to limit the exposure of the samples and prioritize the identification of nitrogen containing compounds, only positive ion spectra were acquired. Analysis was performed at the location of highest deposition thickness, which corresponded to the position that was facing the center of the THS slit during deposition due to the planar nature of the expansion, and was approximately at the center of the sample. Since the EZ-DART samples a large area (2-5mm), ensuring a region of equal deposition for analysis was less relevant than ensuring sampling from a region of high deposition. The THS EZ-DART spectra were background subtracted, using the blank hv-Al foil spectra acquired before each sample, to allow for the analysis of lower intensity species. To allow for some structural analysis, collision induced dissociation (CID) was used to analyze the DART spectra. In CID, the parent molecules responsible for a specific mass peak in the spectrum are accelerated to a high kinetic energy using an electric potential, at which point the excited parents collide with a buffer gas. This collision converts the kinetic energy to internal energy, which results in the breaking of hydrogen-bonded adducts or a covalent bond within the parent molecules and produces an MS/MS spectrum. The resultant spectrum therefore shows how the parent molecules fragment and allows for the identification of structural characteristics and the elucidation of multiple species within a single peak.[44] CID spectra were not background subtracted, leading to some contribution from background in the CID spectra. The CID spectra from the samples were compared with those from the hv-Al blank (shown in the supplemental information), after which only peaks showing major deviations from the blank in both intensity and mass were considered in subsequent analysis.

3.4 Results and Discussion

3.4.1 Comparing the DART spectra of the THS samples produced in four different gas mixtures

DART mass spectra were acquired for THS simulants produced in the following four gas mixtures: N_2-CH_4 (95-5), N_2-CH_4-C_2H_2 (91-5-4, acetylene), N_2-CH_4-C_6H_6 (90-5-5, benzene), N_2-CH_4-C_2H_2-C_6H_6 (86-5-4-5, acetylene and benzene). These spectra, shown in figure 3.3, were all background subtracted prior to analysis to eliminate complications from atmospheric contaminants.

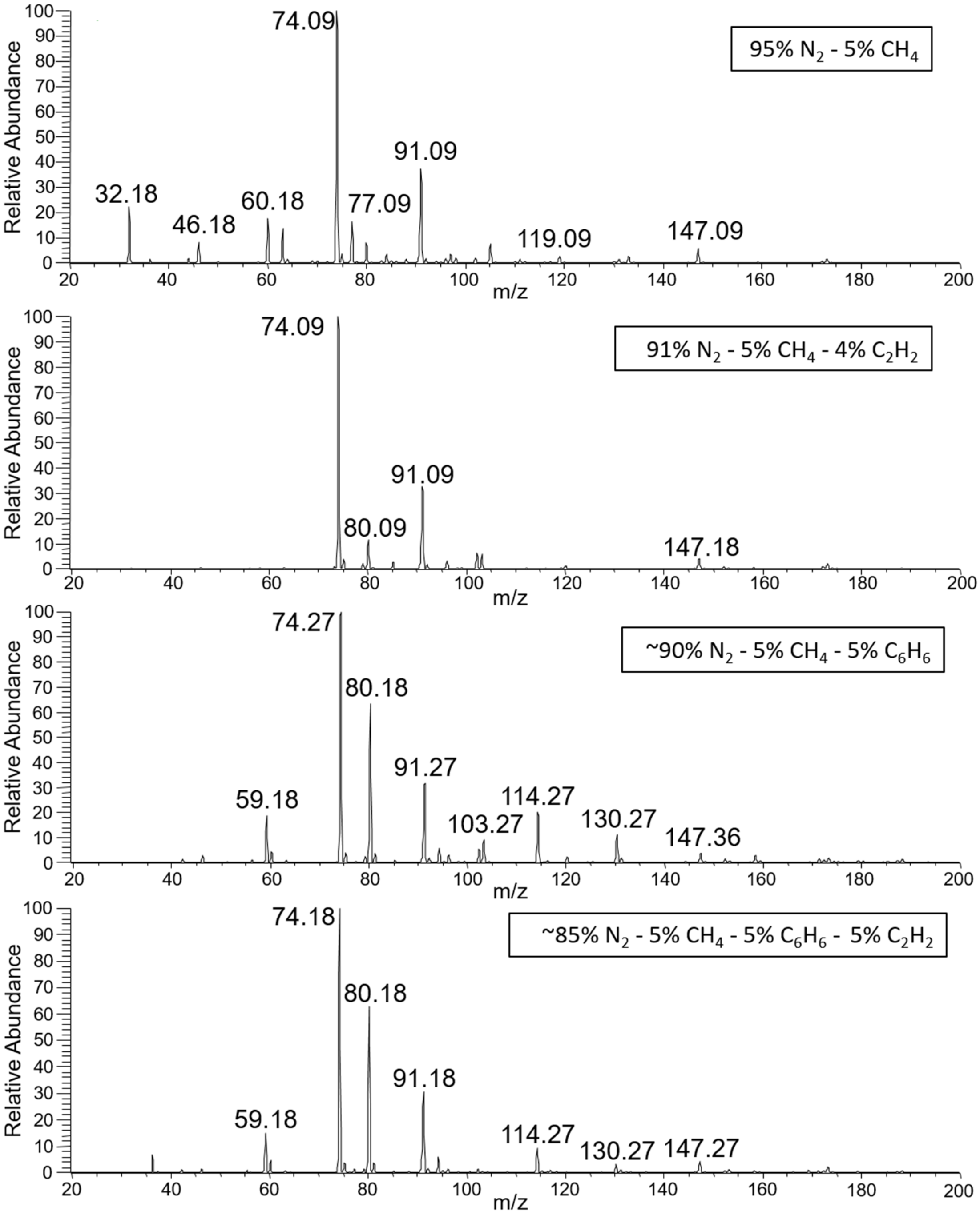

Figure 3.3. EZ-DART mass spectra of THS simulants collected at room temperature with ambient background subtracted. From top to bottom: 95-5 N_2-CH_4, 91-5-4 N_2-CH_4-C_2H_2 (acetylene), 90-5-5 N_2-CH_4-C_6H_6 (benzene), 86-5-4-5 N2-CH_4-C_2H_2-C_6H_6 (acetylene and benzene).

By comparing these four spectra, it is possible to determine the general effects of the different gas mixtures on the solid phase composition. The initial observation is the relative simplicity of all four spectra. Spectra were acquired up to 1000 m/z mass range, but their analysis was limited to the 20-200 m/z mass range due to the scarcity of peaks detected at higher masses. As seen in figure 3.3, the peak intensities drop off above 74 m/z. Furthermore, compared to DART mass spectra of other organic aerosols or petroleum, there are surprisingly few peaks in the THS sample mass spectra, even in the <200 m/z region. While competitive ionization effects may have contributed to this observation, complex spectra (more peaks and higher masses) have been observed in previous studies from samples with similar diversity, making the ionization effect a known minimal contributor. The discussion presented here regarding the types of molecules made in the THS experiment for each gas mixture is limited to the species predisposed to detection by DART-MS, i.e., with suitable volatility and proton affinity for DART ionization. This means that the DART analysis cannot be used to assess what the most abundant species overall are within the samples. On the other hand, by limiting the types of species detectable to high proton affinity compounds, the DART technique has the benefit of simplifying the analysis to mostly nitrogen containing compounds; the main goal of this study. Complementary mass spectrometry techniques will be used in the future to investigate the presence of less volatile and lower proton affinity species such as hydrocarbons.

Another advantage of DART is the ability to detect volatile species trapped within the sample during the experiment. The preservation of these compounds, especially those with high vapor pressures, is likely due to a matrix effect of the solid deposition. Since the solid grains are jet-deposited over long timescales (10-40 hours), it is likely that small volatile molecules become trapped in the solid matrix that develops. This effect has already been observed on grains produced in COSmIC, where argon was trapped in the solid deposit and then evaporated, leaving holes in the deposit layers as seen by SEM. Furthermore, a recent IR study of the THS simulants has shown the disappearance of absorption features over time.[25] This effect could be explained by volatiles trapped within the solid slowly evaporating post deposition. Quickly freezing the samples and acquiring DART mass spectra directly after removal from the freezer, combined with this matrix effect, likely preserves these small volatile compounds and enables their subsequent detection. This matrix effect may also be representative of mechanisms occurring on Titan allowing for increased chemical diversity throughout the atmosphere. As aerosols accumulate in the atmosphere and settle into haze layers, a similar matrix effect could preserve small photochemically reactive organics. This may lead to the transport of more reactive species to the surface, in accumulated aerosol, allowing molecules not expected to be found on the surface to undergo chemistry outside of higher atmospheric layers.

Closer comparison of the DART mass spectra obtained with the four THS simulants shows more details about the effects of the different dopants on the composition of the solid phase. The most intense mass peaks (74, 80, 91 m/z) for all four mixtures are remarkably similar, suggesting that there are favored mechanistic pathways that produce these smaller, more volatile species. Major differences are observed as well. More species are detected for the 95-5 simulant in the <70 m/z mass range compared to the simulants produced in more complex mixtures, while new higher mass species (>91 m/z) are detected in the benzene doped simulants that are not present in the simulants produced in simpler mixtures.

The acetylene doped (91-5-4) simulant presents the simplest spectrum, which contains no major peaks in the <70 m/z mass range and fewer major peaks overall. This could imply that the chemistry induced by the presence of acetylene, a known precursor of benzene, in the gas mixture is mostly hydrocarbon based, and consequently not detectable with DART. The observed simplicity is also suggestive that nitrogen incorporation in this mixture is minimal, which is in agreement with the study in Part II, for which little nitrogen functionality was observed in the IR spectrum. The results of an unpublished x-ray absorption near edge structure (XANES) spectroscopy are also showing a much higher C/N ratio for N_2-CH_4-C_2H_2 mixture compared to N_2-CH_4 mixtures. From this comparison, it appears that acetylene has the most pronounced effect on the products detectable by DART, resulting in the decreased diversity of small polar molecules. This observation may have implications for nitrogen chemistry in Titan's atmosphere that will necessitate further investigation.

The spectra of the benzene doped (90-5-5) sample presents the same major mass peaks (74, 80, 91) as the 95-5 and acetylene doped (91-5-4) simulants, but shows an increase in the 80 m/z peak and the appearance of additional peaks. Therefore, the presence of benzene in the plasma discharge appears to lead to new synthetic pathways that are not occurring in other mixtures. One of the reasons could be that these reactions do not have time to occur during the short residence time of the gas within the active region of the plasma discharge in simpler mixtures where benzene needs to first be produced by chemical reactions. Comparison with the acetylene doped (91-5-4) sample shows that benzene and acetylene each have unique impacts on the chemistry.

For the simulant produced in the mixture with both dopants, acetylene and benzene, the mass spectrum appears to be a combination of the acetylene doped (91-5-4) and benzene doped (90-5-5) simulant spectra, as expected. The two benzene-containing simulants present very similar DART mass spectra, which is consistent with the IR analysis presented in Part II, where the IR spectra of the benzene containing mixtures were almost identical. The benzene chemistry dominates, since the quenching of additional peaks as seen in the acetylene doped (91-5-4) spectrum is not observed, whereas additional peaks from the benzene doped (90-5-5) are still observed with comparable relative intensity. All of these initial observations are suggestive of predicable mechanisms within the THS experiment, leading to quenching of complex chemistry and the resulting domination of smaller components.

3.4.2 Comparing the THS DART spectra acquired at room (17°C) and high (250°C) temperatures

Before further analysis is performed under the assumption that we are observing simpler products related to early and intermediate chemistry, some comparisons are necessary. We first compared the room temperature spectra of the four THS samples to those obtained with higher DART heater temperatures. From prior DART studies of complex organic mixtures, such as petroleum, it has been observed that increasing the temperature of the DART heater can result in the detection of low volatility species as well as species with higher masses. DART spectra were acquired while increasing the heater temperature for each of the four samples. Each sample but the benzene doped (90-5-5) displayed a signal decrease consistent with the loss of volatile species. The DART spectra of the benzene doped simulant at room temperature and 250°C are shown in figure 3.4 for the low mass region.

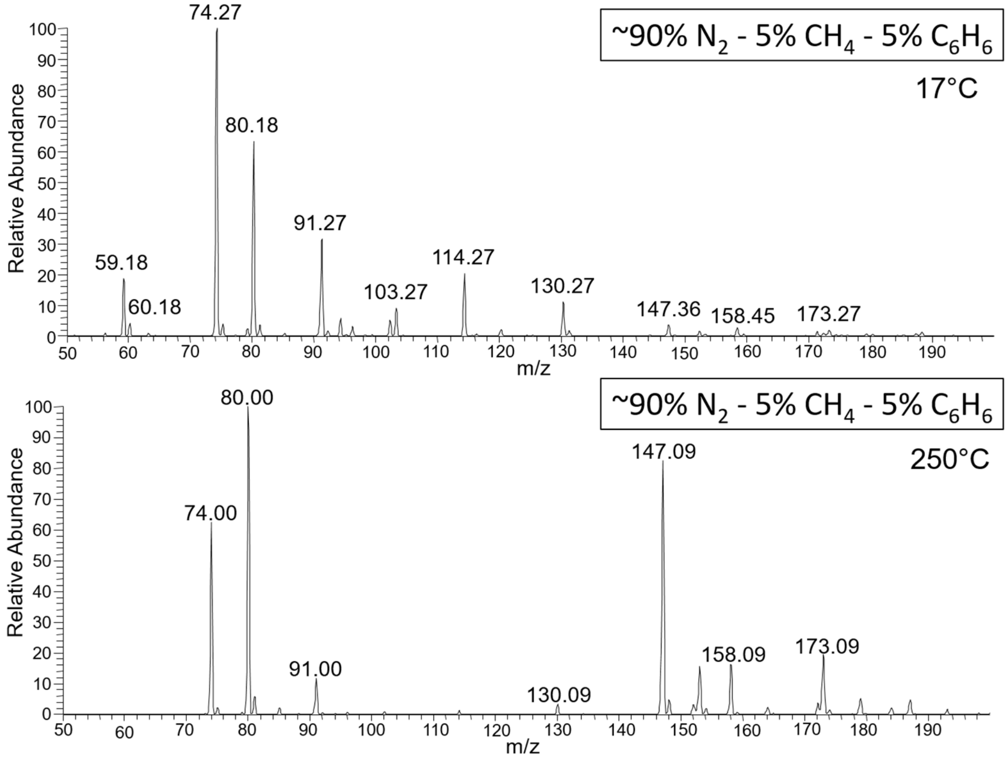

Figure 3.4. DART spectra of the N_2-CH_4-C_6H_6 (90-5-5) sample acquired at two different temperatures: Top: The same spectrum as reported in figure 3.3, collected at room temperature, Bottom: The spectrum collected at a recorded heater temperature of 250°C as measured at the EZ-DART heater.

The mass range of 50-200 m/z is shown since the high temperature spectrum was acquired with mass range of 50-1000m/z to enable the detection of any higher mass species. Since on a few lower intensity peaks were seen at masses >200m/z, a 50-200 m/z range is used for the comparison. The first observation to be made is the major difference between the high temperature DART spectrum of the THS sample and those obtained with other complex organic samples: with the THS sample, an increase in the intensity of the low mass species was observed as opposed to the expected decrease. Furthermore, no new peaks appeared at elevated temperatures in the "gap" regions between the peaks detected in the low temperature spectrum, eliminating the possibility that low volatility-, DART detectable products exist within these regions. These two factors indicate that the products observed follow a predictable pattern biased towards the production of these lower molecular weight species. This supports the hypothesis that the pulsed plasma jet expansion configuration of the THS does not induce an over processing of the analytes, allowing for simpler chemistry to dominate the DART ionizable products.

The observation of products at higher DART heater temperatures for the benzene doped (90-5-5) sample fits with the results of the IR analysis performed in Part II, where the benzene containing samples showed large amounts of aromatic vibrational bands that could be due to polyaromatic hydrocarbons (PAH) polymers as the primary products. An abundance of low volatility polymers would facilitate the preservation of high volatility molecules. These molecules would be trapped in the lower volatility PAH polymers until the DART heater temperature was increased. This hypothesis does, however, call into question why high temperature spectra were not observed for the sample doped with both acetylene and benzene, since the benzene chemistry appears to dominate the DART detectable species. A reason for this difference may be lower production of these species, since the addition of acetylene appears to quench some of the chemistry seen in the 95-5 sample. Another factor may be lower production of the preservative PAH polymers for the 86-5-4-5 mixture. These effects could be confirmed with additional studies on mixtures with various amount of acetylene and benzene dopants, which is beyond the scope of the present study.

The observation of aromatic features in the IR absorption spectrum of the benzene doped samples, and the observations of shifts in some band positions compared to the VIMS data acquired at Titan suggests the THS benzene doped samples are not representative of bulk Titan atmospheric chemistry. However, DART mass spectra obtained for the benzene doped samples could provide insight into the chemistry of a high benzene content microenvironment within Titan's atmosphere. Recently, analyses of CIRS data[45] has allowed the detection of benzene ice in Titan's atmosphere. The condensation of benzene could provide a benzene rich environment in which other atmospheric molecules could participate in aerosol-gas phase reactions, the products of which would not be observed in the bulk of Titan's atmosphere. Products from these local environments may provide a source of molecules not readily synthesized solely by the photochemistry of nitrogen and methane. Thus, the benzene doped samples provide insight into these benzene rich conditions, and possible implications for unique chemistry in Titan's atmosphere.

3.4.3 Comparing the DART spectra of a THS sample to a continuous plasma produced simulant

The second comparison we conducted consisted in looking at the differences between a THS simulant, which shows minimal over-processing as explained above, and a previously studied Titan aerosol simulant produced in a continuous plasma experimental setup, i.e., most likely over-processed. To this end, we chose to compare two aerosols produced from a 95%

nitrogen and 5% methane mixture: the 95-5 simulant produced in the pulsed plasma discharge of the THS setup and a simulant produced in a continuous plasma discharge by Smith et al. at the University of Arizona (apparatus details in He et al[16]). The Arizona simulant has been previously characterized in detail with multiple methods, including electrospray ionization ion cyclotron resonance mass spectrometry (ESI-ICR-MS). In that analysis, a large number of different compounds were found, making it a complex statistical mixture of carbon, hydrogen, and nitrogen.

With the comparison presented here, it is important to keep in mind that ionization by DART is a function of volatility and proton affinity. Since the THS DART mass spectrum was acquired at room temperature, the Arizona aerosol analogue was also tested at room temperature. A lower temperature decreases the likelihood of detecting heavier constituents, since only high volatility species are easily detected without heating. When the Arizona simulant was prepared for analysis a small amount of the powder was placed on hv-Al foil, adhered to the foil using 20 μL of anhydrous methanol, and allowed to dry. After this preparation, the analysis process was the same as for the THS aerosols. While using a solvent does not allow for the most direct comparison, it was required to keep the powder from being dispersed by the DART flow gas.

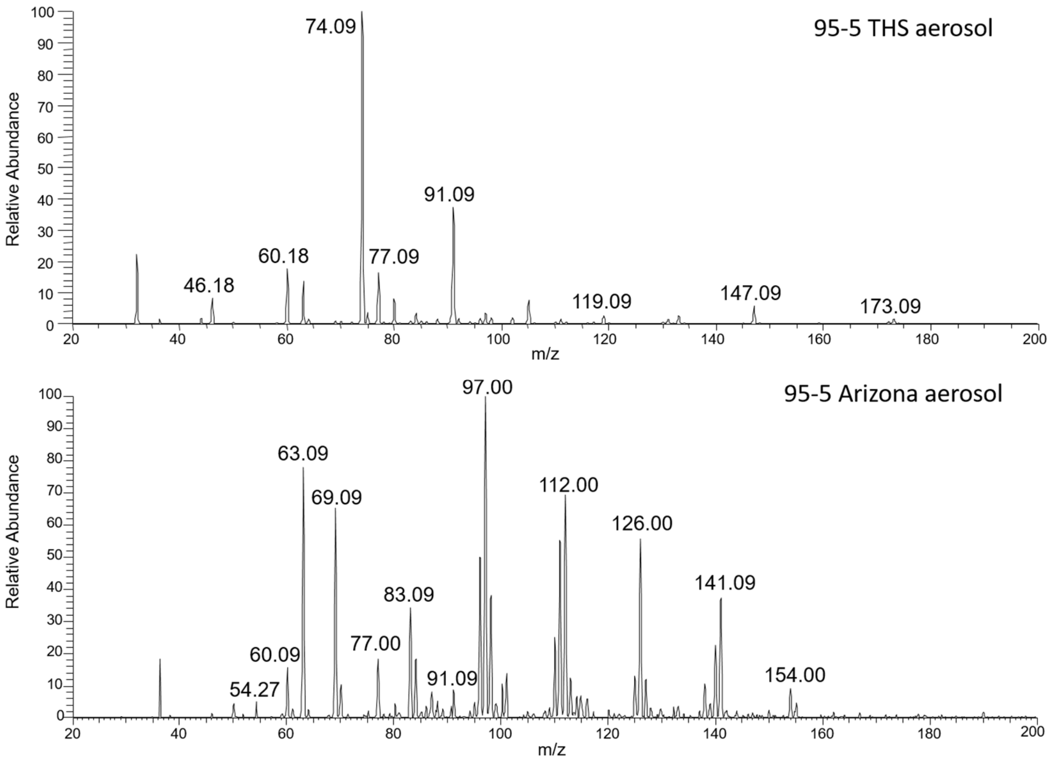

Figure 3.5. Room temperature DART spectra of the (Top) 95%N_2-5%CH_4 THS sample and a (Bottom) 95%N_2-5%CH_4 Titan aerosol simulant sample from the University of Arizona. Since the Arizona aerosol required solvation, a methanol trimer peak is visible at 97 m/z. Both spectra are background subtracted from ambient background.

The DART spectra of the Arizona simulant and the THS simulant acquired at room temperature are shown in figure 3.5. In the spectrum of the Arizona simulant, the base peak at 97 m/z is attributed to the methanol trimer, commonly seen in DART analyses of samples containing methanol. When comparing the two spectra, a difference in complexity between the THS and Arizona simulants is immediately visible: the Arizona simulant shows a greater number of peaks over the entire low mass region. Since ionization with DART is related to proton affinity, it can be assumed that the Arizona simulant contains more nitrogen-bearing compounds, leading to higher proton affinity. This increased nitrogen incorporation is likely related to a more complex chemistry occurring in the continuous plasma discharge of the Arizona experimental setup. In the THS experiment, even though the high energy required to dissociate nitrogen is reached in the pulsed plasma discharge, there is only a short time (< 3μs) during which the nitrogen can react. In the Arizona experimental setup, in which the continuous plasma discharge allows for the continuous dissociation of both nitrogen gas and products over the course of the experiment, resulting in significantly more processing of the Arizona simulant compared to the THS simulant, and the subsequent incorporation of more nitrogen-containing molecules in the Arizona solid aerosols. The higher number of peaks observed in the Arizona sample DART spectrum supports this assessment and the initial hypothesis that the THS experiment allows for the observation of early and intermediate chemical products. The simplicity of the THS simulant DART spectra has allowed a more in depth structural analysis, the results of which are presented below with possible mechanisms for their creation in Titan's atmosphere either reported from prior work or proposed.

3.4.4 Analysis of peaks observed in the THS DART spectra

While the THS DART mass spectra from all four mixtures (figure 3.3) show relatively few peaks, the non-exact mass resolution of the ion trap mass spectrometer used, combined with the propensity of DART ionization to form adducts with both water and ammonia, complicated the analysis. To allow for some structural analysis, collision induced dissociation (CID) was used. As discussed above CID allows for the structural identification through fragmentation. By identifying adducts and fragments ions, molecular formulae could be suggested. Formulae and compounds reported from this data analysis were assigned using possible combinations of carbon, hydrogen, and nitrogen, giving higher consideration to possible structures that could account for losses observed in CID and adduct formation when applicable. Since polar samples have been observed to readily adduct to water and ammonia in prior studies,[46] only polar compounds were assigned as adducts. In addition to adducts and protonated ions, the detection of molecular ions was also considered during the analysis.

CID analysis of all species was not attempted in this work. Only m/z values for which CID spectra were consistent for multiple scans were considered. Since some of these peaks were also concurrent with background, only the ones showing at least an order of magnitude difference in signal intensity with background CID spectra were analyzed (as shown in the supplemental information or SI). Additional CID data recorded but not analyzed in this work are reported in the SI for possible future analysis, pending new insights. Since CID targets a species based on m/z and an isolation width of 2 m/z was chosen (ensure capture of less stable species), the resultant MS/MS can be more complex than expected. High resolution mass spectrometry analysis of a Titan aerosol simulant similar to the Arizona aerosol showed that even a single nominal mass could contain multiple peaks, each with their own possible structural isomers. Although the THS simulant is simpler than the Arizona aerosol, there is still the high probability for multiple species within a single nominal mass and isolation width. As such, the CID spectra shown below are a combination of fragments from each compound within the isolation width. Taking this into consideration, not all fragments in each result CID spectra were identified or discussed in this work. Any compound identifications were made based on readily interpretable fragments with the understanding that contribution from other species was unavoidable. Before going into the details of the CID analysis, we first focus on peaks for which no CID data was obtained but assignments could be made.

3.4.4.1 Peaks at 80 m/z and 32 m/z – no CID

No CID fragmentation products were recorded for the 80 m/z peak. This peak is visible in the 95-5 DART spectrum, but undergoes a slight increase in intensity in the acetylene doped (91-5-4) DART spectrum, and is significantly more intense in the benzene doped (90-5-5) and acetylene and benzene doped (86-5-4-5) DART spectra. This 80 m/z peak could be related to the 79 m/z ion peak observed in the gas phase analysis (see Part 1). The peak at 79 m/z was only observed in the benzene doped (90-5-5) and acetylene and benzene doped (86-5-4-5) samples in the gas phase, which is in agreement with the substantial increase in 80 m/z peak intensity observed in the DART data for those two mixtures. The CID data for the benzene doped (90-5-5) sample, reported in the SI, shows a reaction product of 96 m/z, relating to a reaction with water in the ion trap. CID spectra for the other three mixtures were too low in intensity to be analyzed, which is expected due to their lower intensity compared to the benzene doped (90-5-5) sample.

Because both 79 and 80 m/z were observed in Part 1, the formulae presented in that work were used as the starting point here. While molecular ions are observed with DART, protonated species are more common, so only formulae for 79 Da were considered. Out of the two formulae proposed in that work, pyridine stood out as it has been observed in other Titan aerosol analogues.[29, 47] Because a reaction product was observed at 96 m/z in CID, neat pyridine was also tested with DART to verify if a similar reaction would occur. 80 m/z was observed in the overall DART spectrum for pyridine and 96 m/z was observed in the CID spectrum (shown in the SI), making pyridine the most likely assignment for the 80 m/z peak.

If we consider that pyridine is the molecule observed in all four samples at 80 m/z, a mechanism needs to be proposed to not only explain its synthesis in each condition, but also provide insight into the intensity differences observed between the four samples. The intensity comparison does enable a starting point from which a mechanism can be suggested. The low intensity of the 80 m/z peak in the acetylene doped (91-5-4) sample suggests that acetylene does not play the largest role in the production of pyridine, but still allows for the production of a small amount. Mechanisms for the production of pyridine in Titan's atmosphere typically involve products made from acetylene. When considering the production of pyridine, Wilson and Atreya, 2003 cite that the typically expected mechanism of $C_5H_6 + N \rightarrow C_5H_5N + NH$, which is exothermic by 95 kJ/mol, would be unlikely on Titan due to the large energy barrier for the creation of C_5H_6 and thus cite the $C_4H_5 + HCN \rightarrow C_5H_5N+H$, endothermic by -122 kJ/mol, as a possible minor pathway by which pyridine could be produced.[48] This being a minor pathway is supported by the relatively small production of pyridine in the acetylene-doped (91-5-4) and 95-5 samples.

The inclusion of benzene though appears to be key for the larger relative production of pyridine, considering the substantial increase in the relative intensity of pyridine for mixtures with benzene. The direct substitution of nitrogen into benzene within the higher energy plasma needs to be ruled out as a reactionary route for pyridine production with a benzene dopant. Zhang and associates studied the different products of benzene with various plasmas.[49] In that study, they found that pure nitrogen did not allow for the production of large amount of pyridine, air provided slightly more, and a 1% NO in nitrogen produced the most pyridine. They thus invoked the production of NO radicals in their mechanism for the production of pyridine by direct substitution. As the THS experiment uses UHP nitrogen and methane, NO will not have a mechanistic side effect on the production of pyridine and a different mechanism needs to be invoked. Parker and associates studied different mechanistic pathways for pyridine in an experiment at the Advanced Light Source using vinyl cyanide and phenyl radicals produced by pyrolysis.[50] The production of C_4H_6, proposed as a reactant for the production of pyridine and a possible product from benzene, was not observed in their experiment. This leads to the recombination of vinyl cyanide with either vinyl radical or cyanovinyl radical as the most likely pathways. A computational comparison found that reaction between vinyl cyanide and cyanovinyl radical had no entry barrier, which would allow this reaction to proceed at cold temperatures. Additionally, phenyl radical was cited as the progenitor of cyanovinyl radical through hydrogen abstraction, and the observation of aromatic vibrational modes in the IR analysis of the THS solid samples (Part II) suggests phenyl radical is indeed produced. This mechanism, along with the minor pathway described above, provide evidence for the differing amounts of pyridine production between the four THS samples. The recent observation of vinyl cyanide on Titan 51 and the prior observation of benzene[52, 53] suggest that investigation of this mechanism could be relevant for the production of pyridine on Titan.

Another peak for which CID results were not obtained was 32 m/z observed only for the 95-5 sample. Because this peak was observed in extremely low abundance in the background DART spectrum (as reported in the SI), it can be assumed that it is not due to the presence O_2^+ produced by the EZ-DART source. The only other possibility is methylamine, which can be produced from the recombination of the amino and methyl radicals. Amine IR bands have been reported in Part II for each of the four THS samples, so the observation of the simplest amine is reasonable. The observation of 46 m/z in the 95-5 sample suggests the presence of ethylamine or its isomers, which follows from the production of methylamine with the inclusion of another methyl radical. Production of propylamine, or an isomer, would follow sequentially, and is seen at 60 m/z. These products are expected to be produced in Titan's atmosphere, so their observation is not unprecedented. While CID of these species would be helpful for exact identification, they were too low in mass or intensity to provide spectra in the study presented here. The ease of synthesis for these molecules, combined with the observations of amines in the IR analysis (Part II), make the assignments of these peaks as simple amines the most reasonable conclusion.

As discussed above, the preservation of gaseous and high volatility species has already been observed in prior works using the COSmIC chamber, where argon was trapped in the solid matrix and later released after sample collection. Since the THS samples used in the present study were quickly stored below the boiling temperature of methylamine and ethylamine, their preservation until DART analysis would be considered feasible. The observation of these amines in only the 95-5 sample may be related to a variety of factors, the most likely of which is that benzene and acetylene produce radicals that combine with the methyl or amino radicals from the nitrogen and methane producing different products, some of which not ionizable with DART. The observation of these simple amines in the 95-5 sample, produced in the simplest gas mixture, suggests that the THS experiment can be used to simulate the early stage of Titan's chemistry.

3.4.4.2 74 m/z CID analysis

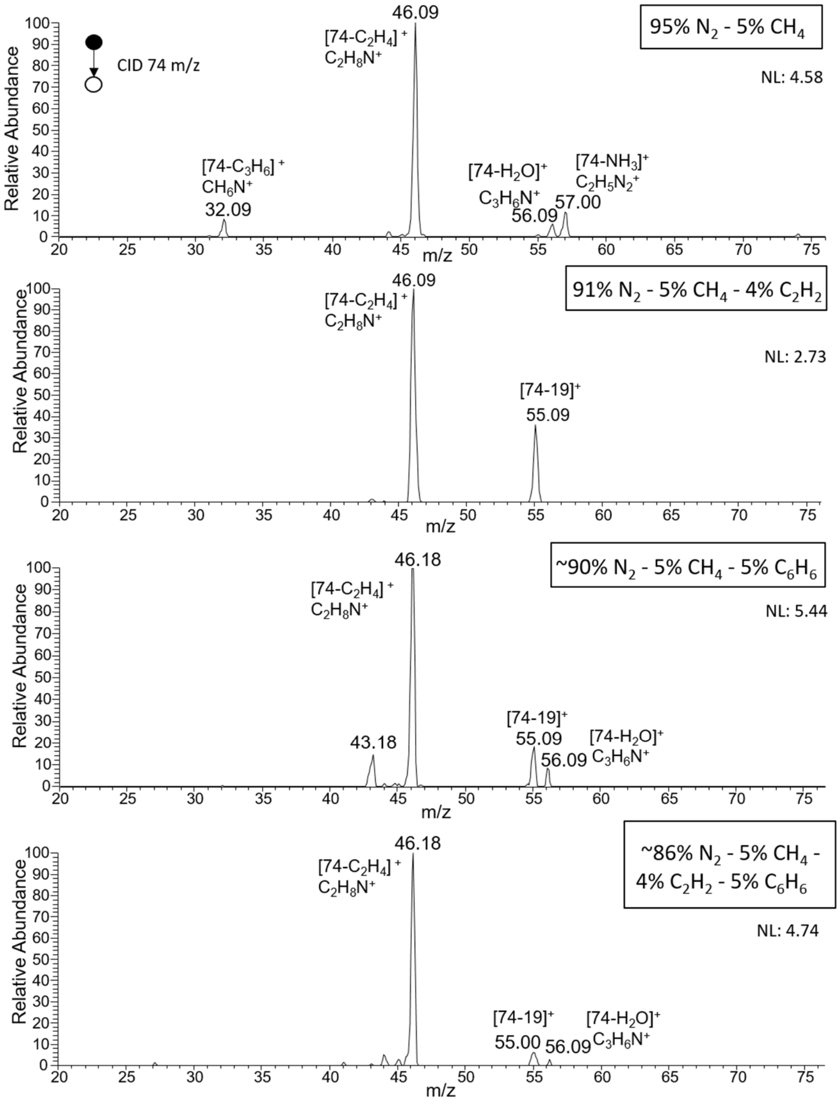

Figure 3.6. CID spectra of the 74 m/z DART peak for each sample, from top to bottom: 95-5 N_2-CH_4, 91-5-4 N_2-CH_4-C_2H2 (acetylene), 90-5-5 N_2-CH_4-C_6H_6 (benzene), 86-5-4-5 N_2-CH_4-C_2H_2-C_6H_6 (acetylene and benzene). Major fragments and losses are labeled. Overall intensity is reported for each spectrum as the normalized target level (NL).

74 m/z is the base peak in the DART mass spectrum for all four samples and was therefore the first target for analysis by CID. The CID spectra for 74 m/z are shown in figure

4.6, displaying the complexity contained within a single peak. Note that the peak at 74 m/z is one of the first peaks for which higher complexity would be expected due to an increased number of possible isomers. Since more isomers are possible within the 74 m/z peak, identifications were made with caution. Conclusions were drawn from the trends between observed species where an exact identification could not be made. Even though 74 m/z is the base peak for each sample, the peaks present in the CID spectra had very low intensity, suggesting the presence of several parent molecules including adducts and isomers at that mass. It is important to note that the CID data enable us to study some of the isomers, but do not always allow for complete characterization of each species within the analyzed peak.

In the CID spectra of the 74 m/z peak, the major product peak observed in all four samples is 46 m/z. Because it results from the loss of 28 Da (C_2H_4 – ethylene) from the parent molecule, this product is most likely ethylamine (protonated in the CID spectrum: $C_2H_8N^+$). For the ethylamine product to consistently be present in the spectra despite their low intensity, it is assumed that multiple routes must be available for the species at 74 m/z to lose 28 Da. Comparison to other MS/MS spectra 54 has led to the assignment of diethylamine for the 74 m/z species that results in the 46 m/z CID product. Additionally the structure of the diethylamine molecules allows for the loss of C_2H_4 from either side, explaining why this product is consistently present even in low intensity spectra. The synthesis of diethylamine likely follows from other smaller amines, with the addition of two methyl radicals directly to the amine. The 46 m/z CID product is the only one that is common to all four THS samples. This demonstrates that even the most abundant mass peak results from the presence of different parent molecules being synthesized in each sample.

In the 95-5 CID spectrum, the 57 and 56 m/z products are adducts with ammonia and water respectively. While the 57 m/z product could be proposed as an amine loss from 74 m/z itself, as opposed to an adduct, that is unlikely for multiple reasons. The most obvious reason is that no peak was observed at 57 m/z in the overall DART spectrum. The loss of 17 Da has been observed from primary amines in prior work involving the EZ-DART 41, but in those cases the loss product was also detected in the overall spectrum. This is not the case for the background subtracted 95-5 DART spectrum presented here (figure 3.3). Also, the most likely compound for which an amine loss would be observed would be methylguanidine, but in that case other CID products would be expected for that species, such as 43 m/z, which is not detected in the 95-5 CID spectrum. For these reasons, we assign the 57 m/z product as being from an ammonia adduct, with the most likely formula being $C_2H_4N_2$ (protonated in the CID spectrum: $C_2H_5N_2^+$), for which aminoacetonitrile and methyl cyanamide are the two stable structural isomers. Other isomers would contain azides, radicals, or permanent charges, all of which would not be expected to form adducts. Because methyl cyanamide would undergo spontaneous trimerization above its melting point, we assign aminoacetonitrile to the 57 m/z species. Aminoacetonitrile has been detected in other Titan simulants as well as in the interstellar medium,[55] and its synthesis from methyl, amino, and cyano radicals is possible in Titan's atmosphere.

The 56 m/z peak in the 95-5 CID spectrum is due to a loss of 18 Da and is identified as a water adduct, commonly observed in DART analysis. The most likely formula for this species would be C_3H_5N (protonated in the CID spectrum: $C_3H_6N^+$), for which two of the most stable isomers are propionitrile and propargylamine. Since both of these products are stable and able to adduct with water, it is difficult to assign 56 m/z to one isomer over another.

Consequently, it is necessary to make comparisons to other analyses to attempt an assignment. Comparison with the IR data reported in Part II suggests a propionitrile identification, since propargylamine contains a terminal alkyne and the corresponding vibration was not observed in the IR spectrum for the 95-5 sample. Additionally, observation of propargylamine would also be expected in the acetylene doped (91-5-4) sample due to the presence of the terminal alkyne, but no 56 m/z product peak is present in the 74 m/z CID spectrum for that mixture. These factors led us to tentatively assign propionitrile to the 56 m/z product ion in the 95-5 sample. The 74 m/z CID spectra for the two benzene doped (90-5-5 and 86-5-4-5) samples also show a peak at 56 m/z, but it is much more difficult to identify. The IR analysis described in Part II reported bands associated with terminal alkynes and amines, in addition to bands for possible nitriles. Due to this discrepancy, the 56 m/z peak cannot be assigned for the benzene doped samples, but likely corresponds to one of the two isomers proposed for the 95-5 sample.

The 32 m/z peak in the 95-5 CID spectrum is the simplest to assign since the 32 m/z mass peak is also observed in the overall DART spectrum and has already been identified as methylamine. In the 74 m/z CID spectrum, this peak is produced from the loss of 42 Da (C_3H_6) from 74 m/z. The 74 m/z species generating this product ion is identified as N-methylpropylamine, with the 42 Da loss corresponding to the loss of the propane from the compound. The presence of this isomer, combined with the low overall intensity of this spectrum, shows that multiple isomers should be expected for any peak analyzed with DART.

The observation of a peak at 43 m/z in the benzene doped (90-5-5) sample is more difficult to assign since it is indicative of a 31 Da loss, possibly methylamine. The 43 m/z peak in this spectrum must have higher proton affinity to retain the ionization over the methylamine, eliminating the possibility of it coming from N-methylpropylamine as assigned in the 95-5 DART spectrum. Taking that into account, the most likely formula for the 43 m/z fragment would be CH_2N_2 (protonated in the CID spectrum: $CH_3N_2^+$), making the original parent formula $C_2H_7N_3$. This would place the most likely identification as methylguanidine for which 43 m/z is an expected fragment. The lack of other fragments expected in the methylguanidine CID spectrum however, makes this identification tentative, and will require additional analysis in the future to confirm.

A product peak at 55 m/z is observed in all CID spectra except for the 95-5 sample. This peak corresponds to a loss of 19 Da and is therefore difficult to assign. It cannot be identified as a water loss from a 73 m/z peak contained in the CID isolation width since there is no 73 m/z peak observed in the overall DART spectrum (not even without background subtraction). This leaves the product as the likely result of a two-step loss process, thus too difficult to identify with the data available, and requiring further analysis in the future.

In summary, with the data obtained through CID analysis of the 74 m/z peak, we can positively identify diethylamine, aminoacetonitrile, propionitrile, and N-methylpropylamine as compounds contained in the 74 m/z peak. The diversity of compounds shows how necessary CID analysis is for the identification of species in these simulants. The synthesis of these species all fit well within mechanisms discussed in earlier works, even though amines have yet to be identified on Titan. The observation of these and other amines in the overall data show the preservation of small molecules over the course of accumulation and analysis. This suggests that these amines could be produced on Titan and be available for synthesis of other products.

3.4.4.3 91 m/z CID analysis

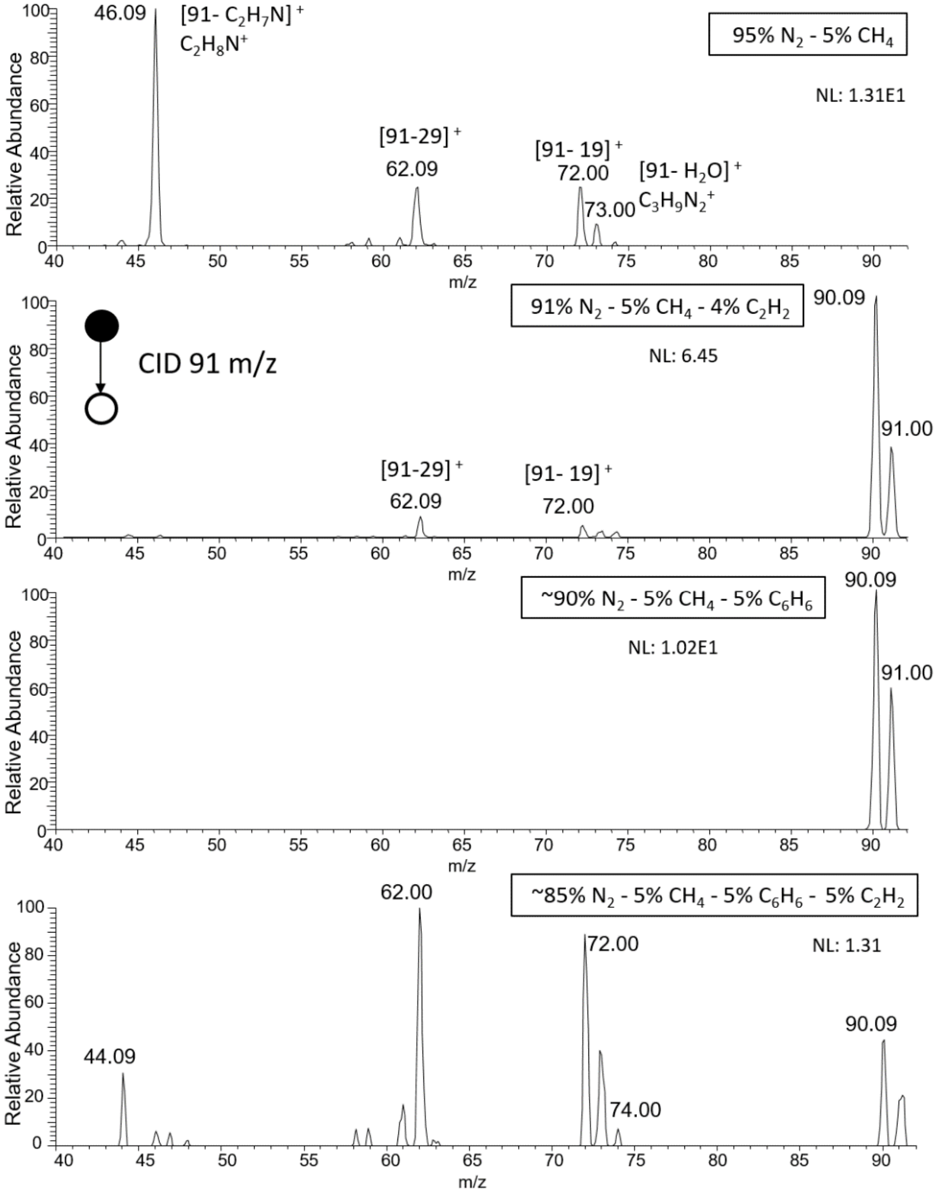

Figure 3.7. CID spectra of the 91 m/z DART peak for each sample, from top to bottom: 95-5 N_2-CH_4, 91-5-4 N_2-CH_4-C_2H_2 (acetylene), 90-5-5 N_2-CH_4-C_6H_6 (benzene), 86-5-4-5 N_2-CH_4-C_2H_2-C_6H_6 (acetylene and benzene). Major fragments and losses are labeled. Overall intensity is reported for each spectrum as the normalized target level (NL). The 86-5-4-5 spectrum is unlabled due to extremely low overall intensity.

Since 91 m/z was the next most intense peak common between all four samples, it was also analyzed with CID. The resulting CID spectra for all four samples are shown in figure 3.7. It should be noted that the CID spectrum of the acetylene and benzene doped (86-5-4-5) sample was very low in intensity and was not extensively analyzed in this work. However, because all peaks in that spectrum were an order of magnitude higher than the background CID, they were still used for comparison. Initial inspection of the four different spectra shows how much impact the inclusion of a dopant can have on the synthesis of different compounds within the THS. The THS chemistry appears to be more diverse in the acetylene and benzene doped (86-5-4-5) sample, with the detection of a broader range of fragments in the CID spectrum. This diversity could also account for the lower intensity of the CID spectrum for this sample, since having many different products contained within one peak would decrease the overall intensity of the CID spectrum. In the CID spectrum of the 95-5 sample, the base peak is at 46 m/z. This 46 m/z product is easily explained as a dimer, since 46 m/z is also observed in the overall DART spectrum for the 95-5 sample, and has been identified in that case as ethylamine. Seeing a dimer for ethylamine is reasonable, considering there is also evidence of a dimer for methylamine at 63 m/z in the overall spectrum for the same sample.

In the 91 m/z CID spectra for the acetylene doped (91-5-4) and benzene doped (90-5-5) samples, the major peaks are 90 and 91 m/z, which suggest the presence of a molecular cation or extremely stable protonated species which does not readily undergo fragmentation, and only loses a single hydrogen when fragmentation does occur. The production of this compound seems to be heavily influenced by the presence of benzene, considering the benzene sample contains no other fragment ions. The observation of 90 m/z is unlikely to be from the isolation width used (i.e. coming from a 90 m/z peak in the DART spectrum), since there is no 90 m/z peak observed in the overall DART mass spectra. This suggests that 91 m/z is a molecular cation, which would be more likely observed for a species with some type of aromaticity or conjugation. The two most probable formulae for 91 m/z are $C_7H_7^+$ and $C_6H_5N^+$. For $C_7H_7^+$, the only likely compounds would be benzyl cation or tropylium cation. Observation of either of these species by DART would be unlikely since both would be produced from the ionization of toluene, which was not detected by EZ-DART when tested as a reference. This compound thus likely contains a ring structure with the formula of C_6H_5N, for which there are several possible isomers, the most stable of which would be ethynylpyrrole or cyclopentadienecarbonitrile. Neither of these are fully conjugated, but they could reasonably be produced in the benzene or acetylene doped mixtures, since amines and nitriles were detected in the IR data for both of these dopants. While the production of either is questionable considering the lack of fragments, an explanation may exist in the ionization process. Indeed, a lack of fragments was also observed for the protonated pyridine observed at 80 m/z in the overall DART spectrum. Because of its similarity with pyridine, in that regard, ethynylpyrrole seems to be a more likely possibility. The synthesis of pyridine was proposed as reasonable due to the inclusion of benzene. It is possible that phenyl radical could also assist in the production of other nitrogen containing rings.

The 73 m/z peak present in the CID spectra of both the 95-5 and acetylene doped (91-5-4) samples is due to a loss of 18 Da, and is thus identified as a water adduct. This product is most likely $C_3H_8N_2$ (protonated in the CID spectrum: $C_3H_9N_2^+$), since $C_4H_{10}N$ does not contain any isomers without a permanent charge. Attempting to assign the $C_3H_8N_2$

is difficult though since there are many possible structural isomers, but comparisons with other analytical data can assist in the characterization. From the IR analysis in Part II, we know that imines have been observed for the 95-5 sample and that no bands corresponding to an N-N bond were reported. A three or four member ring would be unlikely due to the steric strain, leaving possible candidates as an imine, five membered ring with two nitrogen atoms, or an alkene with two amines. A full identification cannot be completed without more data such as subsequent CID, which was not conducted in the present study. Imines and amines are good candidates though since they would be in agreement with both the THS IR analysis and other Titan aerosol simulations and models.

The 72 m/z fragmentation peak observed in both the 95-5 and acetylene-doped samples is from a loss of 19 Da, which is not from a single process and thus not identifiable with the data presented here, similar to the 55 m/z peak from the CID of 74 m/z. The 62 m/z fragment peak detected in both the 95-5 and acetylene doped (91-5-4) samples, corresponds to the loss of 29 Da, which can be assigned to the loss of methylimine, considering imines have been proposed to exist on Titan and also reported in earlier work.[25, 56, 57] After this point, assignment becomes much more difficult, since the 62 m/z fragment does not match expected possible products that, when combined with a methylimine loss, allow for a stable parent compound. This is not a 28 Da loss from 90 m/z since 90 m/z is not observed in the overall unsubtracted mass spectrum and 62 m/z is not seen in the background CID, indicating that it must come from the sample. It is possible that this is another two-step process. The data presented here cannot differentiate between a methylimine loss and a two-step process, but the latter seems to be a more reasonable explanation since two-step process peaks are also seen in the low intensity CID spectra of 74 m/z.

In summary, the CID spectra of the 91 m/z peak are more difficult to analyze and have only led to the identification of an ethylamine dimer, tentatively ethynylpyrrole and an imine or amine with a formula of C3H8N2. The stark contrast seen between the 95-5 sample and the more complex samples indicates that the inclusion of the dopants can not only induce the production of more complex species that cannot be produced with only nitrogen and methane in the truncated chemistry of the THS, but can also suppress the production of certain compounds.

3.4.4.4 114 m/z CID analysis

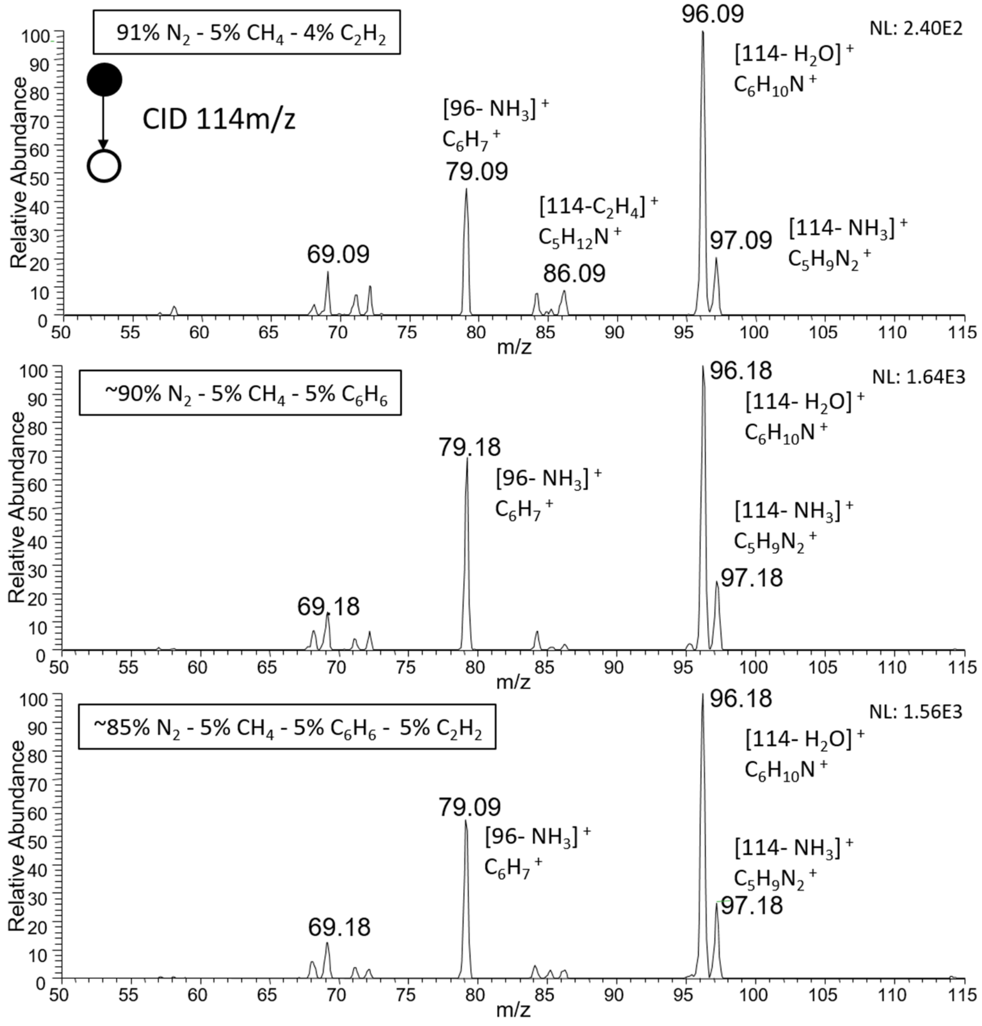

Figure 3.8. CID spectra of the 114 m/z DART peak for the three complex samples, from top to bottom: 91-5-4 N_2-CH_4-C_2H_2 (acetylene), 90-5-5 N_2-CH_4-C_6H_6 (benzene), 86-5-4-5 N_2-CH_4-C_2H_2-C_6H_6 (acetylene and benzene). Major fragments and losses are labeled. Overall intensity is reported for each spectrum as the normalized target level (NL).

The 114 m/z peak appears only in the DART spectra of the doped samples. The intensity of the 114 m/z peak is extremely small in the acetylene doped (91-5-4) sample but still present. In the benzene doped (90-5-5 and 86-5-4-5) samples however, the intensity of the 114 m/z is much higher. In the resultant CID spectra, the first major fragment ion for all three samples is at 96 m/z and corresponds to a loss of 18 Da from the parent ion, therefore identified as a water adduct. The second most intense CID peak, at 79 m/z, is difficult to explain as a fragment from 114, since 35 Da does not add up to a possible fragment by itself, and 35 Da is higher than what we would expect for a two-step process.

In the benzene doped (90-5-5) and acetylene-and-benzene-doped (86-5-4-5) cases the peak intensity for the CID 96 m/z fragment ion was high enough to perform another CID step, shown in figure 3.9. In these MS^3 spectra, 79 m/z appears as a fragment of 96 m/z, indicating that the 79 m/z peak is from two concurrent losses: the loss of the adducted water, followed by a loss of 17 Da an amine from the 96 m/z species. A doubly adducted species, allowing for the loss of both water and ammonia adducts, has never been reported in prior DART studies, indicating that this is an amine loss, not the loss of an ammonia adduct. Previous work with the EZ-DART[41] has shown that primary amines are readily lost with DART sampling, supporting the identification of 79 m/z in the MS/MS spectrum as the loss of a primary amine from 96 m/z. In the case of the 114 m/z CID, the first CID scan could easily have broken the adduct species and also caused the loss of a primary amine, which would explain the 79 m/z peak. In addition, the other major peak at 68 m/z in the MS^3 scan is due to a loss of 28 Da, which could correspond to a loss of CH_2N or C_2H_4. By comparing these losses to other CID spectra of compounds with relevant chemical formulae, we can assign aminopyrimidine to the 96 m/z CID product. This compound would account for the loss of the primary amine, since other similar pyrimidine compounds produce an M-H+ fragment ion, matching the observation of 79 m/z. While other compounds are also possible for these spectra, aminopyrimidine accounts for the two major fragments. Moreover, the presence of a very small amount of 96 m/z in the overall DART mass spectra provides further support for this assignment. Identification of the 97 m/z peak was not attempted due to MS^3 spectra being obtained from that mass. The other peaks in the CID spectra likely correspond to additional isomers from the 114 m/z and were not examined in detail due to their low abundance compared to the aminopyrimidine peaks.

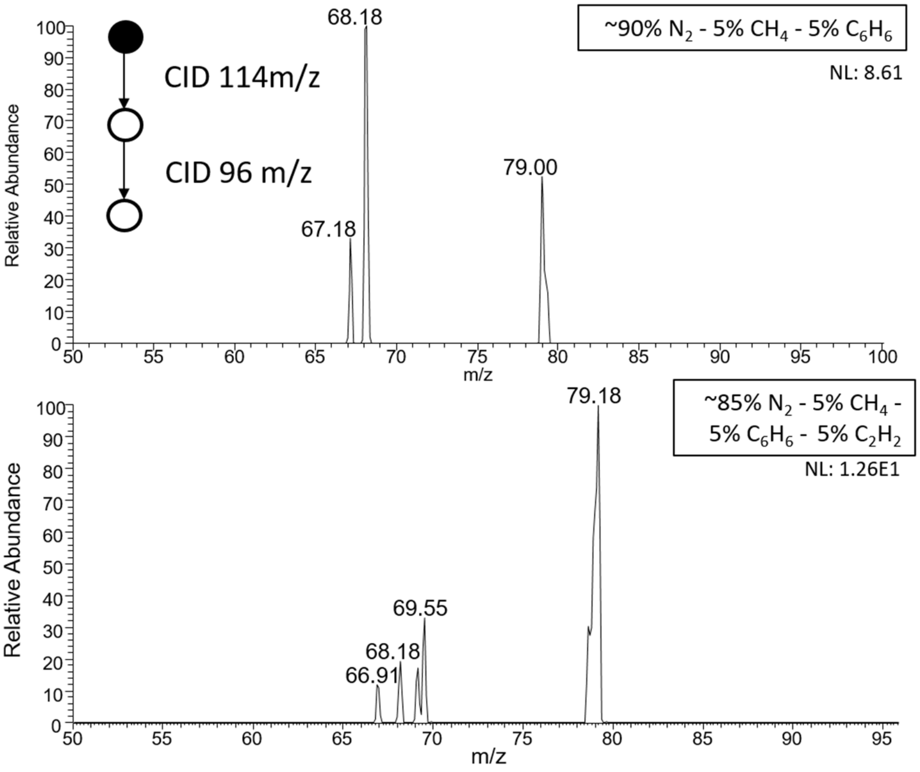

Figure 3.9. MS^3 spectrum of 114 m/z - 79 m/z for the two benzene doped samples, from top to bottom: 90-5-5 N_2-CH_4-C_6H_6 (benzene), 86-5-4-5 N_2-CH_4-C_2H_2-C_6H_6 (acetylene and benzene). Overall intensity is reported for each spectrum as the normalized target level (NL).

The finding of a pyrimidine-type molecule in these samples is of great interest for its prebiotic relevance since pyrimidine is a precursor of nucleobases. The production of aminopyrimidine seems to be enhanced when benzene is present, and therefore it is likely that the synthesis of aminopyrimidine involves a mechanism comparable to that of pyridine, where acetylene can be used for the synthesis but phenyl radical can assist at low temperatures. At high temperature, a mechanism involving hydrogen cyanide and acetylene radical cation is known to produce a pyrimidine cation.[58] In the low-temperature processes of the THS experiment however, no pyrimidine production was observed in the acetylene doped only sample. Consequently, that mechanism is likely not the one responsible for the production of the aminopyrimidine observed in the THS samples. Taking that into consideration, it is likely that phenyl radical provides assistance to the synthesis, similarly to the pyridine production process. Comparing the intensities of the 79 m/z peak in the MS^3 spectra for the benzene doped (90-5-5) and the acetylene and benzene doped (86-5-4-5) samples suggests that aminopyrimidine production is enhanced when both dopants are included. From this perspective, it is possible that both acetylene and hydrogen cyanide are included in the synthesis of aminopyrimidine, but phenyl radical enhances the synthesis at the low temperatures used in the pulsed plasma discharge. This suggests that pyrimidine could be produced on Titan in benzene rich areas, since both hydrogen cyanide and acetylene would be readily available. Considering that the possibility of nucleic bases produced from acetylene on Titan has been discussed in prior work,[59] the observation of aminopyrimidine from the benzene doped samples shows the interest of investigating the benzene Titan chemistry further in future experiments.

3.4.4.5 119 m/z CID analysis

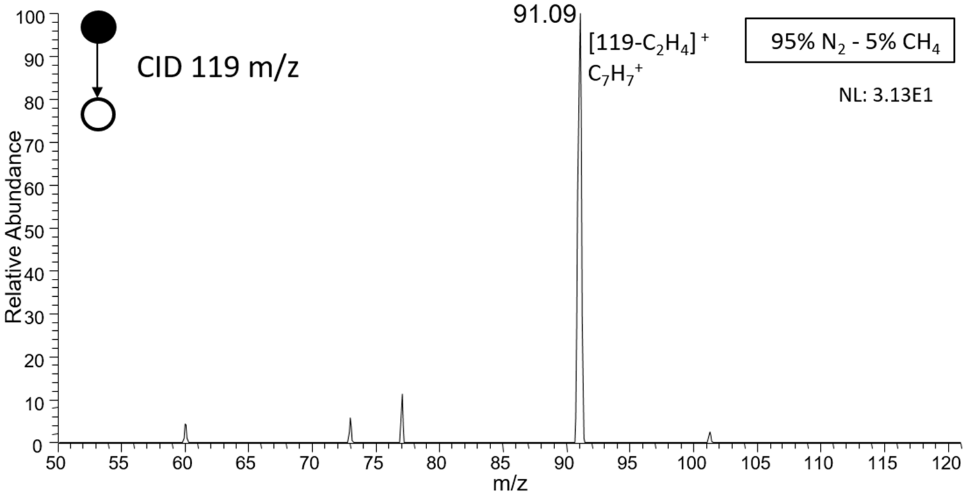

Figure 3.10. CID spectrum of the 119 m/z DART peak for the 95-5 N_2-CH sample. Overall intensity is reported as the normalized target level (NL).

The 119 m/z peak is only observed in the 95-5 sample. The CID analysis of that peak revealed that this compound shows no adduct formation, and only produces a major fragment of 91 m/z from a loss of 28 Da, i.e., either CH_2N or C_2H_4, both of which are possible for this sample considering that imines have been detected in the IR analysis. The high intensity of the 91 m/z peak implies it is a stable fragment produced from a favored fragmentation pathway, suggesting it could be due to a tropylium cation from a toluene-like parent ion. This would imply that the 91 m/z fragment results from a loss of 27 Da only, which would correspond to a hydrogen cyanide (HCN) loss. Such a loss would also be reasonable considering the presence of cyanides in this sample, but the resulting formulae of C_8H_8N for the parent molecule does not produce any viable chemical structure. As a consequence,

C_9H_{10} seems the most likely formula, and methylstyrene the best assignment since it accounts for the observation of a 91 m/z CID fragment resulting from an ethylene loss.

While the observation of hydrocarbons is known to be difficult in DART, α-methylstyrene has been observed before at high temperature,[60] indicating that some assistive ionization processes may be occurring in this sample. This assignment would also account for the lack of adduct formation, which is usually extremely common for DART detectable species. The production of methylstyrene could be questioned as coming from the background, but since this peak was not seen in any other sample and is observable even with background subtraction, that is unlikely. Observation of this compound in only the 95-5 sample is curious, since both benzene and acetylene should contribute to its production. A likely possibility is that the benzene and acetylene are consumed in other processes which prohibit the production of a small aromatic such as methylstyrene. Modeling could provide insight into why this product is only seen for the 95-5 sample and not the others. This could lead to interesting implications for Titan chemistry.

As the molecular mass increases, the exact identification of species via one-step CID becomes difficult due to the increasing number of structural isomers possible. As a consequence, the following CID analyses on higher mass peaks was conducted with a focus on identifying losses and chemical formulae with the most stable and reasonable isomers. Any compound suggestions will need to be studied with higher mass resolution or other methods in the future to identify possible species with increased confidence.

3.4.4.6 130 m/z CID analysis

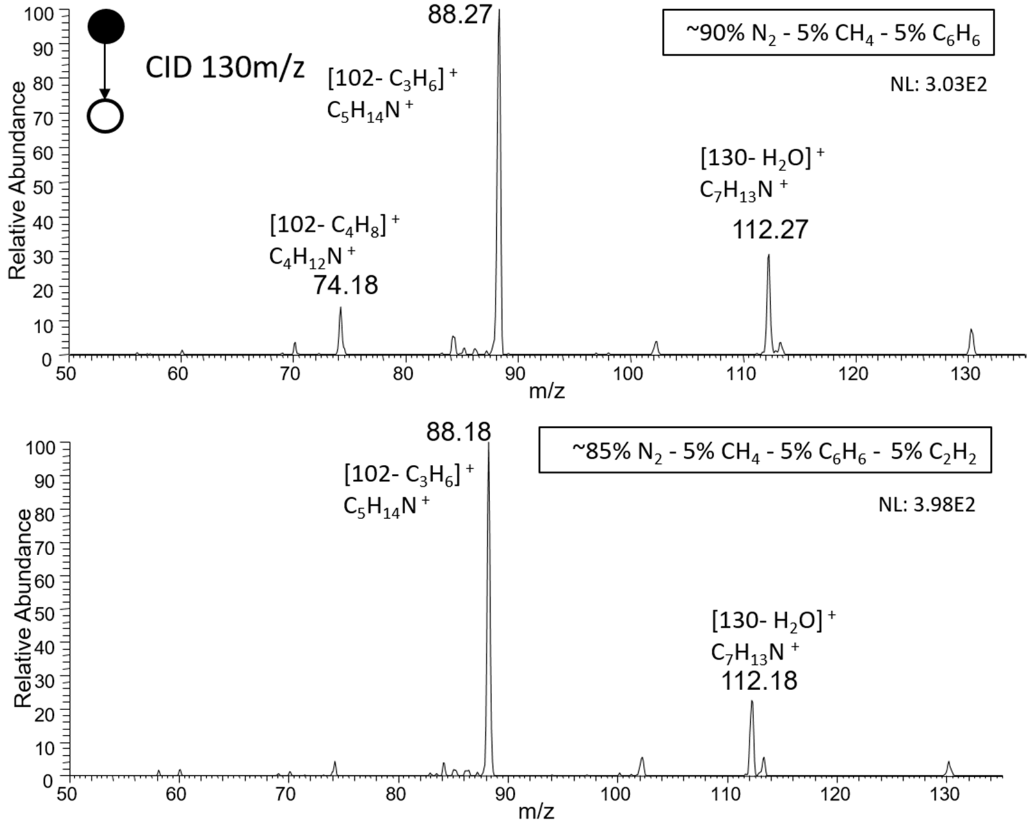

Figure 3.11. CID spectra of the 130 m/z DART peak for the benzene-doped samples from top to bottom: 90-5-5 N_2-CH_4-C_6H_6 (benzene) and 86-5-4-5 N_2-CH_4-C_2H_2-C_6H_6 (acetylene and benzene). Overall intensity is reported for each spectrum as the normalized target level (NL).

The first peak to be analyzed with this method was 130 m/z, shown in figure 3.11. This peak was observed only in the benzene doped (90-5-5) and acetylene and benzene doped (86-5-4-5) samples, and was a more abundant peak in the overall spectrum for the former. Both CID spectra show evidence for a water adduct at 112 m/z. After evaluating different possible formulae, $C_7H_{13}N$ gives the greatest number of likely isomers. Because no peaks due to a 17 Da loss (like the ones observed in the 114 m/z CID spectra) were observed in the 130 m/z CID spectra, it was concluded that the parent molecule(s) did not contain a primary amine. This leaves a secondary amine, tertiary amine or a nitrile group as possible functional groups present in structures for the 130 m/z molecule, which are all reasonable since IR bands corresponding to secondary amines and nitriles have been observed for both these samples. Higher sensitivity would be necessary to perform subsequent CID and obtain an exact identification.

The other major fragment ion in both samples is 88 m/z, corresponding to a loss of C_3H_6 or C_2H_4N from 130 m/z. Taking these losses into account and considering the stable isomers for which one of these two losses are possible, the most likely possibility appears to be the loss of C_3H_6 from $C_8H_{19}N$. This would correspond to a secondary amine, likely comparable to the loss observed in the CID analysis of the 74 m/z DART peak, but there are too many isomers to make an exact structural identification.

The interesting aspect of the two identifications (resulting from the 112 m/z and 88 m/z fragments) is that neither formula is indicative of aromatic constituents, even though 130 m/z is not observed unless benzene is present in the gas mixture. The small amount of 130 m/z species still observed in the CID suggests that there may be some stable aromatic compounds present, but those cannot be confirmed due to the lack of CID fragmentation peaks. Non-aromatic compounds within 130 m/z suggests that the presence of benzene within the initial mixture can induce different chemical pathways, similar to the mechanism proposed for pyridine, that do not always result in aromatic compounds. The complexity of the different chemical pathways caused by the inclusion of these dopants indicates that microenvironments and concentration gradients for molecules such as benzene need to be taken into account for more complex mechanisms in Titan's atmosphere.

3.4.4.7 147 m/z CID analysis

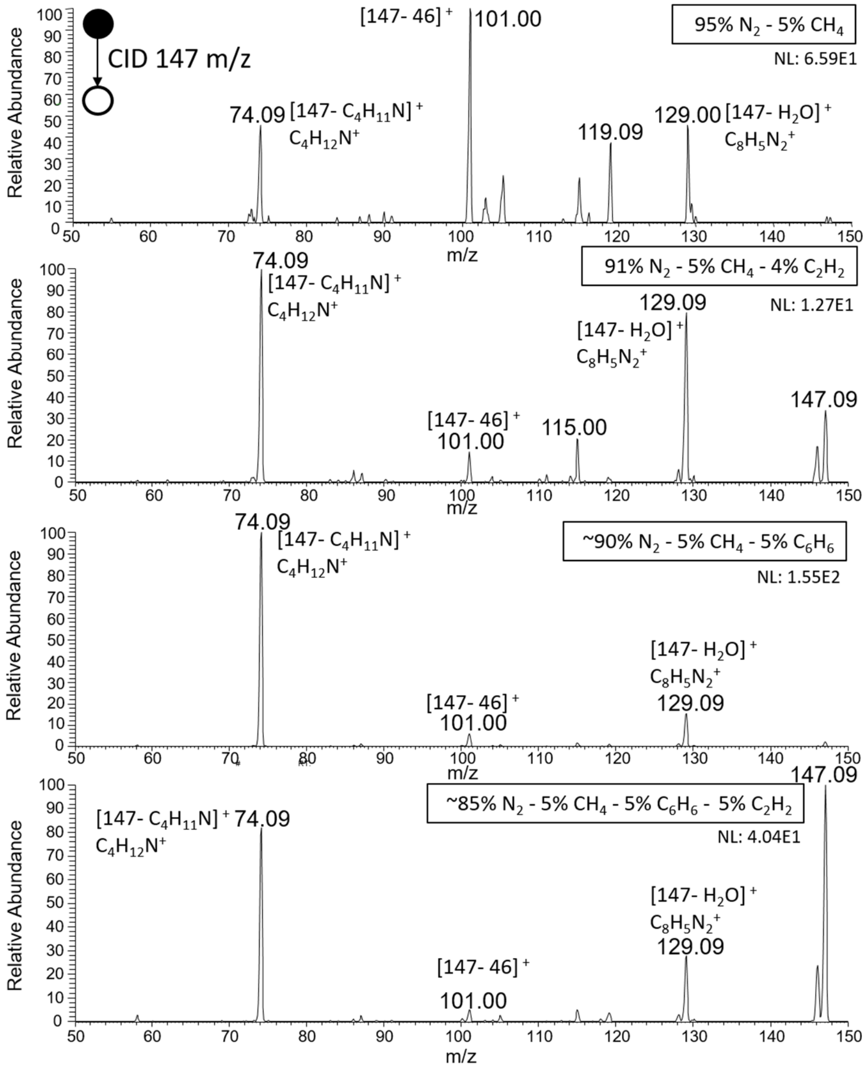

Figure 3.12. CID spectra of the 147 m/z DART peak for the four THS samples, from top to bottom: 95-5 N2-CH4, 91-5-4 N2-CH4-C2H2 (acetylene), 90-5-5 N2-CH4-C6H6 (benzene), 86-5-4-5 N2-CH4-C2H2-C6H6 (acetylene and benzene). Major fragments and losses are labeled. Overall intensity is reported for each spectrum as the normalized target level (NL).

CID spectra for the 147 m/z DART were acquired for all four samples, and are shown in figure 3.12. For all four THS samples, a fragment ion is observed at 74 m/z, which suggests that a dimer of 74 m/z, with a most likely formula of $C_4H_{11}N$, is a constituent of the 147 m/z peak. Since 74 m/z is the major peak in the overall DART spectrum for all four samples, the observation of a proton bound dimer is not surprising.

The next fragment ion investigated was 129 m/z and, due to a loss of 18 Da, was identified as a water adduct. Assignment for this species is difficult, since there are two possible formulae which would allow for stable isomers: $C_7H_{16}N_2$, in which amine isomers are abundant, and $C_8H_4N_2$, in which aromatic nitriles are the most common. Without further CID, possible assignment is based on comparison with the IR analysis of these samples. The IR data reported in Part II shows aliphatic secondary amine, C-N bond, and aromatic nitrile bands were observed for all four samples. The 129 m/z peak overall intensity is much higher in the benzene doped sample (considering the higher NL intensity for the CID spectrum), indicating that benzene is included in its synthesis as either a reactant or assisting in its production, similar to the synthesis of pyridine. Taking this into account, the $C_8H_4N_2$ formula is most likely the highest contributor to this peak, due to the aromaticity allowed by this formula and taking into account the presence of the more unique aromatic nitrile band in the IR of all four samples. The most likely compound for this formula would be dicyanobenzene, but higher sensitivity and subsequent CID will be needed in the future to confirm this identification.

In the acetylene doped (91-5-4) and acetylene and benzene doped (86-5-4-5) samples, an unfragmented 147 m/z peak is observed, suggesting a highly aromatic molecule with little substitution, for which two likely formulae are $C_{11}H_{14}$ and $C_9H_{10}N_2$. Both of these have a high number of isomers which would not be expected to fragment, so one cannot be identified over the other. The other common peaks between the four different samples are 101 m/z and 115 m/z, with the former being the most abundant fragment for the 95-5 sample and an extremely small fragment in the other samples, and the latter being a less abundant fragment for all four samples. The losses these peaks correspond to are difficult to explain: neither 46 Da for the 101 m/z peak nor 32 Da for the 115 m/z peak have an easily identifiable loss formula. These fragment peaks thus most likely result from two-step processes, and cannot be identified without subsequent CID analysis.

The 95-5 sample displays two more fragments: 119 m/z and 105 m/z. The 119 m/z fragment is likely methylstyrene, having been identified via CID of the 119 m/z peak itself, which would likely come from the loss of ethylene from the 147 m/z parent ion. Ethylene loss from an aromatic compound similar to methylstyrene is possible, but more unfragmented parent ion would be expected in this case. The loss of methylimine from 147 m/z would better explain the fragmentation, but identification of a stable isomer for the parent formula $C_{10}H_{12}N$ is difficult, and as such an exact identification cannot be made. $C_{11}H_{14}$ can still be proposed as the most likely formula for the parent molecule though. The 105 m/z fragment, with a loss of 42 Da, would then likely be due to a loss of propene from $C_{11}H_{14}$ as well, with the fragment itself being styrene. This fits with the 119 m/z fragment belonging to methylstyrene. This does not make identification any simpler though due to the possible isomers and the same difficulties in identifying the prior 119 m/z parent. Other identifications were not attempted due to a combination of low abundance, concurrence with background CID spectra, and high number of possible isomers. Overall, the CID analysis of the 147 m/z DART mass peak shows that with increasing mass comes increasing complexity. Many of these assignment difficulties could be addressed in the future with greater sensitivity, enabling more levels of CID analysis.

More CID spectra from these samples, reported in the SI, were not analyzed in this study due to insufficient resolution and the need for more fragmentation steps with increasing mass. The CID data reported here demonstrate the role that a dopant can play in the synthesis of unique compounds and the enhancement of the synthesis for other compounds. While initial proposals were made for many of the compounds identified here regarding synthesis, modeling studies outside the scope of this experimental study will be necessary in the future to confirm synthetic pathways and their relevance for Titan's atmosphere.

3.5 Conclusions

The Part I study demonstrated the capability of the Titan Haze Simulation (THS) experiment to probe the first and intermediate steps of Titan's atmospheric chemistry in the gas phase, and monitor the influence of dopants on the gas-phase chemistry. The Part II study performed the first analysis of the THS solid phase products with SEM and IR, identifying the aerosol growth and the many different chemical functionalities present in the material, and assessing the influence of the dopant on these parameters. Additionally, in Part II, the low temperature characteristics of the plasma were confirmed, demonstrating the THS experiment is representative of the low-temperature conditions on Titan. In this study, we have characterized the composition of the THS solid aerosols, produced in the same gas mixtures utilized in Part II, with DART-MS, building upon the analyzes presented in Parts I and II.

The analysis performed here was the first study of a Titan simulant with DART-MS, demonstrating that the technique can be applied to the study of the solid phase aerosol products without solvation or harsh heating required by other mass spectrometric methods for solid phase analysis. The successful analysis presented here shows that DART-MS is a promising diagnostic tool for the analysis of other Titan simulants to minimize possible reactions from sample preparation methods. Further analysis of other aerosol analogues with DART-MS could allow for a better understanding of any sample changes caused by other analytical methods. The success of this analysis indicates that DART-MS and analytical methods like it should be taken into consideration for *in-situ* applications, such as future missions to Titan and other planetary bodies. The limitations in identifications due to low mass resolution and sensitivity can be addressed in future studies, for which this study will provide a foundation.

The EZ-DART-MS analysis presented here has allowed for multiple insights into the solid-phase THS simulants and their possible implications for Titan atmospheric chemistry. While these results are only applicable for molecules detectable by DART-MS, a large number of compounds were identified.

The results of these analyses show that:

- The DART spectra of the THS samples have demonstrated their surprising simplicity in composition compared to other Titan aerosol analogues for the mass range studied. While other experiments may generate aerosols from a stochastic mixture of C, H, and N, the controlled, truncated chemistry of the THS experiment allows for the production of aerosols from specific chemical pathways, either the first steps of the N_2-CH_4 chemistry or more focused chemical processes when adding dopants to the initial N_2-CH_4 mixture. Contrary to other experiments that use continuous plasma as the energy source, the aerosol analogues produced in the THS are not overly processed in the pulsed plasma and thus could provide insight into early stage chemistry and specific chemical pathways in Titan's atmosphere.

The simplicity of the samples was further confirmed by analysis with a higher temperature DART flow gas. The samples produced in the two simplest mixtures, N_2-CH_4 (95-5) and N_2-CH_4-C_2H_2 (91-5-4) along with the acetylene and benzene doped (86-5-4-5) sample only displayed decreased in intensity when heated as opposed to the expected higher mass species. Only the benzene doped (90-5-5) sample produced a spectrum with higher intensity for some of the peaks already detected at room temperature but no detection of heavier products, confirming the simplicity of the sample. This fits with the analysis performed in Part II showing more complex aromatic production in the benzene doped sample. This analysis at higher temperature also confirmed the ability to complete the DART analysis at room temperature allowing for DART spectra to be obtained without possible degradation from heating.

- The preservation of small molecules detectable with DART analysis indicates that these smaller semi-volatile compounds are preserved during sample collection, likely by being trapped in aerosols. Similar molecules may also be preserved on Titan in the same way during longer scale aerosol accumulation.
- The CID analysis showed several types of nitrogen incorporation, confirming similar observations in the IR analysis of Part II. The most commonly observed nitrogen-compounds in this study were amines and nitriles. The incorporation of nitriles in the Titan simulation laboratory experiment is not surprising since nitriles have been detected on Titan, but the observation of multiple amines experimentally increases the expectation for amines being present on Titan, even though they have not yet been detected there.
- The large differences in the benzene doped (90-5-5) sample compare to the other THS samples provide some interesting insights into the impact high molecular weight dopants can have on the chemistry. While the IR results indicate that it is not the most representative gas mixture for Titan aerosol analogues, the impacts benzene has on the production of different compounds as observed in the DART-MS needs to be taken into consideration. The increased production of some compounds and unique nature of the mixture could have interesting implication for benzene rich regions on Titan, considering variation of the benzene mixing ratio as well as benzene

condensation have been observed depending on altitude and seasonal variations.

The DART analysis presented here has shown the effects of particular dopants on the production, or lack thereof, of particular compounds. For example, the production of small amines is only detected in the 95-5 THS sample, indicating that other mechanisms impede their production in the presence of dopants. Another example is the much larger production of pyridine in the presence of benzene, not only providing support for a mechanism reported in other studies but also showing that these dopants have synthetic impacts beyond their direct inclusion into the observed products. These results justify future studies with other dopants and mechanistic investigations into the implications this analysis may have for Titan atmospheric chemistry.

3.6 Acknowledgements

We would like to thank Mark Smith for providing the Arizona Titan aerosol simulant sample for analysis. The research was funded by NSF award number CHE-1508825. The early part of this work was funded by NASA Astrobiology Institute, Titan as a Prebiotic Chemical System, the Keck Institute for Space Studies, Future Missions to Titan: Scientific and Engineering Challenges, and NASA SMD (SSW). K.T.U. acknowledges financial support from the Harriett Jenkins Pre-Doctoral Fellowship Program. We also thank the Caltech Glass Shop for their assistance in the fabrication of the EZ-DART source and the technical support of R. Walker and E. Quigley (NASA ARC).

3.7 References

1. C. Sagan, W. R. Thompson and B. N. Khare, *Accounts of Chemical Research*, 1992, **25**, 286-292.
2. H. B. Niemann, S. K. Atreya, J. E. Demick, D. Gautier, J. A. Haberman, D. N. Harpold, W. T. Kasprzak, J. I. Lunine, T. C. Owen and F. Raulin, *J Geophys Res-Planet*, 2010, **115**, E12006.
3. H. B. Niemann, S. K. Atreya, S. J. Bauer, G. R. Carignan, J. E. Demick, R. L. Frost, D. Gautier, J. A. Haberman, D. N. Harpold, D. M. Hunten, G. Israel, J. I. Lunine, W. T. Kasprzak, T. C. Owen, M. Paulkovich, F. Raulin, E. Raaen and S. H. Way, *Nature*, 2005, **438**, 779-784.
4. F. Raulin, *Space Science Reviews*, 2005, **116**, 471-487.
5. F. Raulin and T. Owen, *Space Science Reviews*, 2002, **104**, 377-394.
6. W. C. Maguire, R. A. Hanel, D. E. Jennings, V. G. Kunde and R. E. Samuelson, *Nature*, 1981, **292**, 683-686.
7. V. G. Kunde, A. C. Aikin, R. A. Hanel, D. E. Jennings, W. C. Maguire and R. E. Samuelson, *Nature*, 1981, **292**, 686-688.
8. F. M. Flasar, R. K. Achterberg, B. J. Conrath, P. J. Gierasch, V. G. Kunde, C. A. Nixon, G. L. Bjoraker, D. E. Jennings, P. N. Romani, A. A. Simon-Miller, B. Bézard, A. Coustenis, P. G. J. Irwin, N. A. Teanby, J. Brasunas, J. C. Pearl, M. E. Segura, R. C. Carlson, A. Mamoutkine, P. J. Schinder, A. Barucci, R. Courtin, T. Fouchet, D. Gautier, E. Lellouch, A. Marten, R. Prangé, S. Vinatier, D. F. Strobel, S. B. Calcutt, P. L. Read, F. W. Taylor, N. Bowles, R. E. Samuelson, G. S. Orton, L. J. Spilker, T. C. Owen, J. R.

Spencer, M. R. Showalter, C. Ferrari, M. M. Abbas, F. Raulin, S. Edgington, P. Ade and E. H. Wishnow, *Science*, 2005, **308**, 975-978.

9. M. L. Cable, S. M. Hörst, R. Hodyss, P. M. Beauchamp, M. A. Smith and P. A. Willis, *Chemical Reviews*, 2012, **112**, 1882-1909.
10. F. Raulin, C. Brasse, O. Poch and P. Coll, *Chemical Society Reviews*, 2012, **41**, 5380-5393.
11. M. Fulchignoni, F. Ferri, F. Angrilli, A. J. Ball, A. Bar-Nun, M. A. Barucci, C. Bettanini, G. Bianchini, W. Borucki, G. Colombatti, M. Coradini, A. Coustenis, S. Debei, P. Falkner, G. Fanti, E. Flamini, V. Gaborit, R. Grard, M. Hamelin, A. M. Harri, B. Hathi, I. Jernej, M. R. Leese, A. Lehto, P. F. Lion Stoppato, J. J. Lopez-Moreno, T. Makinen, J. A. M. McDonnell, C. P. McKay, G. Molina-Cuberos, F. M. Neubauer, V. Pirronello, R. Rodrigo, B. Saggin, K. Schwingenschuh, A. Seiff, F. Simoes, H. Svedhem, T. Tokano, M. C. Towner, R. Trautner, P. Withers and J. C. Zarnecki, *Nature*, 2005, **438**, 785-791.
12. S. M. Hörst, *Journal of Geophysical Research: Planets*, 2017, **122**, 432-482.
13. E. Sciamma-O'Brien, N. Carrasco, C. Szopa, A. Buch and G. Cernogora, *Icarus*, 2010, **209**, 704-714.
14. N. Sarker, A. Somogyi, J. I. Lunine and M. A. Smith, *Astrobiology*, 2003, **3**, 719-726.
15. H. Imanaka, B. N. Khare, J. E. Elsila, E. L. O. Bakes, C. P. McKay, D. P. Cruikshank, S. Sugita, T. Matsui and R. N. Zare, *Icarus*, 2004, **168**, 344-366.
16. C. He, G. Lin, K. T. Upton, H. Imanaka and M. A. Smith, *The Journal of Physical Chemistry A*, 2012, **116**, 4760-4767.
17. H. Imanaka and M. A. Smith, *Geophysical Research Letters*, 2007, **34**.

18. H. Imanaka and M. A. Smith, *Proceedings of the National Academy of Sciences*, 2010, **107**, 12423-12428.
19. R. Thissen, V. Vuitton, P. Lavvas, J. Lemaire, C. Dehon, O. Dutuit, M. A. Smith, S. Turchini, D. Catone, R. V. Yelle, P. Pernot, A. Somogyi and M. Coreno, *The Journal of Physical Chemistry A*, 2009, **113**, 11211-11220.
20. B. Cunha de Miranda, G. A. Garcia, F. Gaie-Levrel, A. Mahjoub, T. Gautier, B. Fleury, L. Nahon, P. Pernot and N. Carrasco, *The Journal of Physical Chemistry A*, 2016, **120**, 6529-6540.
21. C. Szopa, G. Cernogora, L. Boufendi, J. J. Correia and P. Coll, *Planetary and Space Science*, 2006, **54**, 394-404.
22. G. Alcouffe, M. Cavarroc, G. Cernogora, F. Ouni, A. Jolly, L. Boufendi and C. Szopa, *Plasma Sources Sci T*, 2010, **19**.
23. N. Carrasco, F. Jomard, J. Vigneron, A. Etcheberry and G. Cernogora, *Planetary and Space Science*, 2016, **128**, 52-57.
24. E. Sciamma-O'Brien, C. L. Ricketts and F. Salama, *Icarus*, 2014, **243**, 325-336.
25. E. Sciamma-O'Brien, K. T. Upton and F. Salama, *Icarus*, 2017, **289**, 214-226.
26. A. Somogyi, C. H. Oh, M. A. Smith and J. I. Lunine, *Journal of the American Society for Mass Spectrometry*, 2005, **16**, 850-859.
27. A. Somogyi, M. A. Smith, V. Vuitton, R. Thissen and I. Komaromi, *Int J Mass Spectrom*, 2012, **316**, 157-163.
28. A. Somogyi, R. Thissen, F. R. Orthous-Daunay and V. Vuitton, *Int J Mol Sci*, 2016, **17**.
29. M. C. Pietrogrande, P. Coll, R. Sternberg, C. Szopa, R. Navarro-Gonzalez, C. Vidal-Madjar and F. Dondi, *Journal of Chromatography A*, 2001, **939**, 69-77.

30. M. Morisson, C. Szopa, N. Carrasco, A. Buch and T. Gautier, *Icarus*, 2016, **277**, 442-454.
31. M. E. Monge and F. M. Fernandez, in *Ambient Ionization Mass Spectrometry*, The Royal Society of Chemistry, 2015, DOI: 10.1039/9781782628026-00001, pp. 1-22.
32. M. E. Monge, G. A. Harris, P. Dwivedi and F. M. Fernandez, *Chem Rev*, 2013, **113**, 2269-2308.
33. X. Ding and Y. Duan, *Mass Spectrometry Reviews*, 2015, **34**, 449-473.
34. W. Romão, L. V. Tose, B. G. Vaz, S. G. Sama, R. Lobinski, P. Giusti, H. Carrier and B. Bouyssiere, *Journal of The American Society for Mass Spectrometry*, 2016, **27**, 182-185.
35. K. A. Schilling Fahnestock, L. D. Yee, C. L. Loza, M. M. Coggon, R. Schwantes, X. Zhang, N. F. Dalleska and J. H. Seinfeld, *The Journal of Physical Chemistry A*, 2015, **119**, 4281-4297.
36. M. N. Chan, T. Nah and K. R. Wilson, *Analyst*, 2013, **138**, 3749-3757.
37. R. B. Cody, J. A. Laramée and H. D. Durst, *Analytical Chemistry*, 2005, **77**, 2297-2302.
38. L. Song, S. C. Gibson, D. Bhandari, K. D. Cook and J. E. Bartmess, *Analytical Chemistry*, 2009, **81**, 10080-10088.
39. R. B. Cody, *Analytical Chemistry*, 2009, **81**, 1101-1107.
40. R. B. Cody and A. J. Dane, *Journal of The American Society for Mass Spectrometry*, 2013, **24**, 329-334.
41. K. Upton, K. Schilling and J. Beauchamp, *Analytical Methods*, 2017, **9**, 5065-5074.
42. B. H. P. Broks, W. J. M. Brok, J. Remy, J. J. A. M. van der Mullen, A. Benidar, L. Biennier and F. Salama, *Physical Review E*, 2005, **71**, 036409.
43. L. Biennier, A. Benidar and F. Salama, *Chemical Physics*, 2006, **326**, 445-457.

44. A. R. Johnson and E. E. Carlson, *Analytical Chemistry*, 2015, **87**, 10668-10678.
45. Vinatier S. et. al., *Icarus*, submitted.
46. J. H. Gross, *Analytical and Bioanalytical Chemistry*, 2014, **406**, 63-80.
47. P. Ehrenfreund, J. J. Boon, J. Commandeur, C. Sagan, W. R. Thompson and B. Khare, *Adv Space Res*, 1994, **15**, 335-342.
48. E. H. Wilson and S. K. Atreya, *Planetary and Space Science*, 2003, **51**, 1017-1033.
49. Z. Zhang, X. Gong, S. Zhang, H. Yang, Y. Shi, C. Yang, X. Zhang, X. Xiong, X. Fang and Z. Ouyang, *Scientific Reports*, 2013, **3**, 3481.
50. D. S. N. Parker, R. I. Kaiser, O. Kostko, T. P. Troy, M. Ahmed, B.-J. Sun, S.-H. Chen and A. H. H. Chang, *Physical Chemistry Chemical Physics*, 2015, **17**, 32000-32008.
51. M. Cordiner, M. Y Palmer, C. A. Nixon, S. B. Charnley, M. J. Mumma, P. G. J. Irwin, N. A. Teanby, Z. Kisiel and J. Serigano, 2015.
52. V. Vuitton, R. V. Yelle and J. Cui, *Journal of Geophysical Research: Planets*, 2008, **113**, E05007.
53. Y. Sekine, S. Lebonnois, H. Imanaka, T. Matsui, E. L. O. Bakes, C. P. McKay, B. N. Khare and S. Sugita, *Icarus*, 2008, **194**, 201-211.
54. Q. Wu, H. Shi, Y. Ma, C. Adams, T. Eichholz, T. Timmons and H. Jiang, *Talanta*, 2015, **131**, 736-741.
55. A. Belloche, K. M. Menten, C. Comito, H. S. P. Müller, P. Schilke, J. Ott, S. Thorwirth and C. Hieret, *A&A*, 2008, **482**, 179-196.
56. J. C. Loison, E. Hébrard, M. Dobrijevic, K. M. Hickson, F. Caralp, V. Hue, G. Gronoff, O. Venot and Y. Bénilan, *Icarus*, 2015, **247**, 218-247.

57. N. Balucani, F. Leonori, R. Petrucci, M. Stazi, D. Skouteris, M. Rosi and P. Casavecchia, *Faraday Discussions*, 2010, **147**, 189-216.

58. A. M. Hamid, P. P. Bera, T. J. Lee, S. G. Aziz, A. O. Alyoubi and M. S. El-Shall, *The Journal of Physical Chemistry Letters*, 2014, **5**, 3392-3398.

59. Y. A. Jeilani, C. Fearce and M. T. Nguyen, *Physical Chemistry Chemical Physics*, 2015, **17**, 24294-24303.

60. A. Mess, J. P. Vietzke, C. Rapp and W. Francke, *Anal Chem*, 2011, **83**, 7323-7330.

3.8 Supplemental Information

3.8.1 CID Spectra of 80 m/z

The CID spectra from the 90-5-5 N_2-CH_4-C_6H_6 (benzene) sample and neat pyridine are shown below. Both display the reaction product with water as the only peak.

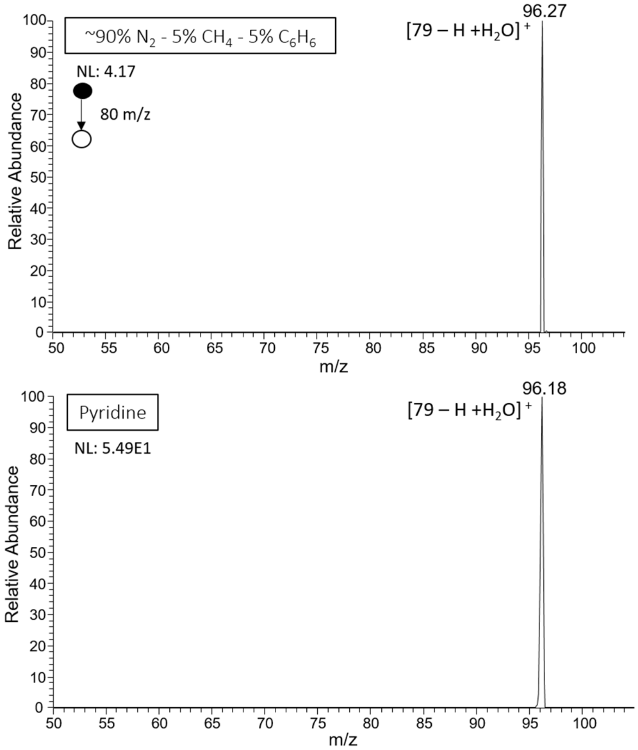

Figure 3.13. Top: Spectrum for the CID of 80 m/z from the 90-5-5 N_2-CH_4-C_6H_6 (benzene) sample. Bottom: Spectrum for the CID of 80 m/z from neat pyridine. Overall intensity is reported for each spectrum as the normalized target level (NL).

3.8.2 CID Spectra of 173 m/z and Discussion

The fragments from 173 m/z are more complicated, since the losses seems to suggest two very different molecular formula making up the peak. The fragment as 113 m/z is from a loss of $C_2H_8N_2$ and is suggestive of the complex formula $C_8H_{20}N_4$. While high degrees of nitrogenation for these molecules is not impossible, it would be unlikely to be favored due to low stability. Even though this species produces the base fragment for 173 m/z, the fact that the parent ion is in low abundance for all four samples increases the support for this formula. The C_2H_4 and C_3H_6 losses are suggestive of $C_{10}H_{23}N_2$, due in part to the high number of isomers that could enable those losses.

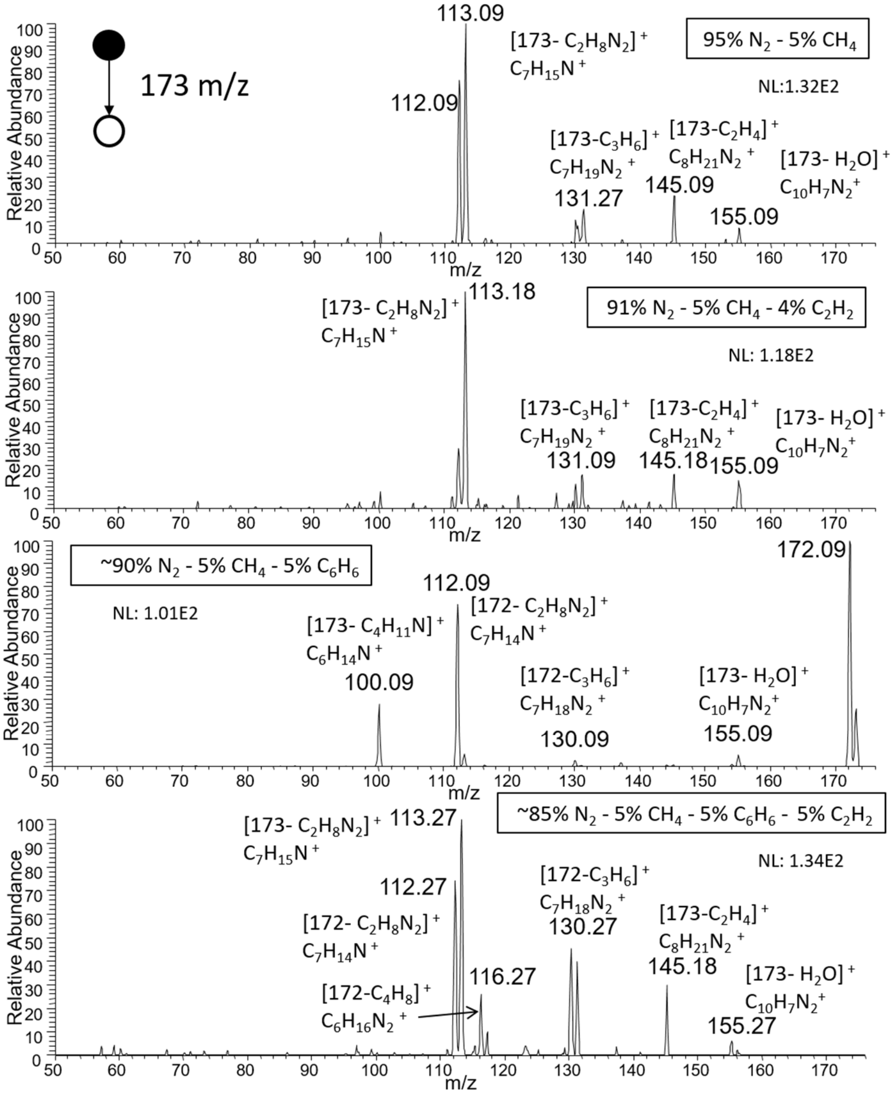

Figure 3.14. The CID of 173 m/z for each sample going, from top to bottom : 95-5 N_2-CH_4, 91-5-4 N_2-CH_4-C_2H_2 (acetylene), 90-5-5 N_2-CH_4-C_6H_6 (benzene), 86-5-4-5 N_2-CH_4-C_2H_2-C_6H_6 (acetylene and benzene). Major fragments and losses are labeled. Overall intensity is reported for each spectrum as the normalized target level (NL).

3.8.3 Spectra without background subtraction and background spectra for each sample

Shown below are all the spectra used for background subtraction and their respective spectra prior to subtraction. The subtraction was performed with the Xcalibur software suite.

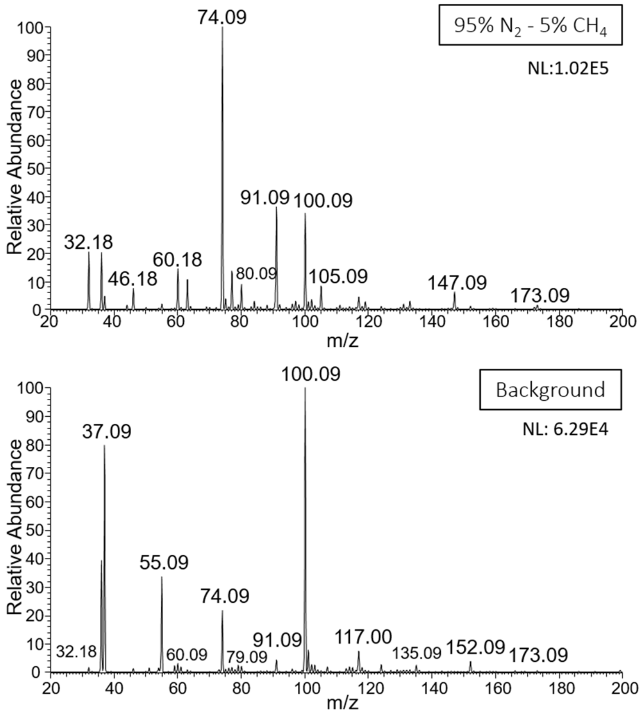

Figure 3.15. Top: Spectrum for the 95-5 N_2-CH_4 sample without background subtraction. Bottom: Background spectrum used for subtraction from the 95-5 N_2-CH_4 spectrum. Overall intensity is reported for each spectrum as the normalized target level (NL).

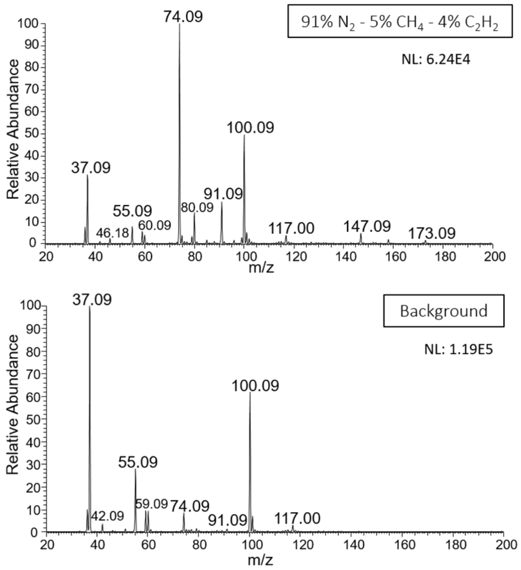

Figure 3.16. Top: Spectrum for the 91-5-4 N_2-CH_4-C_2H_2 (acetylene) sample without background subtraction. Bottom: Background spectrum used for subtraction from the 91-5-4 N_2-CH_4-C_2H_2 (acetylene) spectrum. Overall intensity is reported for each spectrum as the normalized target level (NL).

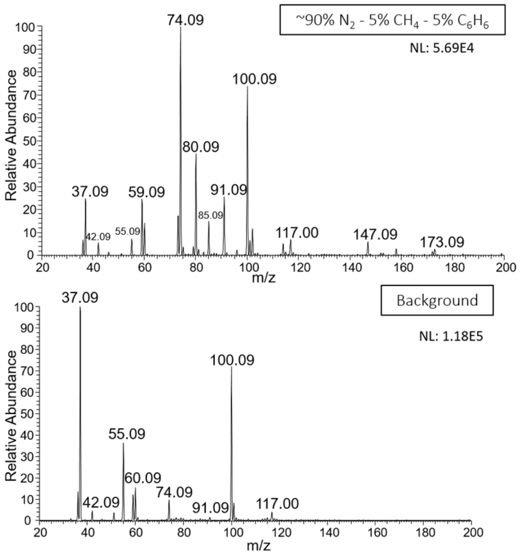

Figure 3.17. Top: Spectrum for the 90-5-5 N_2-CH_4-C_6H_6 (benzene) sample without background subtraction. Bottom: Background spectrum used for subtraction from the 90-5-5 N_2-CH_4-C_6H_6 (benzene) spectrum. Overall intensity is reported for each spectrum as the normalized target level (NL).

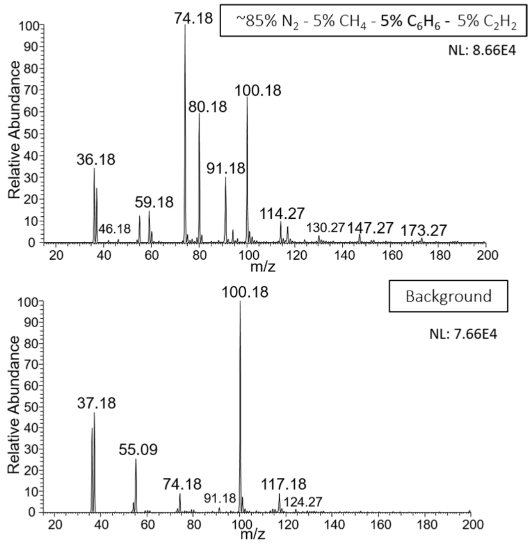

Figure 3.18. Top: Spectrum for the 86-5-4-5 N_2-CH_4-C_2H_2-C_6H_6 (acetylene and benzene) sample without background subtraction. Bottom: Background spectrum used for subtraction from the 86-5-4-5 N_2-CH_4-C_2H_2-C_6H_6 (acetylene and benzene) spectrum. Overall intensity is reported for each spectrum as the normalized target level (NL).

3.8.4 CID of studied peaks from atmospheric background

The figures below show CID of peaks from an atmospheric background taken after the original samples and background were acquired. If any similarities to peaks from CID of the same peaks in the sample are seen, any peaks analyzed for the sample were higher in intensity. All background CID were acquired under the same conditions used for the samples. CID of 80 m/z in atmospheric background produced no fragments. Overall intensity is reported for each spectrum as the normalized target level (NL).

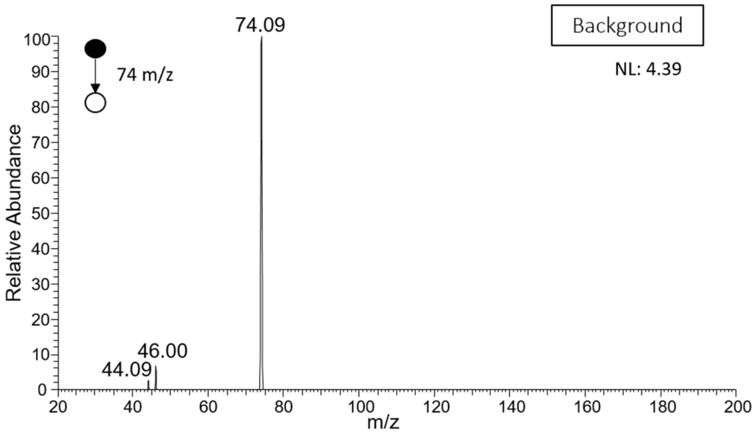

Figure 3.19. CID of the 74 m/z present in atmospheric background.

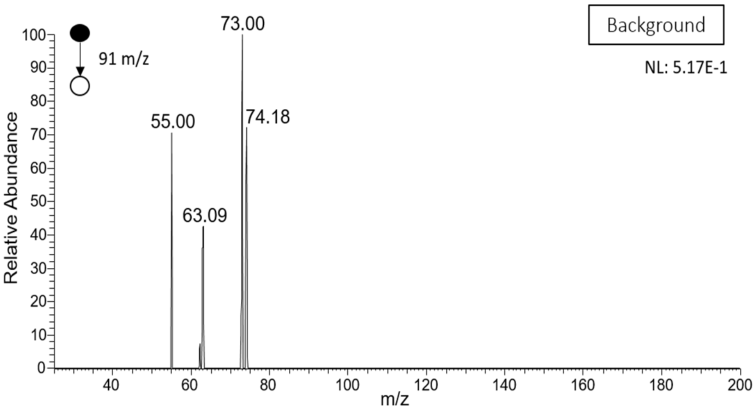

Figure 3.20. CID of the 91 m/z present in atmospheric background.

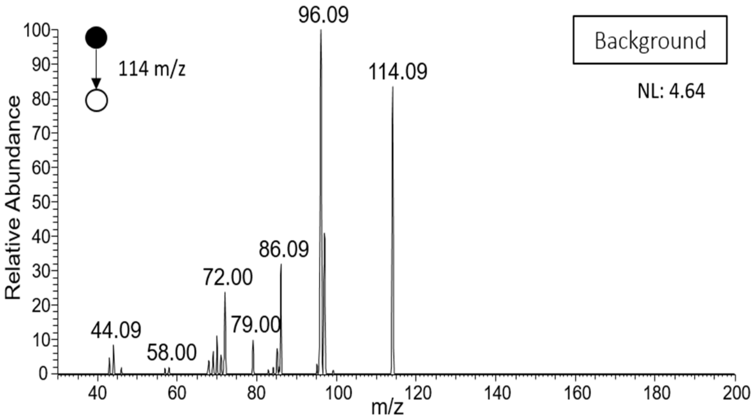

Figure 3.21. CID of the 114 m/z present in atmospheric background.

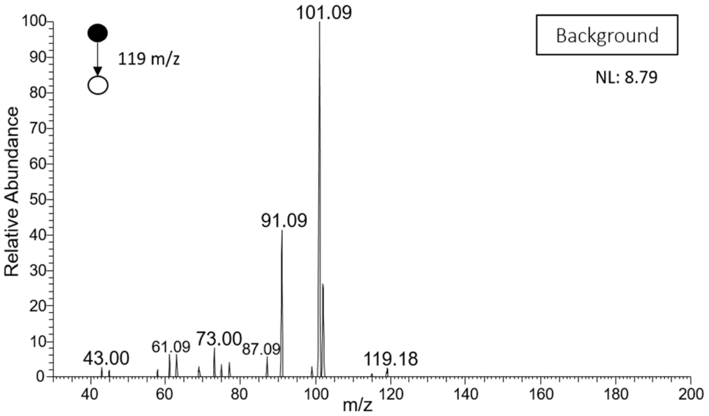

Figure 3.22. CID of the 119 m/z present in atmospheric background.

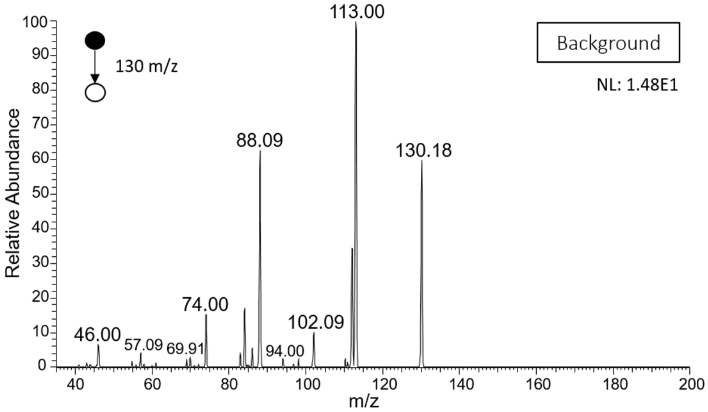

Figure 3.23. CID of the 130 m/z present in atmospheric background.

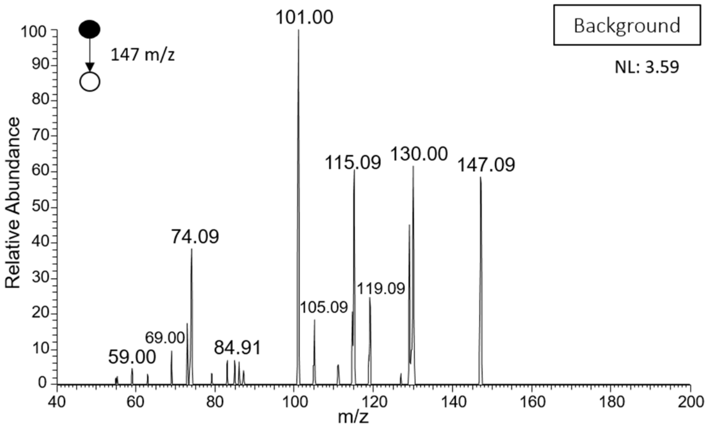

Figure 3.24. CID of the 147 m/z present in atmospheric background.

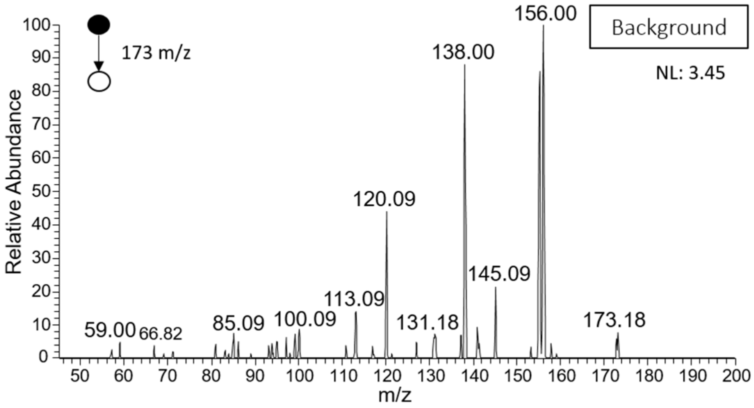

Figure 3.25. CID of the 173 m/z present in atmospheric background.

Chapter 4

ANALYSIS OF TITAN AEROSOL SIMULANTS THROUGH SOLID PHASE MICROEXTRACTION GAS-CHROMATOGRAPHY MASS SPECTROMETRY: A MISSION APPLICABLE ANALYTICAL METHOD FOR SPACE ENVIRONMENTS

4.1 Abstract

Saturn's moon Titan possesses a dense atmosphere comprising mostly nitrogen and methane, with a rich assortment of organic molecules and aerosols. Laboratory based synthesis of simulated Titan aerosols, called tholins, has produced molecules with rich chemical diversity and functionality over a wide range of molecular weights. This diversity has made the tholins difficult to characterize and the need to identify the specific structures of compounds remains. To allow for identification of compounds of various chemical functionalities and sizes, a solid phase microextraction gas chromatography mass spectrometry (SPME-GC-MS) method is proposed. The method allows for the preconcentration of semi-volatile compounds of both polar and non-polar functionalities, their analysis by GC, and subsequent structural identification by MS. This method is applied to a tholin sample generated by a hot plasma discharge in a nitrogen and methane atmosphere. Compounds with an array of molecular weights and structures are identified, spanning the major chemical functionalities expected on Titan. Many of the compounds identified are those seen in prior analyses, but some new compounds of astrobiological interest are also

seen. The large number of compounds successfully characterized suggests that this SPME-GC-MS method would be effective for inclusion on a future lander mission to Titan or other icy worlds.

4.2 Introduction

Due to the discoveries of the Cassini-Huygens mission to the Saturn system, the icy moon of Titan presents an astrochemically interesting target for further study.[1-3] The reasons for this interest are many, such as the nitrogen-methane atmosphere,[4, 5] geographical features including lakes,[6] dunes,[7] and valleys indicative of flowing liquid,[8] and the proposed water-ammonia ocean under the surface.[9] The atmosphere has been one of the most studied aspects of Titan, since its composition may resemble that of an early Earth[10, 11] and is optically opaque due to an abundance of organic aerosols.[10] These aerosols are proposed to consist of diverse organic molecules with elemental compositions comprising carbon, nitrogen and hydrogen.[12, 13] Low molecular weight species such as hydrogen cyanide and acetylene are formed in abundance by various excitation processes in the upper atmosphere.[10, 13-17] The production of more complex species, such as benzene, require complicated reaction mechanisms.[1, 2, 17] With this diversity, precursors to molecules such as amino acids may be readily synthesized, increasing the interest in Titan's chemistry to the astrobiological community. Indeed, amino acid synthesis was observed in studies involving aged Titan aerosol simulants.[18] All of these factors make Titan an interesting target for the study of its atmospheric and surface chemistry.

Studies have been performed to replicate Titan aerosols in the hope of increasing understanding regarding their formation and chemistry. These studies take both Titan like conditions and experimental constraints into consideration when performing aerosol generation.[19-24] The atmosphere, consisting of 90-98% nitrogen and 2-10% methane, is the easiest to replicate.[19] While many different ratios have been tested, the 95% nitrogen and 5% methane ratio has been accepted as the most representative.[25] The low temperature conditions of 95-150K can be readily accommodated, but the lower pressure of 10^{-6}-10^{-7} mbar at 1000 km[26] where the solar photon flux peaks in Titan's atmosphere,[27] is much more difficult to implement. Low pressure increases timescales for reaction, so pressures are typically increased to allow for increased accumulation of aerosol. The energy sources used to produce the aerosol are also varied, with UV light,[21] cold plasma,[28-30] and hot plasma discharges[31] being the most common. While each method of excitation has benefits and detractions, hot plasma discharges produce a large amount of aerosol sufficient for evaluating the efficacy of different analytical methods. Studies on such aerosols will help to inform the choice of analytical methodologies and instrument design for future missions to examine the complex chemistry of the atmosphere and surface of Titan.

A range of different analyses have been performed on simulated Titan aerosols, or tholins, to better understand their chemical composition and the possible implications of that composition for interesting chemistry on Titan. These investigations have found a large number of compounds, with various degrees of nitrogen incorporation, and the expectation of multiple structural isomers of the same chemical composition.[19, 20, 31-34] It becomes highly probable that a subset of these isomers are astrobiologically significant. The large amount of complexity expected in these samples drives the need for analytical methods that can separate different compounds, either by structure or chemical functionality. The use of derivatization is one such possibility, but it typically allows only for the analysis of a single chemical functionality.[35, 36] Additionally, the ability to detect other compounds of interest could be impaired if they are unintentionally changed during the derivatization process.

Prior analyses have encountered problems with differing solubilities of tholin components. Different solution phase extractions have been attempted, but there always remains an insoluble fraction.[19, 31, 34, 37] Prior analyses of tholins in the presence of water have found that some compounds readily react, producing amino acids.[18] While an interesting observation, chemical transformations that accompany solvent addition impair the ability to identify structures of nascent tholin components. Microfluidic based methods have been proposed for future Titan missions, but typically target a single chemical functionality out of the many expected within the aerosol.[36] Ideally, one of the analytical methods included in a Titan mission would allow for the analysis of multiple chemical functionalities simultaneously and without the use of solvents.

Since hydrocarbons and nitriles are expected to occur in abundance on Titan, gas chromatography (GC) has been considered the best at both simultaneous analysis of multiple functionalities and avoiding chemical change through solvation. Pyrolysis based GC has been the most widely studied solvent free method, even having been included on the Huygens lander.[4, 5, 38-41] While the chemical data obtained from that instrument was beneficial to understanding Titan, the instrument was designed primarily for the analysis of atmospheric gases, and was unable to provide chromatographic data due to valve failure during the mission. Additionally the GC method used by that instrument relied on heating the aerosol collected during descent with an aerosol pyrolyzer.[41] Several other methods have also utilized pyrolysis for volatilization, with GC methods to determine which heavier compounds could be detected in Titan aerosols.[39, 40, 42] While these studies have successfully analyzed and identified a variety of organic molecules in different tholin samples, the compounds detected are rarely more complex than benzene. A difficulty with pyrolysis is that it can chemically change the sample, and other work has found that it both induces polymerization and releases hydrogen cyanide.[43] The atmospheric aerosols of Titan are expected to comprise mostly smaller molecules, with larger polymers being unlikely. So while GC enables the broad analysis desired in instrumentation for mission applications, pyrolysis presents difficulties.

A different GC method involves the use of solid phase microextraction (SPME) to preconcentrate gas or solution phase analytes prior to desorption in the GC inlet. SPME-GC has been attempted on tholin samples in the past, but those samples were obtained through discharges in a nitrogen-methane-hydrogen atmosphere in the presence of water.[44, 45] Additionally, the collected tholin was reacted to not only derivatize nascent molecules, but also to fractionate hydrophobic and hydrophilic components.[35, 46] While the SPME analysis for these tholins concentrated on the identification of polyaromatic hydrocarbons (PAHs), neither fraction produced positive results with SPME extraction.[44, 45] Another study using SPME extraction of tholins synthesized in the same manner was able to identify multiple complex aromatics compounds, including PAHs, when extraction was performed after multiple freeze-thaw cycles.[46] Simpler compounds were not detected, as the study focused on the detection of substituted aromatics and PAHs with SPME. While relevant for the study of icy worlds, the majority of Titan tholins are produced with the exclusion of water. This is due to water ice not being present where photochemistry occurs, and thus it will have little if any impact on the chemistry of Titan aerosols. Since more complex compounds are expected to be less abundant in these aerosols compared to smaller nitriles and hydrocarbons, the identification of only substituted aromatics and PAHs with this prior SPME work leads to the need to examine additional SPME extraction methods.

Other SPME studies have been applied to solid phase samples for the identification of small volatile organic compounds (VOCs). Most of these studies concentrate on VOCs released from plant matter, such as leaves and flowers.[47, 48] Additional studies have been performed to examine different volatile products from gas phase reactions simulating those seen in Earth's atmosphere contributing to the production of aerosols.[49-52] These extractions use both high temperature and room temperature conditions, depending on the sample and VOC of interest. These studies report not only great success in the detection of simple VOCs, but also that some of the compounds detected are different from those seen with direct gas phase analysis alone. The success of these studies supports the conjecture that SPME-GC can detect small organics simultaneously with larger more complex molecules from samples such as tholins.

To accomplish the desired analysis of a diverse range of compounds, a study was performed on two different tholin samples considered representative of Titan, using SPME-GC-MS with the goal of assessing and developing a possible mission applicable analytical method. Additionally the study is designed to allow for the analysis of tholins without solvent extraction or excessive heating. The SPME extraction was performed with two different fiber media to better understand its impact on the molecules detected. The results presented in this study show that a wide variety of molecules can be readily detected with SPME extraction and that the fiber media greatly impact the compounds seen in the resultant chromatogram. Both simple and complex molecules are identified with fewer hydrocarbons detected than with other GC studies. The ability to perform GC on less volatile compounds without pyrolysis or solvent extraction, especially using water, make this SPME method one that should be considered for inclusion in future missions to icy worlds, particularly Titan.

4.3 Experimental Methods

4.3.1 Production of Tholins

The two tholin samples examined in this study were produced in a similar manner. The synthesis of T1 performed by Smith and associates at the University of Arizona, and described in detail in prior publications,[23, 31] is summarized here. A gas mixture of 95% nitrogen and 5% methane is flowed inside a high vacuum stainless steel and glass reaction chamber at a temperature of 195K. The flow rate maintained a constant pressure of 850 Pa. An AC electrical discharge, with a current of approximately 100 mA was applied with an estimated discharge exposure time of 2 seconds. Synthesis was continued for 72 hours, after which the vessel was warmed to room temperature under vacuum for 24 hours, and the solid then collected under a nitrogen atmosphere. This sample has been exposed to ambient atmosphere prior to testing. It was stored under ambient atmosphere, but in the dark and frozen, for two years prior to testing.

While T2 has only just recently been investigated, it was synthesized by Hörst and associates at John's Hopkins University in a similar manner.[53] The 95% nitrogen and 5% methane gas mixture was exposed to an AC glow plasma in a ultra-high vacuum reaction chamber at room temperature under a consistent gas flow maintaining a chamber pressure of 400 Pa. After synthesis the reaction chamber was evacuated for 24 hours at room temperature, and the solid was then collected under ambient atmosphere. The samples have since only been exposed to nitrogen atmosphere and stored in the dark at room temperature prior to testing.

4.3.2 Extraction and analysis by SPME-GC-MS

Each extraction, a graphic for which is shown in figure 4.1, was performed using a separate vial for each tholin. All tholins were weighed and placed into 2 mL GC autosampler vial and sealed with a Teflon-faced silicone rubber septum and screw cap. Both samples of T2 were placed in vials while under a nitrogen atmosphere in a glove-bag. Approximately 4 mg were used for each aliquot to allow for comparison. The 100 µm PDMS fiber (Supleco, Bellafonte PA) was held in a manual sample holder during use and the 75 µm CAR/PDMS field sampler assembly (Sigma Aldrich, St. Louis, MO) was used as provided. Each fiber was conditioned prior to use and cleaned between extractions as specified in their respective manuals. All extractions were performed at 60°C with the fiber inserted into the vial headspace. The temperature was held constant during extraction by placing the sample vial in a temperature controlled Teflon coated graphite SCP Science Digi heating block (SCP Science, Champlain, NY). The PDMS extractions were performed for 1 hour and the CAR/PDMS extractions for 15 minutes. Temperature was monitored for the duration of the extraction, with the vial being heated only during the extraction process.

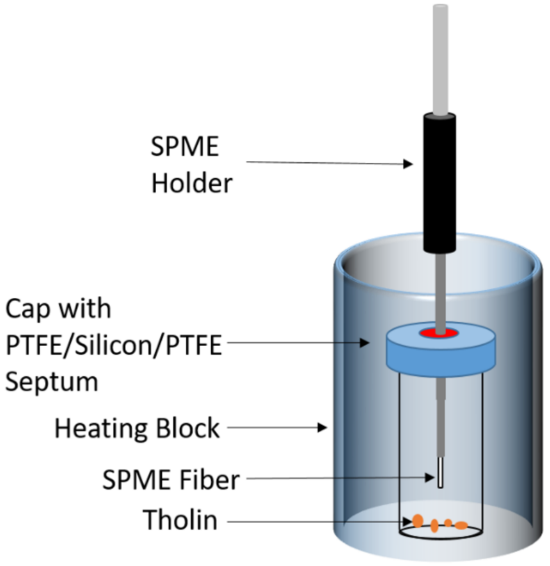

Experimental Steps

If tholin is unexposed to atmosphere:
1. Place tholin in 2 mL vial inside nitrogen filled glove bag

If tholin is exposed, place in vial.

Next steps apply to all tholins
1. Seal 2mL vial with cap and use Teflon tap around cap-vial seal
2. Place SPME holder needle into vial
3. Place vial with SPME needle into heating block
4. Dispense SPME fiber into headspace
5. Allow for adsorption
6. Return fiber to SPME holder
7. Remove sample from heating block

Figure 4.1. A graphic, along with experimental steps, for the extraction process. Extra steps for unexposed samples are specified.

Immediately following extraction, the fiber was inserted into the split-splitless GC inlet at 200°C for 3 minutes under splitless inlet conditions. A new, deactivated, 2mm ID liner was used (Sky liner, Restek Corp., Bellafonte PA). Helium was used for the inlet purge and carrier gas. A 30m x 0.25mm ID x 0.25 µm film thickness 5%-phenyl-arylene-95% dimethylpolysiloxane stationary phase column (Zebron ZB-5MS, Phenomenex, Torrance, CA) was used. For the PDMS extractions the column oven temperature program began at -55°C for 3 minutes followed by ramps to 65°C at 20°C/min, to 130°C at 1.5°C/min, and finally to 200°C at 30°C/min with a final 1 minute hold. With CAR/PDMS extractions the temperature program began at -55°C for 3 minutes, with a ramp to 150°C at 3°C/min, a 3 minute hold at 150°C, a ramp to 200°C at 8°C/min with a final 1 minute hold. Cooling was accomplished by liquid nitrogen. A 5 minute solvent delay was used for all analyses to mitigate effects of the large air peak desorbed from the fibers. The GC-MS instrument used for this study was a Waters Micromass GCT Premier (Waters Corp., Milford, MA) with a mass resolution of 7000 at 219 m/z, from a lock mass peak obtained with heptacosafluorotributylamine, and a mass accuracy of ± 5 mDa. Spectral accumulation was performed in centroid mode.

4.3.3 Standards and Identification

Standards obtained for this study included benzene (HPLC grade), pyrimidine (98%), adiponitrile (99%), succinonitrile (99%), methenamine (99%), dimethylaminoacetonitrile (97%), 2-methylglutaronitrile (99%), propionitrile (99%), 3-pyridinecarbonitrile (98%), tertbutylnitrile (98%), benzonitrile (99%), isobutyronitrile (99%), glutaronitrile (99%), pentanenitrile (99%), and 4-methylpentanenitrile. All were obtained from Sigma Aldrich. Standard solutions were made in milliQ water at 200 µg/mL to 50 µg/mL in 2 mL GC autosampler vials. Headspace extraction was performed for 1 minute to 1 hour depending on the fiber and the standard tested. Compounds not identified by standards were matched used the NIST 2005 EI mass spectrometry library.

4.4 Results and Discussion

The overall chromatogram for the PDMS extraction of both tholins is shown in figures 4.2a and 4.2b, with the CAR/PDMS extraction for T1 shown in figure 4.2c. Retention times are labeled and all identified compounds are tabulated in Table 4.1. In all of these chromatograms peaks corresponding to siloxanes are seen as major peaks. The prevalence of these species is due in part to the nature of the SPME fibers containing siloxanes. A larger contributing factor is the extraction method. These extractions were performed in headspace for longer timescales compared to most other work performed with SPME. Even though T2 was sealed under nitrogen, there is atmospheric leaking over the extraction timescale. Furthermore, the septum is formed from silicone rubber, presenting a large possible source of siloxanes. This contamination is easily removed between sampling by baking out the fibers and ensuring no siloxanes are observed prior to extracting a new tholin sample. Presence of the siloxanes was also confirmed in "blank" extractions done in new, clean, empty vials. As such, the observation of siloxanes is not a major concern and within expectations for this method.

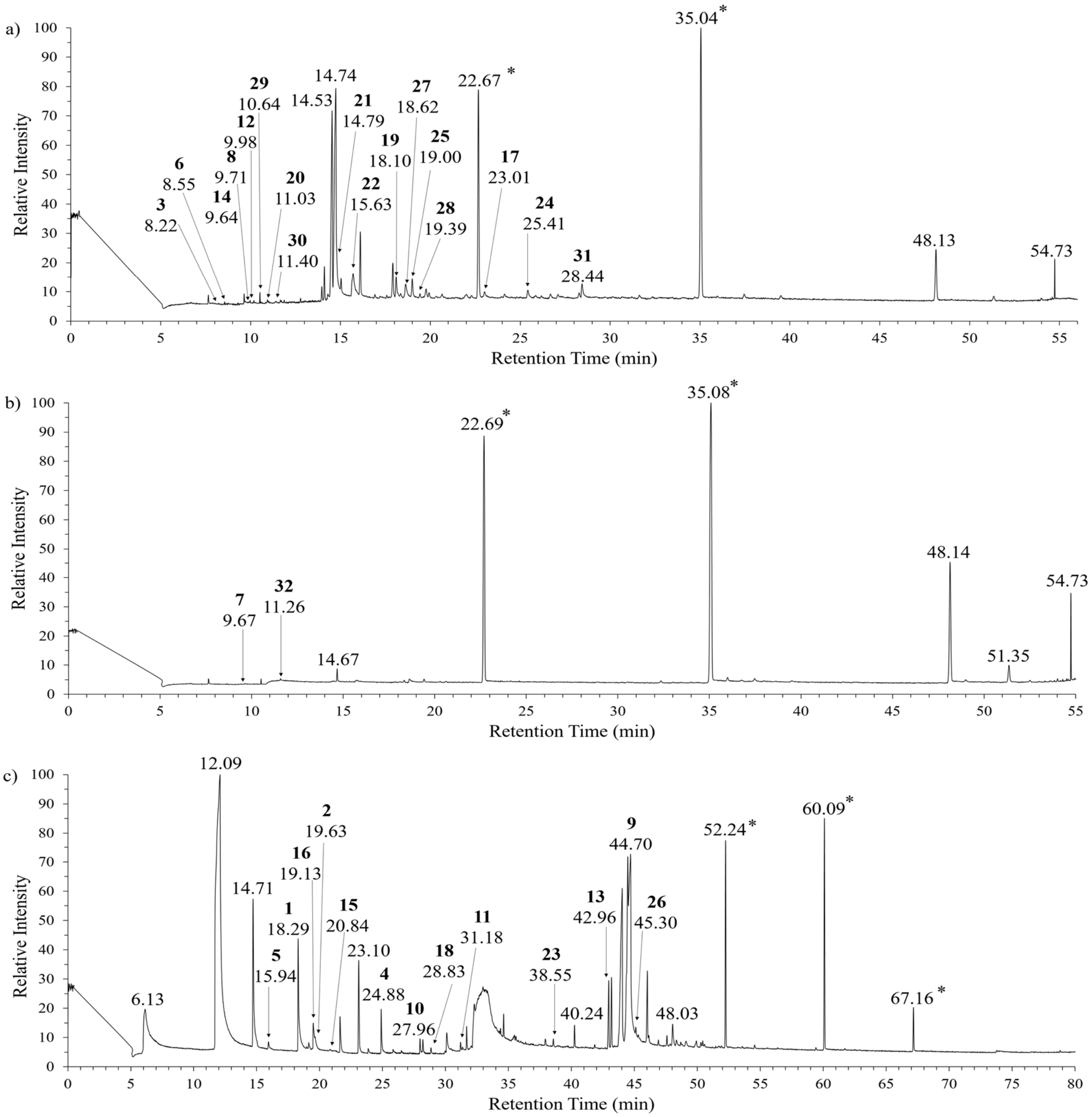

Figure 4.2. a) Total ion chromatogram (TIC) for the PDMS extraction of T1 b) TIC for the PDMS extraction of T2 c) TIC for the CAR/PDMS extraction of T1. Bold numbers refer to the peak number value in Table 4.1. Siloxanes are labeled with an asterisk.

Peak Number	Compound Name	T1		T2
		CAR/PDMS RT (min)	PDMS RT (min)	PDMS RT (if different)
1	propionitrile	18.29	n.d.	n.d.
2	2-methyl-2-propenenitrile	19.63	n.d.	n.d.
3	isobutyronitrile	21.62	8.22	n.d.
4	butanenitrile	24.88	n.d.	n.d.
5	cyclopentane	15.94	n.d.	n.d.
6	benzene	23.10	8.55	X
7	pyridine	n.d.	n.d	9.67
8	pyrimidine	n.d.	9.71	n.d.
9	succinonitrile	44.70	n.d.	n.d.
10	2-methyl-2-butenenitrile	27.96	n.d.	n.d.
11	methylallylcyanide	31.18	n.d.	n.d.
12	pentanenitrile	31.67	9.976	X
13	tertbutylnitrile	42.96	n.d.	n.d.
14	dimethylaminoacetonitrile	30.08	9.64	n.d.
15	methylcyclopentane	20.84	n.d.	n.d.
16	hexane	19.13	n.d.	n.d.
17	1H-pyrrole-3-carbonitrile	n.d	23.01	X
18	3-methyl-butanenitrile	28.83	n.d.	n.d.
19	glutaronitrile	43.86	18.10	X
20	4-methylpentanenitrile	32.98	11.03	n.d.
21	benzonitrile	43.78	14.79	n.d.
22	3-pyridinecarbonitrile	45.10	15.63	n.d.

23	1-methylethylidene propanedinitrile	38.55	n.d.	n.d.
24	adiponitrile	49.09	25.41	X
25	2-methylglutaronitrile	44.46	19.00	n.d.
26	cyclohexanecarbonitrile	45.30	n.d.	n.d.
27	2,4-diaminopyrimidine	n.d	18.62	X
28	alpha-methylstyrene	49.29	19.39	X
29	2,4-dimethylheptane	n.d	10.64	X
30	2,3,4 trimethylhexane	n.d	11.40	X
31	hexamethylenetetramine	56.37	28.43	n.d.
32	4,5-diethyloctane	n.d	n.d	11.256

Table 4.1. Compounds Identified in SPME Extraction of Tholins. All compounds identified by either standards or library matches and their retention times are reported. All retention times (RT) are reported in minutes corresponding to the specified extraction. If the compound was not detected no detection (n.d.) is reported. For the T2 column an X indicates the same RT as observed for the PDMS extraction for T1. The peak number refers to the bold peak labels in figure 4.2.

The first thing to note for the chromatograms is the large number of eluted species for the PDMS extraction of T1. There is a tight clustering of peaks between 13 and 20 minutes, with other clearly evident peaks at other retention times. Many of these peaks are broad or display shoulders, which suggests the possibility of co-elution of multiple components. Since the detection method used in this study is electron impact mass spectrometry it allows for identification of co-eluting species. Electron impact produces characteristic mass fragments for different compounds, dependent on both chemical functionality and compound size. This combined with the exact mass resolution of the mass spectrometer allows for an extracted ion chromatogram (EIC) to be obtained. An EIC shows peaks for a particular mass, which can then be used to make identifications of compounds with a desired chemical functionality easier even in the presence of multiple co-eluted species. Some of these EIC and representative mass spectra are shown in the subsequent analysis of different functional groups below.

The second overall observation from these chromatograms is how different the CAR/PDMS extraction for T1 is to the PDMS extractions for both tholins. While both display a large number of peaks, those identified in the CAR/PDMS extraction are much more separated. The broad nature of many peaks in this chromatogram is suggestive of compounds that are not easily resolved, which likely correspond to highly polar compounds. The implications of this are discussed below, but it makes those regions of the chromatogram difficult to use for identification. As such the majority of the identifications discussed below correspond to either retention times outside of those peaks, or species that can be readily resolved with an EIC. A large number of peaks have these specifications, and multiple compounds are identified that are not seen on the PDMS fiber extraction (figure 4.2a). Using a combination of EICs for both fibers along with comparison to compounds found in prior analyses, some of the organic compounds of interest in the material are identified and described below.

4.4.1 Analysis of Organic molecules

4.4.1.1 Amines

Amines are of interest due to both their likelihood on Titan and their biological significance. While the detection of primary amines is desirable for their astrobiological significance, they are difficult to detect with most GC columns without significant care. Simple primary amines do produce a distinctive fragment in EI, $CH_2NH_2^{\bullet+}$ with a mass of 30.034 Da. This fragment, the EIC for which is shown in figure 4.10, is seen in the CAR/PDMS extraction chromatogram for both tholins, but the peak is too broad to enable analysis. As such simple primary amines cannot be readily analyzed with this SPME-GC method, which is to be expected considering the difficultly of their analysis with GC and possible losses due to volatility. A more complex primary amine can be detected by examining different distinctive fragments. This includes 2,4-diaminopyrimidine seen on the PDMS fiber for both tholin samples at 18.62 min and identified based on library matching. While a complex amine is interesting, finding a compound containing four nitrogen atoms and multiple primary amines shows that a large amount of chemical complexity is possible for these samples, even in the smaller molecules produced. This shows that this method can detect more complex primary amines within these tholins.

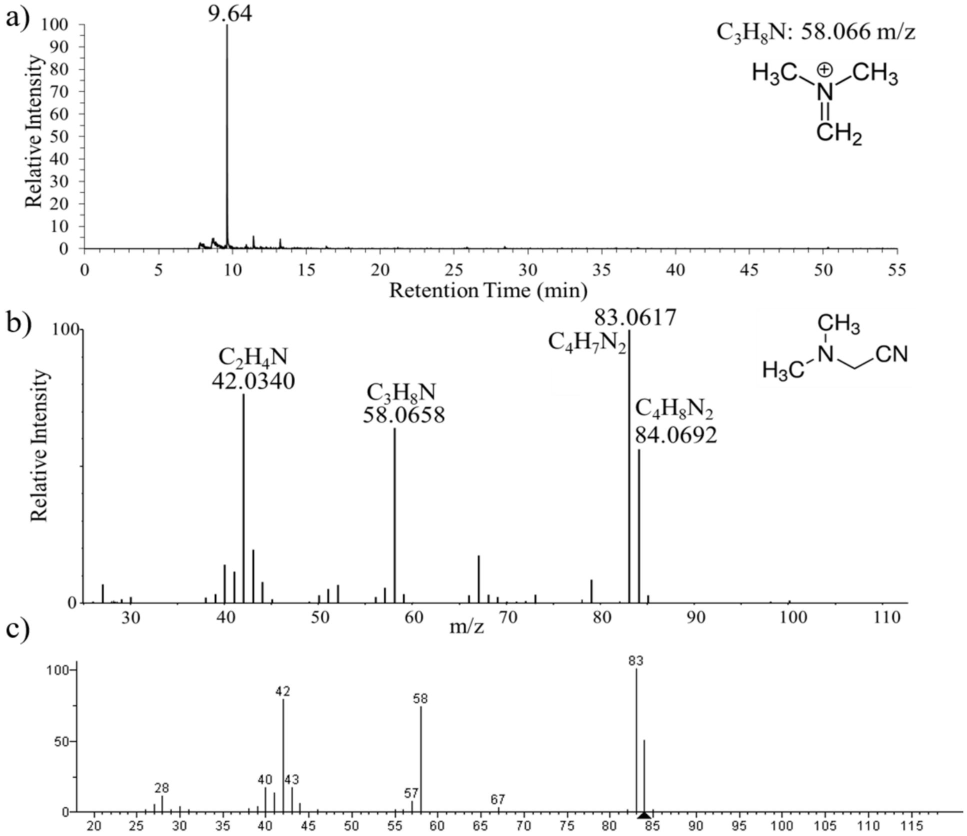

Figure 4.3. a) EIC of 58.066 m/z for the entire chromatographic run with the structure of the targeted ion shown. b) The EI mass spectrum for the 9.64 minute peak with relevant fragments labeled and the compound structure shown. Both are from the T1 PDMS extraction. c) EI library match spectrum from NIST library.

More highly substituted amines become more difficult to identify, since there are fewer distinctive EI fragments as the complexity of the substitution increases. One or two methyl groups on a secondary or tertiary amine respectively do produce identifiable fragments, even if the other sidechain is more complex. The EIC for the simple tertiary amine fragment from the PDMS fiber extraction for T1 is shown in figure 4.3. The single large peak was identified as dimethylaminoacetonitrile by comparison with a standard. This peak was seen in T1 only and extracted by both fibers, showing SPME can detect small tertiary amines. The detection of this amine is of astrobiological interest since it is the doubly methylated form of aminoacetonitrile. That small primary amine is considered a prebiotic molecule since it reacts with water to produce glycine, the simplest amino acid.[18] The production of dimethylaminoacetonitrile in one of these tholins increases the likelihood that the simpler precursor is also made, and is either undetectable with this method or has undergone further reaction during the synthesis process.

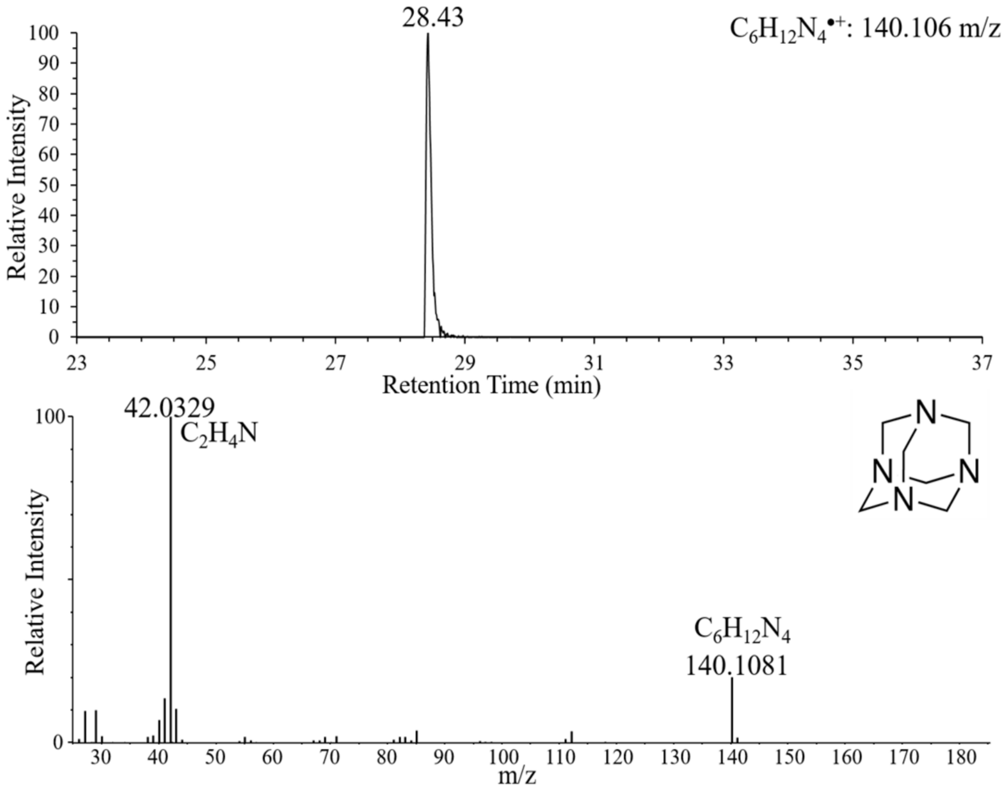

Figure 4.4. Top: EIC for 140.106 m/z for the time range of interest to hexamethylenetetramine from the T1 PDMS chromatogram. Bottom: EI mass spectrum for 28.43 minutes with relevant fragments labeled.

The most unique molecule detected within T1 was hexamethylenetetramine, a four nitrogen molecule with a structure resembling a cage. It was detected on both fibers for T1 with the longest retention time for any identified compound. It was also one of the few compounds with more than two nitrogen atoms, with 2,4-diaminopyrimidine being the only other four nitrogen compound detected. Hexamethylenetetramine was also seen in nuclear magnetic resonance (NMR) studies of T1,[34] indicating the ability of this SPME-GC method to detect compounds found with other analytical methods. It also shows that SPME-GC enables the simultaneous detection of both small and complex molecules. This simultaneous detection is important since the majority of GC methods in prior tholin sample analysis have concentrated on the identification of small molecules, and any larger molecules detected have been mostly hydrocarbons without the high nitrogen incorporation seen in hexamethylenetetramine. While this amount of nitrogen incorporation may not readily occur on Titan, the ability to detect such molecules in mission applications is important in case they are present. In this way this SPME-GC method presents an analytical possibility for much broader identification than could be accomplished with other prior studied GC-MS methods.

4.4.1.2 Aromatics

For aromatic molecules identifying simple, substituted, and heterocyclic compounds is important. Aromatic compounds can be easier to identify with EI due to their stability. They do not readily fragment and can be identified based off of EICs for the molecular ion as opposed to a fragment ion. Benzene is one of the simplest, and the EIC of a characteristic benzene fragment is shown in figure 4.5 for the PDMS extraction of T1. There are a variety of peaks, some of which are background ions and are labeled accordingly. The identification of benzene at 8.55 minutes is important since it was confirmed in Titan's atmosphere through the Cassini NIMS and any analytical method proposed for the identification of diverse compound types should be able to detect it along with other more complex molecules.

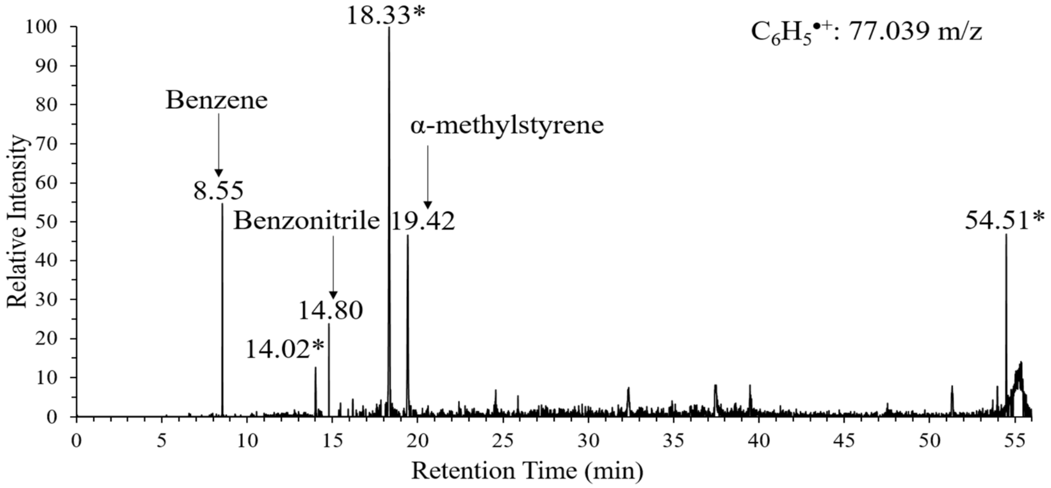

Figure 4.5. EIC for 77.039 m/z from the PDMS chromatogram for T1 with identified peaks labeled and background contaminants marked with an asterisk.

Other more substituted benzene molecules can also be identified, including α-methylstyrene and benzonitrile. While the former is a common background ion, it was not seen in the background chromatogram and must originate from the tholins themselves. α-Methylstyrene is unique in that it only contains carbon and hydrogen, while also containing one of the few nonaromatic alkenes identified. Since acetylene has also been seen in Titan's atmosphere, benzene molecules substituted with unsaturated hydrocarbons are expected, and the detection of α-methylstyrene fits with those expectations. Benzonitrile is a simple substituted benzene and one of the most likely substituted aromatics on Titan considering the prevalence of hydrogen cyanide and benzene in the photochemically active atmospheric regions. Additionally it has been seen in other analyses of tholins and thus is an expected observation.[38, 40, 42] Other substituted benzene molecules could contribute even more to Titan's chemistry and the detection of simpler variants indicates that more complex benzene molecules could possibly be detected.

Heterocyclic aromatic compounds are more common in the tholin samples compared to homocyclic aromatics due to the abundance of nitrogen and the high energy synthetic methods used. Some of these heterocyclic aromatics are expected to occur in Titan's atmosphere, making their detection important. The identified compounds of this type were all on the PDMS extractions and include 3-pryidinecarbonitrile, 2,4-diaminopyrimidine, and 1-H-pyrrole-3-carbonitrile detected in both tholin samples, pyrimidine detected in T1, and pyridine detected in T2. The variety in complexity is an expected observation since reactive nitrogen is abundant in these synthetic methods, but the different chemistry seen is interesting. This variability showcases the need for comparative studies when developing a suitable analytical method for tholin characterization.

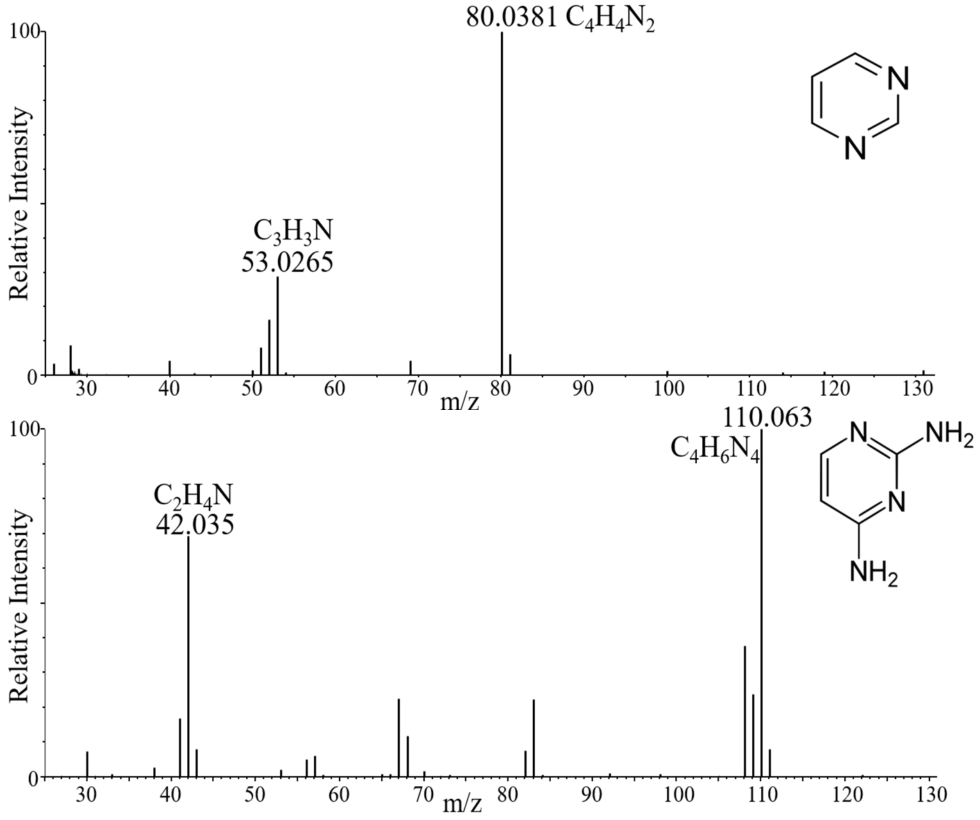

Figure 4.6. Both EI mass spectra are taken from T1 PDMS chromatogram. Top: EI mass spectrum for pyrimidine with relevant fragments labeled. Bottom: EI mass spectrum for 2,4-diaminopyrimidine with relevant fragments labeled.

The detection of 2,4-diaminopyridimidine in both tholins increases the likelihood that the precursor pyrimidine is produced in T2 as well. The difficultly in the identification of pyrimidine likely stems from the pyridine present in T2, which has a retention time close to pyrimidine, but elutes as broad peak with high intensity. Pyrimidine and dimethylaminoacetonitrile both display retention times very close to that seen for pyridine, but elute in much narrower peaks. This presents a possible concern for application of this GC method, since the aerosols on Titan are expected to contain similar molecules. Once molecules of concern, such are pyridine, are identified the oven temperature ramps can be modified in subsequent experimental studies to account for closely eluting species, allowing for optimization of GC oven methods prior a Titan mission. The mass spectra for both pyrimidine and 2,4-diaminopyridimidine, shown in figure 4.6, also display why identification of aromatics can be difficult. Even though both compounds have the same heterocyclic base, they do not display the same characteristic fragment for pyrimidine alone. As such, the identification of substituted heterocycles cannot be based off extracting the mass of the common base alone, and so each aromatic would need to be identified individually.

The detection of pyridine and pyrimidine molecules within the tholins presents promising possibilities for astrobiology. While both have been identified in tholins with prior analyses,[38-40, 42] the identification of substituted pyridine and pyrimidine deviates from those prior data. Substituted pyrimidines comprise three of five nucleic bases present in DNA and RNA. Additionally pyridine forms the basis for multiple biological molecules such as alkaloids. The presence of substituted versions of these heterocycles indicates their possible inclusion in more advanced chemistry in Titan's atmosphere.

The last heterocycle detected, 1-H-pyrrole-3-carbonitrile, displays similar chemistry to the 3-pyridinecarbonitrile, and the precursor pyrrole was not detected in either tholin. The reason may be similar to pyridine, considering their similar chemistry. They are both single nitrogen aromatics and thus pyrrole is likely to elute broadly as well. The detection of the subsisted molecule means pyrrole was likely produced during the synthesis of the tholins and either lost to evaporation or subsequent reaction. This assumption is further supported with the detection of 1H-pyrrole in other tholin samples analyzed with pyrolysis-GC.[39, 40] To confirm the retention time for this molecule in future analyses, standards and possibly doping the tholins with pyrrole would be required. Finding 1-H-pyrrole-3-carbonitrile does indicate that smaller molecules readily react to produce more complex versions. Such reactions could also be expected in Titan's atmosphere, especially considering the likely production of cyanide radicals in large scale.

4.4.1.3Nitriles

The nitrile functionality is found in the largest number of molecules within T1, with many of the most intense chromatographic peaks displaying nitrile functionality. Nitriles are also one of the most readily identified fragments in the EICs. This is because the McLafferty rearrangement for alkyl nitriles produces a distinctive fragment with a monoisotopic mass of 41.027 Da. Since this fragment is 12 mDa larger than C3H5 it can be selected for in an EIC without isolating the hydrocarbon fragment, which significantly simplifies analysis and identification. The EIC for 41.027 Da is shown in figure 4.7 for part of the total chromatogram of the PDMS extraction of T1. In this EIC, species other than nitriles can be seen due to some compounds, such as nitrogenated aromatics, also producing a 41.027 Da fragment, including aromatic nitriles. While many of these compounds have been discussed in detail above, it shows how common nitrile chemistry is in these tholin samples. The commonality of nitrile substitution on compounds of multiple additional functionalities supports the idea that nitrile containing isomers will be common.

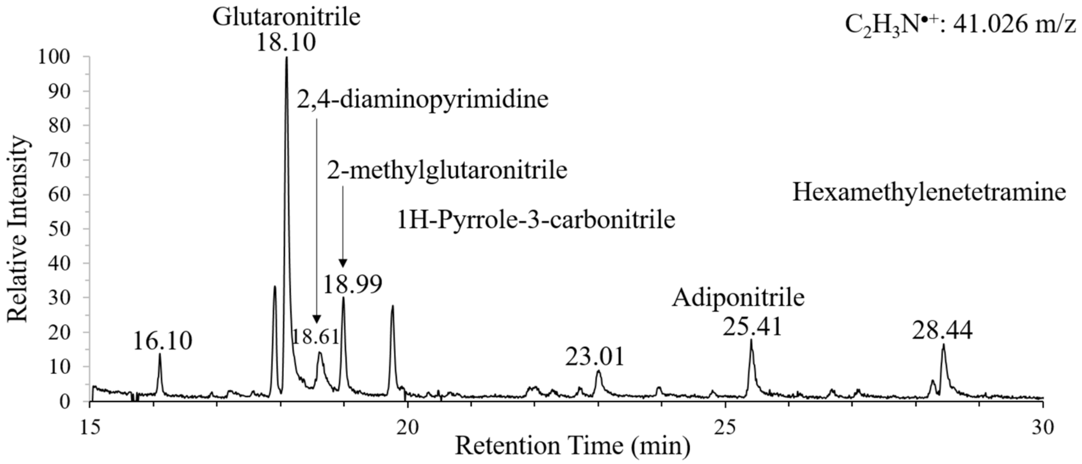

Figure 4.7. EIC for 41.027 m/z for the T1 PDMS extraction for the retention times of 15-30 minutes. The numbers refer to the compounds in Table 4.1. More than just nitriles are seen due to the mass also matching other possible fragments. An isolation window of 0.01 Da was used to improve chromatographic resolution while still eliminating the hydrocarbon fragment.

The other mononitriles identified in the material are similar to those identified in prior pyrolysis-GC studies of other tholins.[38-40, 54] They also comprise the largest diversity of identified compounds, including small and large alkyl chains. Alkenes are also identified in methylallylcyanide and 2-methyl-2-propenenitrile, both only seen on the CAR/PDMS extraction for T1. Other mononitriles identified include propionitrile, isobutyronitrile, tertbutylnitrile, 3-methyl-butanenitrile, pentanenitrile, and 4-methylpentanenitrile. These were identified by a mixture of standards and library matching and the conditions for their detection are shown in Table 4.1. Some of these nitriles comprise the smallest compounds seen in the extraction, with the next smallest non-nitrile being cyclopentane. These small nitriles could be indicative of smaller hydrocarbon precursors that were not identified with this method but seen with prior GC analyses.[38, 40, 54] This also supports the presence of nitriles as the most common functionality in these tholin samples, and their contributions to more complex chemistry. The identification of multiple nitriles of various sizes is well within expectations for this sample, but also supports the use of SPME-GC for the identification of both small and large compounds in the same extraction.

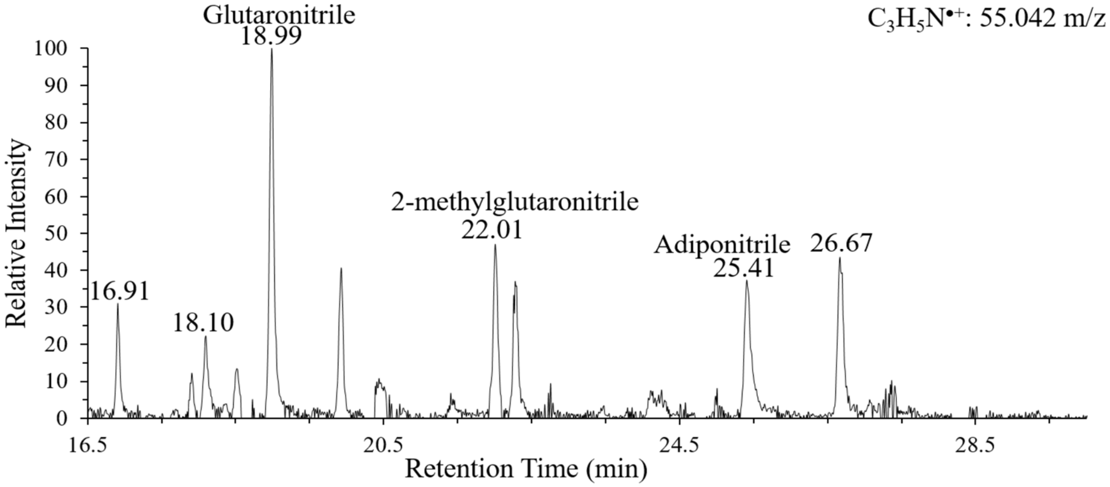

Figure 4.8. EIC for 55.042 m/z from the T1 PDMS extraction. The numbers refer to the compounds in Table 4.1.

Dinitriles are also seen in both fiber extractions and both tholin samples as shown in Table 4.1. The dinitriles seen also include the other alkene observed in the sample, 1-methylethylidene propanedinitrile, also only detected in the CAR/PDMS extraction. The identification of alkene containing nitriles on the CAR/PDMS fibers suggests that media is more effective at extracting alkenes. This may also be complicated by the smaller size of these alkene containing nitriles. The other dinitriles identified in this material include succinonitrile, glutaronitrile, and adiponitrile. These are all alkyl dinitriles and much larger, being four, five, and six carbons respectively. These dinitriles are more difficult to identify, since the McLafferty rearrangement is also seen but does not unambiguously identify dinitriles. The alkyl dinitriles typically produce fragments for C_3H_5N at 55.042 Da, and for C_3H_4N at 54.034 Da. These fragments correspond to breaking along the alkyl chain, and the EIC for the former is shown in figure 8. There are multiple other compounds with this fragment seen in the EIC, but the similarity of the fragments in these chromatographic peaks likely makes the identification difficult. It is most likely that these unidentified peaks correspond to isomers of other alkyl dinitriles, the confirmation of which would require testing with additional standards. This data shows that SPME-GC allows for the extraction of nitriles with various sizes and polarities, with the actual number being extensive. Since nitriles are the most commonly expected functional group in Titan aerosols, the effectiveness of this SPME-GC method for their extraction suggests it would be well suited for their *in-situ* analysis.

4.4.1.4 Hydrocarbons

Hydrocarbons produced in the tholin samples are difficult to detect. This is due to multiple factors, including the lack of solubility in solvents used for analyses such as electrospray ionization, high volatility, and the lack of distinctive chemical functional groups that can be derivatized or preselected for using specialized analytical conditions. The analysis of hydrocarbons is typically performed by GC, since the technique can analyze nonpolar compounds effectively. One of the difficulties with the analysis of hydrocarbons by the GC-MS used in this work is the high amount of co-elution with aliphatic nitrile species. Many aliphatic nitriles contain similar ion fragments to those seen in hydrocarbons which, combined with the high amount of co-elution observed for the molecules, minimizes the usefulness of an EIC for identification.

Compared to the nitriles there are relatively few hydrocarbons detected, even though they are expected to be the next most abundant type of compound due to the GC column selection and comparison with prior pyrolysis-GC analyses of tholin samples.[39, 42] There are many possibilities behind this observation. One is that the hydrocarbons are readily lost from the tholins during collection due to their volatility. Another is that the hydrocarbons may not adhere as readily to the fibers as the more polar compounds, or may adhere extremely well and not readily desorb in the GC inlet. Two different fibers were tested in this study, the PDMS and CAR/PDMS, the latter of which is known to be much more adsorbent for small volatiles. When testing each fiber with T1, more hydrocarbons were seen using the CAR/PDMS compared to the PDMS alone. This seems to suggest that a more adsorbent media may be necessary to see hydrocarbons from tholins.

The observation of a hydrocarbon in T2 on the PDMS fiber not seen in T1, and little else other than broadly eluted amines in the CAR/PDMS extraction of T2 (shown in figure 4.9) suggests another possibility. The complexity of the tholin samples could lead to oversaturation of the SPME fiber media, lowering the dynamic range of the method for less abundant species or those with lower specificity of binding for the fiber media. This could be readily addressed through optimization of the SPME fiber media. While 100 μm PDMS and CAR/PDMS SPME fibers are well suited for volatiles, 7 or 3 μm PDMS are better suited for semi-volatile non-polar compounds, providing a ready point for future optimization of hydrocarbon detection. Some inferences can be drawn from the hydrocarbons identified in the sample. Few hydrocarbons overall are identified for T1, with the most abundant peaks occurring for the CAR/PDMS extraction. In that extraction the only hydrocarbons readily identified are cyclopentane, methylcyclopentane, and hexane. Not being able to detect these hydrocarbons on the PDMS fiber extraction does indicate that a more adsorbent fiber media is necessary to detect small hydrocarbons, which fits with the CAR/PDMS fiber being well suited to gases and low molecular weight compounds. The larger hydrocarbons identified in T2 include 2,3,4 trimethylhexane, 2,4-dimethylheptane, and 4,5-diethyloctane, all of which are only seen on the PDMS extraction and the first two of which are also seen in T1 in very small quantities. This may be due to lower production, unsuitability of the SPME fiber media, or losses over time due to volatility or atmospheric exposure since T1 is older and has been exposed to air multiple times prior to this study, compared to the newer T2 that has only been exposed to atmosphere during initial collection. Modeling of mechanisms that enable the synthesis of these hydrocarbon products or their precursors under Titan conditions may enable anticipation of smaller hydrocarbons to target in future studies.

4.5 Conclusion

A SPME-GC method has been presented for the extraction and analysis of tholins considered representative of Saturn’s moon Titan. Two different SPME fiber types have been tested on two different tholin samples and found to allow for the successful identification of a wide range of compounds with various sizes and chemical functionalities. The majority of the compounds detected are larger semi-volatiles, filling a gap in prior pyrolysis-GC analyses which focused on smaller compounds. Functionalities identified comprised mostly nitriles, as expected from theses earlier studies. Amines, hydrocarbons, and aromatics were also identified. While many of these compounds have been identified in prior work some new compounds, such as 2,4-diaminopyrimidine, have been identified that are of particular astrobiological interest. The additional identification of hexamethylenetetramine, seen in prior NMR studies, solidifies the ability of this method to identify a wide variety of compounds. These characteristics makes this SPME-GC method worthy of consideration for inclusion in future missions to study the aerosols of Titan's atmosphere and surface.

The present study is exploratory and as such there are factors impacting the effectiveness of the method for the identification of molecules such as amines and high sensitivity analysis. These factors would need to be addressed prior to mission application. Major issues include oversaturation of the SPME fiber media and subsequent lower dynamic range, the specificity of binding for both the fiber media and the GC column for analytes of interest, large headspace volume, and long extraction timescales. The impact of oversaturation on the dynamic range for some compounds and ways to mitigate it have been addressed above. To address specificity of binding for the fiber media, a variety of fiber media could improve both sensitivity and detection, while also positively impacting dynamic range. While 2D-GC could be considered as a way to address the specificity of binding for the GC-column, considering it has been used in successful analysis of tholins by pyrolysis-GC[39] and petroleum sample characertization,[55] it would be extremely difficult to implement during a lander mission. An alternative would be the inclusion of ancillary columns optimized for compounds for which the primary column had lower binding specificity. The final issues of headspace volume and extraction timescales could be readily mitigated with engineering controls and increased optimization. Since the issues of this exploratory study can be readily addressed with further work, SPME should be consider for inclusion on any future lander mission to Titan considering its success with the analysis of these samples.

If the SPME method proposed here was to be included on a future mission to Titan, the overall protocol could be easily adapted. An aerosol collection media, such as a Teflon filter, could be loaded onto a sample carousel, allowing for sequential exposure during descent into Titan's atmosphere. Upon landing, the collection media would be heated in the presence of the fiber media of choice. Here, the headspace volume would be minimized while the fiber media surface area maximized to ensure maximum absorption of the analytes. From there, the fiber media could readily be desorbed in the inlet area of a mission GC-MS. Analysis of aerosols on the surface would necessitate a modified setup. The Huygens probe detected volatiles from the surface after landing due to either heating of the probe itself during descent or heating of aerosol collected on the outside of the GC inlet.[5] Any volatiles released from heating due to descent could be measured by exposing the fiber media to the heated volatiles. Detecting less volatile molecules would require an IR source for heating the targeted sampling area, such as an IR bulb with an appropriate reflector, combined with a camera to monitor any physical changes to the surface. The fiber media could then be exposed to the heated surface in a similar manner as discussed above. These methods could be modified further for application of this SPME method to other icy world missions, such as investigations of Europa or Enceladus. There, SPME would enable the detection of volatile organic compounds dissolved in ice or liquid water, considering that many other SPME methods have been designed for the detection of trace organics in water.[56-57]

4.6 Acknowledgements

We would like to thank Mark Smith and Sarah Hörst for providing the tholin samples for analysis. The research was funded by NSF award number CHE-1508825. The early part of this work was funded by NASA Astrobiology Institute, Titan as a Prebiotic Chemical System, and the Keck Institute for Space Studies, Future Missions to Titan: Scientific and Engineering Challenges. K.T.U. acknowledges financial support from the Harriett Jenkins Pre-Doctoral Fellowship Program.

4.7 References

1. F. M. Flasar, R. K. Achterberg, B. J. Conrath, P. J. Gierasch, V. G. Kunde, C. A. Nixon, G. L. Bjoraker, D. E. Jennings, P. N. Romani, A. A. Simon-Miller, B. Bézard, A. Coustenis, P. G. J. Irwin, N. A. Teanby, J. Brasunas, J. C. Pearl, M. E. Segura, R. C. Carlson, A. Mamoutkine, P. J. Schinder, A. Barucci, R. Courtin, T. Fouchet, D. Gautier, E. Lellouch, A. Marten, R. Prangé, S. Vinatier, D. F. Strobel, S. B. Calcutt, P. L. Read, F. W. Taylor, N. Bowles, R. E. Samuelson, G. S. Orton, L. J. Spilker, T. C. Owen, J. R. Spencer, M. R. Showalter, C. Ferrari, M. M. Abbas, F. Raulin, S. Edgington, P. Ade and E. H. Wishnow, *Science*, 2005, **308**, 975-978.
2. V. G. Kunde, A. C. Aikin, R. A. Hanel, D. E. Jennings, W. C. Maguire and R. E. Samuelson, *Nature*, 1981, **292**, 686-688.
3. W. C. Maguire, R. A. Hanel, D. E. Jennings, V. G. Kunde and R. E. Samuelson, *Nature*, 1981, **292**, 683-686.

4. H. B. Niemann, S. K. Atreya, S. J. Bauer, G. R. Carignan, J. E. Demick, R. L. Frost, D. Gautier, J. A. Haberman, D. N. Harpold, D. M. Hunten, G. Israel, J. I. Lunine, W. T. Kasprzak, T. C. Owen, M. Paulkovich, F. Raulin, E. Raaen and S. H. Way, *Nature*, 2005, **438**, 779-784.
5. H. B. Niemann, S. K. Atreya, J. E. Demick, D. Gautier, J. A. Haberman, D. N. Harpold, W. T. Kasprzak, J. I. Lunine, T. C. Owen and F. Raulin, *J Geophys Res-Planet*, 2010, **115**, E12006.
6. E. R. Stofan, C. Elachi, J. I. Lunine, R. D. Lorenz, B. Stiles, K. L. Mitchell, S. Ostro, L. Soderblom, C. Wood, H. Zebker, S. Wall, M. Janssen, R. Kirk, R. Lopes, F. Paganelli, J. Radebaugh, L. Wye, Y. Anderson, M. Allison, R. Boehmer, P. Callahan, P. Encrenaz, E. Flamini, G. Francescetti, Y. Gim, G. Hamilton, S. Hensley, W. T. K. Johnson, K. Kelleher, D. Muhleman, P. Paillou, G. Picardi, F. Posa, L. Roth, R. Seu, S. Shaffer, S. Vetrella and R. West, *Nature*, 2007, **445**, 61-64.
7. N. Lancaster, *Science*, 2006, **312**, 702-703.
8. J. T. Perron, M. P. Lamb, C. D. Koven, I. Y. Fung, E. Yager and M. Ádámkovics, *Journal of Geophysical Research: Planets*, 2006, **111**.
9. R. D. Lorenz, B. W. Stiles, R. L. Kirk, M. D. Allison, P. P. del Marmo, L. Iess, J. I. Lunine, S. J. Ostro and S. Hensley, *Science*, 2008, **319**, 1649-1651.
10. M. G. Trainer, A. A. Pavlov, H. L. DeWitt, J. L. Jimenez, C. P. McKay, O. B. Toon and M. A. Tolbert, *Proceedings of the National Academy of Sciences*, 2006, **103**, 18035-18042.
11. A. L. Zerkle, M. W. Claire, S. D. Domagal-Goldman, J. Farquhar and S. W. Poulton, *Nature Geosci*, 2012, **5**, 359-363.

12. Y. Sekine, S. Lebonnois, H. Imanaka, T. Matsui, E. L. O. Bakes, C. P. McKay, B. N. Khare and S. Sugita, *Icarus*, 2008, **194**, 201-211.
13. E. H. Wilson and S. K. Atreya, *Planetary and Space Science*, 2003, **51**, 1017-1033.
14. J. C. Loison, E. Hébrard, M. Dobrijevic, K. M. Hickson, F. Caralp, V. Hue, G. Gronoff, O. Venot and Y. Bénilan, *Icarus*, 2015, **247**, 218-247.
15. H. Imanaka and M. A. Smith, *Proceedings of the National Academy of Sciences*, 2010, **107**, 12423-12428.
16. F. Raulin and T. Owen, *Space Science Reviews*, 2002, **104**, 377-394.
17. V. Vuitton, R. V. Yelle and J. Cui, *Journal of Geophysical Research: Planets*, 2008, **113**, E05007.
18. S. M. Horst, R. V. Yelle, A. Buch, N. Carrasco, G. Cernogora, O. Dutuit, E. Quirico, E. Sciamma-O'Brien, M. A. Smith, A. Somogyi, C. Szopa, R. Thissen and V. Vuitton, *Astrobiology*, 2012, **12**, 809-817.
19. M. L. Cable, S. M. Hörst, R. Hodyss, P. M. Beauchamp, M. A. Smith and P. A. Willis, *Chemical Reviews*, 2012, **112**, 1882-1909.
20. A. Somogyi, C. H. Oh, M. A. Smith and J. I. Lunine, *Journal of the American Society for Mass Spectrometry*, 2005, **16**, 850-859.
21. B. Cunha de Miranda, G. A. Garcia, F. Gaie-Levrel, A. Mahjoub, T. Gautier, B. Fleury, L. Nahon, P. Pernot and N. Carrasco, *The Journal of Physical Chemistry A*, 2016, **120**, 6529-6540.
22. C. Szopa, G. Cernogora, L. Boufendi, J. J. Correia and P. Coll, *Planetary and Space Science*, 2006, **54**, 394-404.

23. H. Imanaka, B. N. Khare, J. E. Elsila, E. L. O. Bakes, C. P. McKay, D. P. Cruikshank, S. Sugita, T. Matsui and R. N. Zare, *Icarus*, 2004, **168**, 344-366.
24. S. M. Hörst, *Journal of Geophysical Research: Planets*, 2017, **122**, 432-482.
25. E. Sciamma-O'Brien, N. Carrasco, C. Szopa, A. Buch and G. Cernogora, *Icarus*, 2010, **209**, 704-714.
26. M. Fulchignoni, F. Ferri, F. Angrilli, A. J. Ball, A. Bar-Nun, M. A. Barucci, C. Bettanini, G. Bianchini, W. Borucki, G. Colombatti, M. Coradini, A. Coustenis, S. Debei, P. Falkner, G. Fanti, E. Flamini, V. Gaborit, R. Grard, M. Hamelin, A. M. Harri, B. Hathi, I. Jernej, M. R. Leese, A. Lehto, P. F. Lion Stoppato, J. J. Lopez-Moreno, T. Makinen, J. A. M. McDonnell, C. P. McKay, G. Molina-Cuberos, F. M. Neubauer, V. Pirronello, R. Rodrigo, B. Saggin, K. Schwingenschuh, A. Seiff, F. Simoes, H. Svedhem, T. Tokano, M. C. Towner, R. Trautner, P. Withers and J. C. Zarnecki, *Nature*, 2005, **438**, 785-791.
27. V. A. Krasnopolsky, *Icarus*, 2009, **201**, 226-256.
28. E. Sciamma-O'Brien, C. L. Ricketts and F. Salama, *Icarus*, 2014, **243**, 325-336.
29. E. Sciamma-O'Brien, K. T. Upton and F. Salama, *Icarus*, 2017, **289**, 214-226.
30. G. Alcouffe, M. Cavarroc, G. Cernogora, F. Ouni, A. Jolly, L. Boufendi and C. Szopa, *Plasma Sources Sci T*, 2010, **19**.
31. C. He, G. Lin, K. T. Upton, H. Imanaka and M. A. Smith, *The Journal of Physical Chemistry A*, 2012, **116**, 4760-4767.
32. A. Somogyi, M. A. Smith, V. Vuitton, R. Thissen and I. Komaromi, *Int J Mass Spectrom*, 2012, **316**, 157-163.
33. A. Somogyi, R. Thissen, F. R. Orthous-Daunay and V. Vuitton, *Int J Mol Sci*, 2016, **17**.
34. C. He, G. Lin and M. A. Smith, *Icarus*, 2012, **220**, 627-634.

35. M. Ruiz-Bermejo, C. Menor-Salván, S. Osuna-Esteban and S. Veintemillas-Verdaguer, *Origins Life Evol B*, 2007, **37**, 123-142.
36. M. L. Cable, A. M. Stockton, M. F. Mora and P. A. Willis, *Analytical Chemistry*, 2013, **85**, 1124-1131.
37. N. Carrasco, I. Schmitz-Afonso, J. Y. Bonnet, E. Quirico, R. Thissen, O. Dutuit, A. Bagag, O. Laprévote, A. Buch, A. Giulani, G. Adandé, F. Ouni, E. Hadamcik, C. Szopa and G. Cernogora, *The Journal of Physical Chemistry A*, 2009, **113**, 11195-11203.
38. P. Ehrenfreund, J. J. Boon, J. Commandeur, C. Sagan, W. R. Thompson and B. Khare, *Adv Space Res*, 1994, **15**, 335-342.
39. M. McGuigan, J. H. Waite, H. Imanaka and R. D. Sacks, *J Chromatogr A*, 2006, **1132**, 280-288.
40. M. C. Pietrogrande, P. Coll, R. Sternberg, C. Szopa, R. Navarro-Gonzalez, C. Vidal-Madjar and F. Dondi, *Journal of Chromatography A*, 2001, **939**, 69-77.
41. G. Israel, C. Szopa, F. Raulin, M. Cabane, H. B. Niemann, S. K. Atreya, S. J. Bauer, J. F. Brun, E. Chassefiere, P. Coll, E. Conde, D. Coscia, A. Hauchecorne, P. Millian, M. J. Nguyen, T. Owen, W. Riedler, R. E. Samuelson, J. M. Siguier, M. Steller, R. Sternberg and C. Vidal-Madjar, *Nature*, 2005, **438**, 796-799.
42. M. Morisson, C. Szopa, N. Carrasco, A. Buch and T. Gautier, *Icarus*, 2016, **277**, 442-454.
43. R. Hodyss, Dissertation (Ph.D.), The California Institute of Technology, 2006.
44. M. Ruiz-Bermejo, C. Menor-Salván, J. L. de la Fuente, E. Mateo-Martí, S. Osuna-Esteban, J. Á. Martín-Gago and S. Veintemillas-Verdaguer, *Icarus*, 2009, **204**, 672-680.

45. M. Ruiz-Bermejo, C. Menor-Salván, E. Mateo-Martí, S. Osuna-Esteban, J. Á. Martín-Gago and S. Veintemillas-Verdaguer, *Icarus*, 2008, **198**, 232-241.
46. C. Menor-Salvan, M. Ruiz-Bermejo, S. Osuna-Esteban, G. Munoz-Caro and S. Veintemillas-Verdaguer, *Chem Biodivers*, 2008, **5**, 2729-2739.
47. A. M. Santos, T. Vasconcelos, E. Mateus, M. H. Farrall, M. D. R. Gomes da Silva, M. R. Paiva and M. Branco, *Journal of Chromatography A*, 2006, **1105**, 191-198.
48. N. Yassaa and J. Williams, *Journal of Chromatography A*, 2007, **1141**, 138-144.
49. G. Duporté, M. Riva, J. Parshintsev, E. Heikkinen, L. M. F. Barreira, N. Myllys, L. Heikkinen, K. Hartonen, M. Kulmala, M. Ehn and M.-L. Riekkola, *Environmental Science & Technology*, 2017, **51**, 5602-5610.
50. Juita, B. Z. Dlugogorski, E. M. Kennedy and J. C. Mackie, *Industrial & Engineering Chemistry Research*, 2012, **51**, 5645-5652.
51. G. E. Orzechowska and S. E. Paulson, *The Journal of Physical Chemistry A*, 2005, **109**, 5358-5365.
52. F. Reisen, S. M. Aschmann, R. Atkinson and J. Arey, *Environmental Science & Technology*, 2003, **37**, 4664-4671.
53. S. M. Hörst, Yoon, Y.H., Parker, A.H., Li, R., de Gouw, J., and M.A. Tolbert., *Submitted*, 2017.
54. L. Torokova, J. Watson, F. Krcma, V. Mazankova, N. J. Mason, G. Horvath and S. Matejcik, *Contributions to Plasma Physics*, 2015, **55**, 470-480.
55. G. S. Frysinger and R. B. Gaines, *Hrc-J High Res Chrom*, 1999, **22**, 251-255.

56 J. J. Langenfeld, S. B. Hawthorne, D. J. Miller, *Analytical Chemistry*, **1996,** *68*, 144-155

57 R. Eisert, K. Levsen, *Journal of Chromatography A*, **1996,** *733*, 143-157

4.8 Supplemental Information

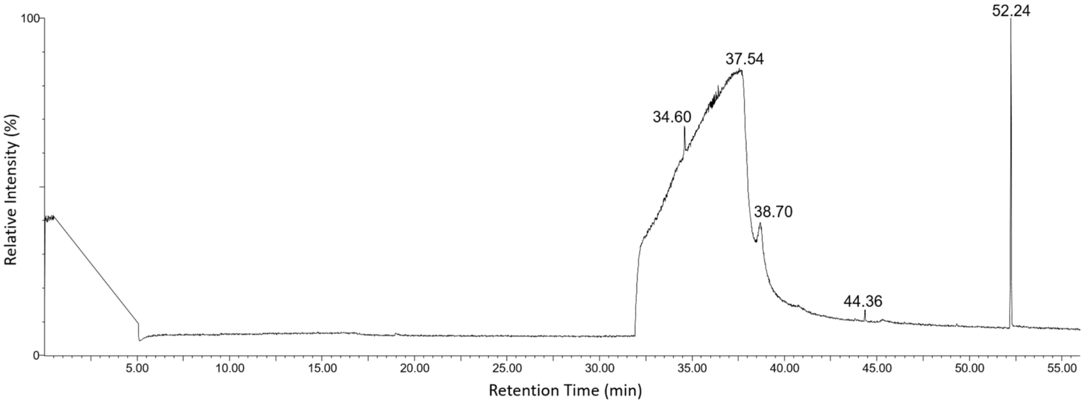

Figure 4.9. CAR/PDMS extraction of T2 showing a large siloxane peak at 52.24 and a very large peak that cannot be identified.

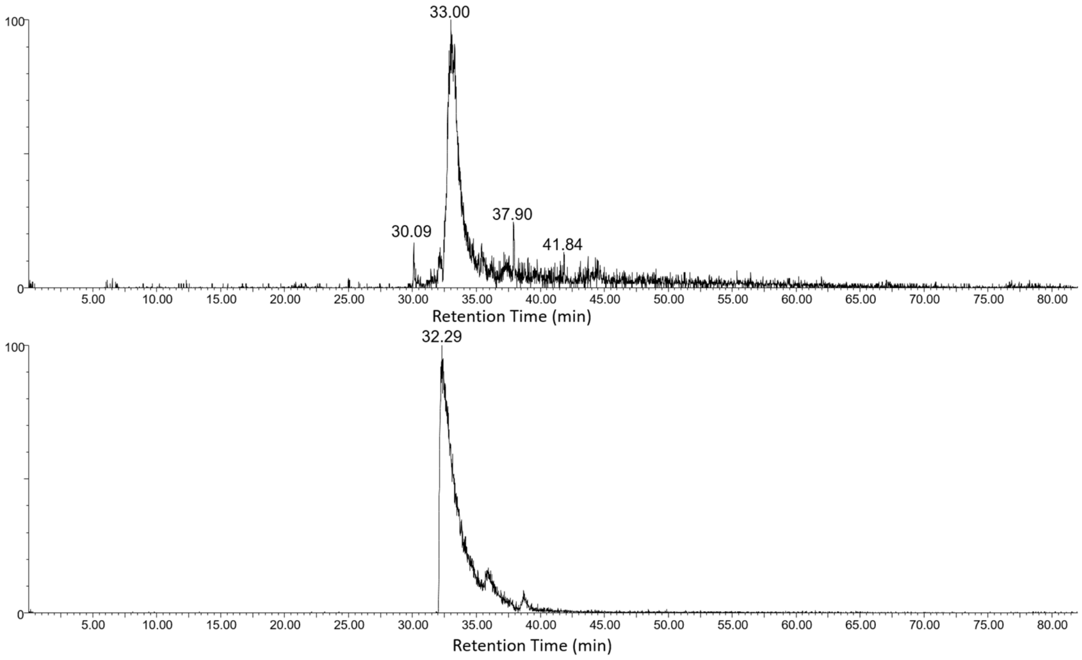

Figure 4.10. The EIC of 30.034 m/z from the CAR/PDMS extraction of each tholin. This fragment is characteristic for a primary amine. Top: EIC of 30.034 m/z for T1 Bottom: EIC of 30.034 m/z for T2.

Chapter 5

HIGHLY SELECTIVE COMPLEXATION WITH 18-CROWN-6 ETHER SEQUESTERS PRIMARY AMINES IN SIMULATED TITAN AEROSOL FOR ENHANCED DETECTION AND STRUCTURAL ANALYSIS

5.1 Abstract

The aerosols present on Saturn's moon of Titan are proposed to contain molecules composed of carbon, nitrogen, and hydrogen. These aerosols have been simulated under laboratory conditions and found to be difficult to analyze due to their chemical complexity and the inclusion of a large number of different molecules. One particular expected functionality that has been the target of prior analyses are primary amines. Alkyl primary amines have been identified in prior work, but bulk primary amine identification and structural identification of said amines remains difficult. To not only identify a variety of primary amines but also obtain this additional structural information, a host-guest supramolecular complex with 18-crown-6 ether is utilized, enabling the identification of primary amines with minimal sample processing. The use of a MS^3 neutral loss method with an ion trap mass spectrometer allows for the unambiguous identification of primary amines and also the elucidation of some structural information. Compounds with nitrile functionality are identified, in addition to phenyl containing molecules. Both of these compound types present interesting implications for astrobiology and the complexity of primary amines possible in Titan's atmosphere.

5.2 Introduction

The Cassini-Huygens mission brought to light many interesting features of Saturn's moon Titan. While the lakes of methane and ethane[1], dunes[2], and river valleys[3] are all interesting, the atmosphere presents a more astrobiologically intriguing target. Titan's atmosphere is composed of nitrogen (90-98%) and methane (2-10%) with other trace gases.[4,5] The UV irradiation of this atmosphere produces molecules with various amounts of nitrogen incorporation that condense into aerosols and descend to the 95K surface.[6-8] Investigations of these aerosols by the Huygens lander found a large amount of chemical complexity, with even more complexity possible within molecules too large for detection with the mass spectrometer present on the mission.[5, 9] This has increased interest in the aerosols found on this moon and driven the desire to study these complex aerosols and characterize any prebiotic molecules found within.

To better study Titan's aerosols, simulants called tholins are made in the laboratory using a variety of different energy methods (discharge, cold plasma, UV), pressures, temperatures, and gas mixtures to simulate the atmosphere and induce chemistry.[10-25] The resultant brown to orange colored solid is then collected for subsequent analysis. These samples have been studied using a variety of methods including but not limited to nuclear magnetic resonance,[13, 14] gas chromatography,[16, 17, 26-29] UV and IR spectroscopy,[11, 15, 20, 30, 31] and electrospray mass spectrometry.[18, 21, 22, 27, 32] While all of these different methods help to provide useful information, most allow only for chemical functionality or chemical formulae to be determined. For methods that allow both pieces of information to be obtained along with some structural identification there tend to be complications with particular functional groups or the identification of larger molecules within the mixture.

Amines are one functional group of astrobiological interest, due to their prevalence in common biological molecules such as amino acids. Amines are likely present in Titan aerosols and tholins but are difficult to detect with methods such as gas chromatography.[10] Aliphatic primary amines in tholins have been studied using a lab-on-a-chip capillary electrophoresis method with fluorescence detection.[33] The use of fluorescence necessitated the use of covalent derivatization conditions and matching of the resultant capillary electrophoresis peaks to readily available standards. While such a method is well suited to eventual in-situ mission applications, the need for standards necessitates complimentary methods for bulk identification prior to later characterization with mission applicable methodology. The desire to selectively identify a large variety of primary amines in these tholins makes this problem well suited to the use of host-guest supramolecular chemistry.

Supramolecular chemistry is a well-known area of physical organic chemistry, involving the formation of a larger subunit from two different molecules bound by non-covalent interactions such as hydrogen bonds or electrostatic forces.[34-36] The many interactions found within supramolecular chemistry often take inspiration from similar interactions found in biology.[37] There, supramolecular chemistry is responsible for the self-assembly of common structures such as the DNA double helix[38, 39] and the β-sheets of proteins.[40] Due to the prevalence and stability of these supramolecular assemblies,[38, 41-44] these types of interactions are utilized in multiple applications, from molecular recognition[45] to catalysis,[39] making supramolecular assemblies well suited for many analytical methods. One supramolecular assembly commonly used for analytical characterization is a host-guest complex.[45-48] In these interactions a host molecule binds, in a reversible manner, with the smaller guest molecule containing a specific chemical functionality for which the host is sensitive.[43] These host-guest complexes are commonly seen in biology with enzymes and substrates, but are also used to assist in chemical synthesis and drug delivery.[37, 47] The versatility and selectivity of host-guest chemistry ability makes these complexes an attractive option for the analysis of tholins.

A major driver in the analysis of tholins are methods that enable the identification and characterization of target molecules within the mixture using minimal sample processing.10 Many other analytical methods used for such samples rely on covalent derivatization and subsequent chromatography.[49-51] These methods can increase experimental timescales and complicate the analysis if the necessary solvents or conditions are incompatible with certain compounds present, a known concern with the analysis of tholins considering their low solubility. Host-guest chemistry presents an alternative since they are typically sensitive to a particular functional group and can often be employed with milder conditions than covalent derivatization. The analysis of complex organic mixtures such as tholins usually relies on mass spectrometry, due to its ability to elucidate both chemical formula from the mass to charge ratio and structure by either conjunction with chromatography or the use of tandem mass spectrometry.[52-54] The host-guest complex used in the analysis of amines in tholins should take into account steps ease detection by mass spectrometry. The important factors in host selection are an increase in the mass range, especially if the proposed guest is small, facilitating the formation of a charged complex since mass spectrometry relies on detection of charged molecules, and that the host-guest complex is strong enough to survive the ionization process.

A selective host for primary amines is 18-crown-6 ether, shown in figure 5.1. This host is known to strongly complex to cations such as potassium, and also hydrogen bonds well with hydronium ion.[48, 55-60] This same hydrogen bonding has been used to complex 18-crown-6 ether to primary amines found in peptides and proteins,[61, 62] with complexation to secondary amines also observed.[48] This hydrogen bonding preserves the positive charge of the guest, making it well suited as a host for mass spectrometry.[55, 62] Additionally the crown ether complex has been characterized as stronger in the gas phase compared to solution. This phenomenon has been used to probe the solution phase structure of peptide-crown ether complexes during sampling by electrospray mass spectrometry.[61] 18-crown-6 ether has also been used with a variety of solvents to enable the separation of amino acids in capillary electrophoresis.[63] These factors and the ease with which this selective host-guest complex can be formed make it an ideal host for the study of primary amines in tholins.

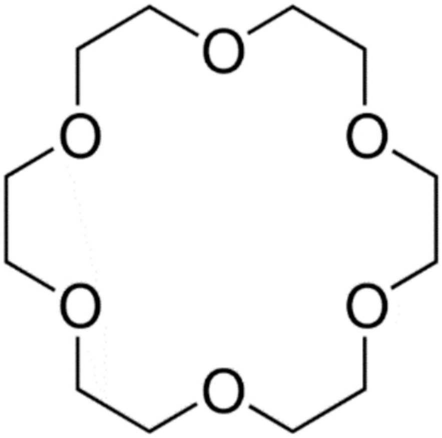

Figure 5.1. 18-crown-6 ether structure

In this study we probe the multiple different primary amines present within two tholin samples by 18-crown-6 ether complexation and analysis by MS/MS[64] and tandem MS^3 mass spectrometry, the latter employing a neutral loss (NL) scan instrumental method. This second method allows for the determination of both which molecules are bound to the crown ether and identification of some structure. The results from this study indicate that a large number of different molecules readily form complexes and primary amines comprise all of the guest molecules readily identified. The majority of those identified appear to follow set structural tendencies with some deviations. Since there are a large number of structural isomers possible within the material, identifications for the majority of compounds are limited to most likely chemical formulae. The breadth of data possible from this experiment would enable further identifications with increased sensitivity, resolution, or integration with chromatography. The range of primary amines identified by the 18-crown-6 ether host-guest complex show the suitability of the technique to enable the bulk identification of primary amines which has proven difficult with other methods. Additionally, the comparison of a new tholin to one that has undergone aging shows that while these amines are quite volatile compared to other species, they can still be identified even with decreased abundance. This has important implications for the identification of these primary amines in other tholin samples generated with lower yield methods or in other types of samples where the identification of low abundance primary amines is desired.

5.3 Experimental Methods

5.3.1 Titan Aerosol Simulants

The Titan aerosol simulants, or tholins, studied in this work have been well studied in other electrospray mass spectrometry experiments and their syntheses, described in detail in prior publications,[14, 18, 21] are summarized below. The new tholin was produced in a U-shaped glass reaction chamber held at 195K. A gas mixture of 95% nitrogen and 5% methane, with a flow rate of 6 atm L h^{-1} and a pressure of 1000 Pa, was exposed to a 60 Hz AC (10V peak to peak) discharge with a current of 30mA. After a typical run consuming 8 mol of gas, the solid was collected in a dry, oxygen free glove box and sealed until testing. Time and exposure between collection and testing were minimized for this sample.

The aged tholin was produced in a very similar manner, with a slightly modified apparatus.[14] A linear high vacuum stainless steel and glass reaction chamber held at 195K was filled with a mixture of 95% nitrogen and 5% methane. Gas flow during the 72 hour reaction time period was maintained to hold the chamber at 850 Pa. The reaction was accomplished by exposing the gas mixture to an AC electrical discharge with a current of 100 mA and an estimated discharge exposure time of 2 seconds. After synthesis the chamber was warmed to room temperature for 24 hours under vacuum and the solid collected under a nitrogen atmosphere. The collected solid has been exposed to and stored under ambient atmosphere in a dark freezer for two years prior to this study.

5.3.2 Materials and Methods

The dichloromethane used in the new tholin part of this study was dried using magnesium sulfate to ensure minimum water content in the solvent. 2mg/mL of new tholin was added to the dried dichloromethane, with no color change observed for the solution. 18-crown-6 ether was added to this solution to a concentration of 1-2mM. This mixture was electrosprayed on a Thermo LCQ Deca ion trap mass spectrometer. Instrumental parameters were modified to maximize the detection of the peaks of interest, resulting in a higher than normal 6.5 KV electrospray needle voltage. Two types of collision induced dissociation (CID) were used to study the sample. The first was in source CID, utilizing an innate setting within the LCQ with voltage settings between 0-12V. This applies a voltage to the octapole guide prior to trapping, allowing for fragmentation of any weak non-covalent bonds within the sample. The second was the traditional CID method, both MS/MS and MS^3 on selected peaks to confirm the formation of the complex and identify any structural possibilities.[64]

Different parameters were utilized for the study of the aged tholin. The anhydrous methanol (99.8%), anhydrous toluene (99.8%) and 18-crown-6 ether (99%) were all obtained from Sigma Aldrich. 3.8 mg of the aged tholin was dissolved in a 50/50 mixture of methanol and toluene with a 100 μM concentration of 18-crown-6 ether. While incomplete solvation was observed, the solution did display the color change expected with reasonable tholin solvation. This mixture was allowed to sit for at least 20 minutes to allow for maximum solvation prior to testing. The resultant mixture was electrosprayed using a Thermo LTQ-XL ion trap mass spectrometer. The instrumental parameters were tuned to ensure detection of the peaks of interest. A neutral loss (NL) method setting within the Xcalibur software was used to perform MS3 NL scans, using CID, on the top 50 peaks. An isolation width of 2 m/z was used for both the MS2 and MS3 scans. Data were accumulated for 10 minutes, for which 13 separate cycles of 50 NL scans were performed. From these data, peaks targeted in at least 5 of the 13 cycles were used for subsequent analysis due to low intensity in the initial spectrum and the large number of observed peaks preventing analysis of all peaks of interest in each cycle.

5.4 Results

5.4.1 New Tholin

18-crown-6 ether has been characterized to show stronger interactions with guest molecules in solvents such as chloroform or dimethylformamide, or larger solvents like n-octanol.[48, 60] The increased stability of the complex in these solvents is proposed to be caused by the reorganization that occurs when the guest binds, which is readily accommodated with solvent environments that display decreased hydrogen boning to the oxygen atoms in the crown ether.[48] Additionally since 18-crown-6 ether readily binds to water, an easily dried or anhydrous solvent was necessary. These factors drove the selection of dichloromethane for this portion of the analysis, prioritizing complex formation over the solvation of the tholin sample.

The resultant electrospray mass spectrum can be seen in figure 5.2. The protonated 18-crown-6 and its water complex are the two most intense species, which is to be expected considering the high concentration of the crown ether and its ease of ionization. The species seen at lower mass display the characteristic pattern of peak envelopes expected of the electrospray mass spectrum of tholin samples. This is seen with the consistent 14 m/z difference between the respective peaks. The higher mass species thus contain compounds complexed to the 18-crown-6 ether. The first series, identified by triangles in figure 5.2, corresponds to an amino nitrile series. These compounds have a general overall structure of $NH_2(CH_2)_xCN$, where the x=1-6 for this spectrum. Some of the compounds in this series are of astrobiological interest. The smallest in this series corresponds to aminoacetonitrile, identified by prior analyses of this sample and a prebiotic molecule that readily becomes the smallest amino acid glycine upon reaction with water.[27] The identification of multiple compounds in this series is important due to the inclusion of the nitrile group, believed to be a common functionality in Titan aerosols due to the abundance of hydrogen cyanide produced in the atmosphere.[10, 65] As such, the identification of compounds containing nitriles confirms that other nitrogen containing functional groups will not complicate the formation of the host-guest complex. The second series is not as readily identified but is based on an ion of 110 Da, with up to four additional methylenes. Since both series are regular it can be assumed that they are mostly linear, with the smaller ions necessitating linearity and the larger ions allowing for more variability. This linearity can be assumed since the region around the primary amine should have minimal steric hindrances to allow for the crown ether to move through multiple structural confirmations.

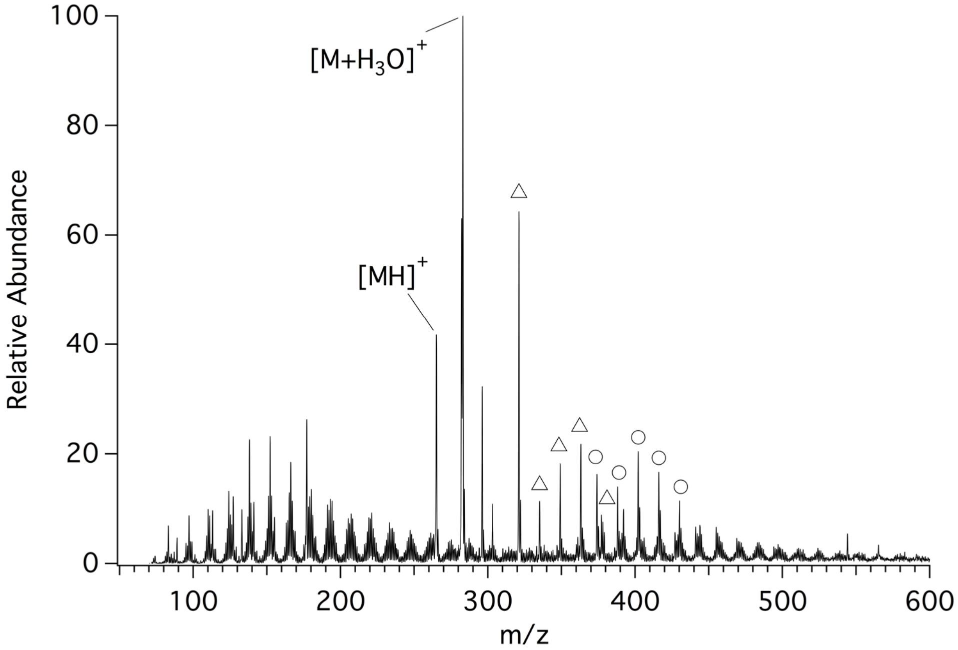

Figure 5.2. The overall mass spectrum for the 18-crown-6 ether and new tholin mixture. The 265 m/z species corresponds to protonated 18-crown-6 ether while the 283 m/z species corresponds to the water adduct. The triangles identify the amino nitrile series while circles correspond to the 110 Da series. Reproduced with permission from Hodyss 2006.[64]

Other possible guests for the 18-crown-6 ether need to be taken into account. It is easily seen from figure 5.2 that the crown ether readily binds with water, and it would also be possible to observe a complex with protonated secondary amines or imines. Both of these guests would display weaker binding compared to a primary amine guest. To take advantage of this difference, in source CID was used, shown in figure 5.3, with the intensities for each peak compared as the voltage was increased. It can been seen that the peaks corresponding to the two identified series do not readily drop off as voltage is applied, indicating they are strongly bound. The amino nitrile series appears to be the most strongly bound, considering the first peak in the series only drops to half intensity at 12V, while the peaks corresponding to the 110 Da series drop off to half intensity by 8V. These data indicate though that the two series identified in figure 5.2 correspond to only primary amine complexes.

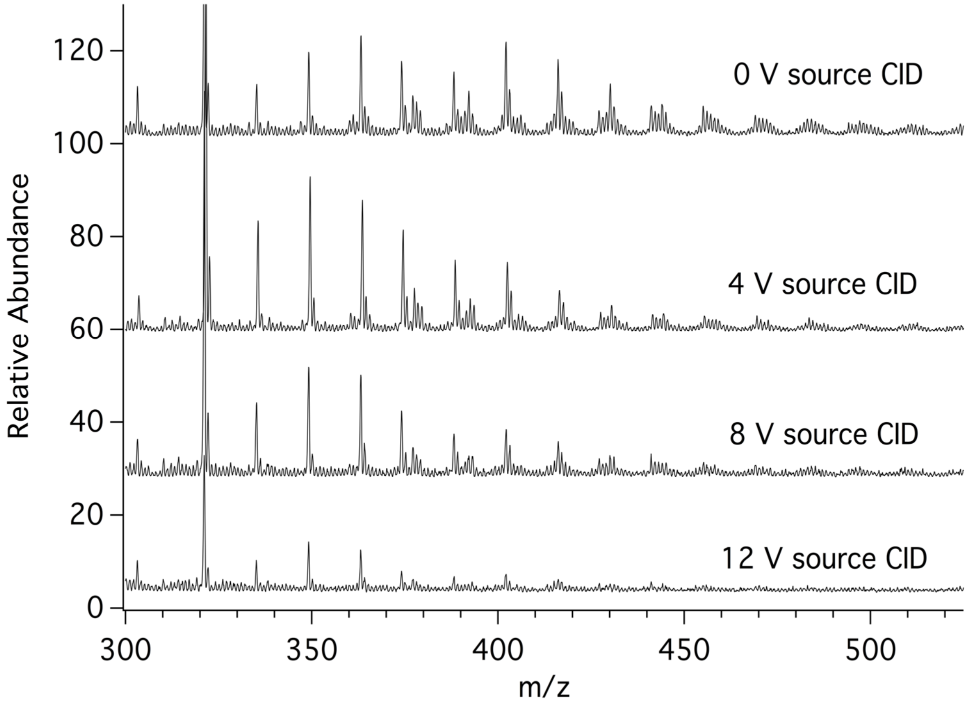

Figure 5.3. In source CID spectra for the 300-550 m/z region of the new tholin and 18-crown-6 ether sample. Reproduced with permission from Hodyss 2006.[64]

This initial experiment shows that the 18-crown-6 ether can successfully complex to primary amines within a tholin sample without competition from other protonated ions within the mixture. While these results are promising, the high discharge voltage is concerning for the analysis of the aged tholin. This could lead to decreased abundances of the molecules of interest and low ionization efficiency complicating their detection. As such, experimental protocols were modified to facilitate a more thorough analysis of the aged tholin.

5.4.2 Aged Tholin

The selection of a different solvent for this experiment was an important first step due to multiple complicating factors. The solvents that enable the strongest complex formation with 18-crown-6 ether are known to not electrospray well, as seen in high electrospray needle voltage required in the analysis of the new tholin discussed above. Since a decreased amount of amines were expected in the aged tholin[20] a more efficient electrospray solvent was necessary to maximize detection. While most solvents are usable with 18-crown-6 ether, aprotic solvents are found be much more effective at dissolving the Titan aerosol simulants, which are well known to be difficult to solvate regardless of solvent type.[10] To allow for maximum solvation of the sample, increase host-guest complex formation, and still enable analysis by electrospray mass spectrometry, an anhydrous mixture of methanol and toluene was used. This solvent mixture was used in prior electrospray analyses of petroleum mixtures,[53] which contain high quantities of polar and non-polar compounds similar to tholins. The anhydrous nature of the solvents also limited the binding of the crown ether to water, decreasing competitive binding. The non-polar nature of the toluene is proposed to enable improved host-guest complex formation in solution, which is necessary to optimize the creation of the much stronger gas phase complex. While full solvation of the tholin was not observed, solvation was similar to that reported in electrospray analyses of this material with a methanol/acetonitrile mixture,[21] enabling a reasonable comparison to prior work.

The overall mass spectrum for the aged tholin and 18-crown-6 ether mixture is shown in figure 5.4 below. The displayed mass range of this spectrum eliminates the intense protonated 18-crown-6 ether at 265 m/z and the 18-crown-6 ether and water complex at 283 m/z, both of which are evident in the new tholin spectrum shown in figure 5.2. A large number of different peaks are easily seen, with multiple different mass envelopes and peak intensities demonstrating the complexity of the material. While the preservation of a permanent charge would make the 18-crown-6 ether complexes the expected high intensity peaks, the high number of isomers combined with the aged nature of the tholin means that no complexes can be assumed and more investigation is required.

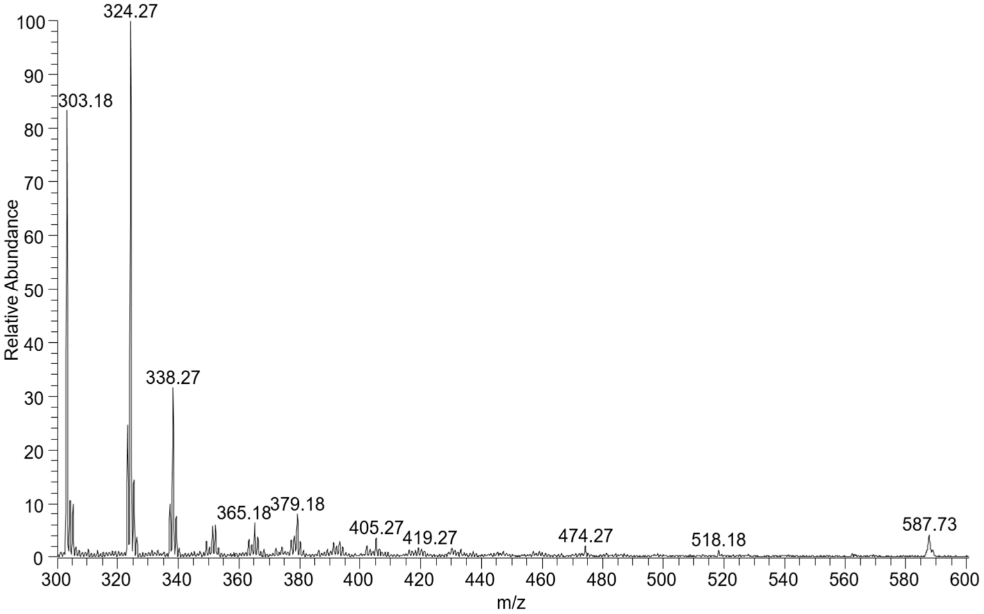

Figure 5.4. The overall mass spectrum for the 18-crown-6 ether and aged tholin mixture. The 303 m/z species corresponds to potassium cation complexed to the 18-crown-6 ether.

To properly identify crown ether complexes and obtain the greatest amount of structural information the use of tandem MS^3 mass spectrometry with neutral loss (NL) scans was utilized. A NL scan allows for the determination of complexes with the crown ether by scanning for crown ether loss (-265 m/z) from the parent peak using an automated method targeting the 50 most intense peaks in the overall spectrum. The initial scan for a NL from the parent is important due to the large number of different compounds likely within the isolation width (2 m/z) used. Not only is the complexed species and any isomers it contains targeted with this initial MS/MS scan, any molecules present in the tholin with the same nominal mass as the complex will also be fragmented. While this leads to complicated MS/MS spectra as seen in some figures below, the fragment corresponding to the NL species is readily identified by this method. Additionally the preservation of the protonated amine makes the NL species the highest intensity peak observed in the MS/MS spectra for the majority of compounds examined, which further simplifies analysis.

If the NL of 264 Da, corresponding to 18-crown-6 ether, is detected, the initial fragment ion is further fragmented which provides structural information. In the case of primary amines the loss of 17 Da is seen, corresponding to the loss of the amine group as the figures below. Other fragments can lead to additional structural information, which can assist with identification. In the case of an ion trap mass spectrometer this identification can be complicated by the presence of isomers. The use of the NL scan helps to eliminate some of the isomers from the parent, but multiple isomers could still be isolated if each have the ability to complex to the crown ether. The structure of the complex itself can provide some insight for identifications, such as low steric hindrance around the primary amine being necessary as discussed above.

Taking the observed data into consideration, peaks reporting a loss indicative of a primary amine along with their proposed chemical formulae are shown in Table 1. These data show compounds that were either explicitly identified as showing a primary amine loss or, for >368 m/z and 374 m/z, based on the presence of the 265 m/z peak (protonated 18-crown-6 ether) in the NL loss scan. The fragments corresponded to the guest molecule for the latter compounds were either outside the mass range or low abundance in the NL scan spectra. Even without that extra confirmation, multiple different species can still be identified and analyzed. From an overall examination of the data it is interesting to note that the most intense species in the initial spectrum does not correspond to complexed species, as expected due to aging related losses from the tholin sample. This supports the use of a NL mass spectrometry method to confirm the presence of complexes if a low abundance of primary amines is expected.

Complexed Species Mass (m/z)	MS^2 NL Peak	Most Likely Neutral Formula(e)	Proposed Structural Series Carbon Number		
			Alkyl Amine	Amino Nitrile	1 Degree Unsaturation
310	46	C_2H_7N*	2		
321	57	$C_2H_4N_2$*		1	
338	74	$C_4H_{11}N$*	4		
339	75	$C_3H_{10}N_2$*			
349	85	$C_4H_8N_2$*		3	
350	86	$C_5H_{11}N$*			5
351	87	$C_4H_{10}N_2$*			
352	88	$C_5H_{13}N$*	5		
353	89	$C_4H_{12}N_2$*			
363	99	$C_5H_{10}N_2$*		4	
364	100	$C_6H_{13}N$*			6
365	101	$C_5H_{12}N_2$*			
366	102	$C_6H_{15}N$*	6		
368	104	C_7H_5N, $C_4H_{13}N_3$*			
372	108	C_7H_9N, $C_5H_5N_3$			
374	110	$C_5H_7N_3$, $C_3H_4N_5$*°			
377	113	$C_6H_{12}N_2$		5	
378	114	$C_7H_{15}N$, $C5H_{11}N_3$			7
380	116	C_7H1_7N	7		
386	122	$C_8H_{11}N$			
391	127	$C_7H_{14}N_2$		6	
392	128	$C_8H_{17}N$, $C_6H_{13}N_3$			8
394	130	$C_8H_{19}N$	8		
401	137	$C_8H_{12}N_2$			
402	138	$C_7H_{11}N_3$, $C_5H_8N_5$°			
403	139	$C_8H_{14}N_2$			
404	140	$C_9H_{17}N$, $C_7H_{13}N_3$			
405	141	$C_8H_{16}N_2$		7	
406	142	$C_9H_{19}N$			9
416	152	$C_8H_{13}N_3$, $C_6H_{10}N_5$°			
417	153	$C_9H_{16}N_2$			
418	154	$C_{10}H_{19}N$, $C_8H_{15}N_3$			
419	155	$C_9H_{18}N_2$		8	
420	156	$C_{10}H_{21}N$, $C_8H_{17}N_3$			10
430	166	$C_9H_{15}N_3$, $C_7H_{12}N_5$°			
431	167	$C_{10}H_{18}N_2$, $C_8H_{14}N_4$			
433	169	$C_{10}H_{20}N_2$		9	

474	210	$C_{14}H_{27}N$, $C_{12}H_{23}N_3$			

Table 5.1. Data from the NL scan of the aged tholin and 18-crown-6 ether complex. Peaks from the overall mass spectrum, their NL scan mass, and most likely chemical formulae for the neutral guest molecule are shown. Those marked with an asterisk showed a 265 m/z peak in the NL scan but no MS3 scan of the guest were obtained. Structural series for the proposed formula are tabulated, with the number corresponding to the number of carbons present in the molecule for the alkyl amines, the number of methylene groups for the amino nitrile, and highest number of carbons possible for the unsaturated series. Those marked with a ° correspond to the 110 Da series identified in the new tholin spectrum shown in figure 5.2.

5.5 Discussion

5.5.1 New Tholin

Since the results shown above for the new tholin indicate the only complexes between 18-crown-6 ether and primary amines were observed for the identified series, further analysis could be attempted. One peak targeted for additional analysis was 416 m/z, the fourth in the 110 Da series. The MS/MS data, shown in the top spectra of figure 5.5, displays fragments corresponding to both the loss of 264 Da, the loss of the crown ether, and protonated crown ether. A peak corresponding to the water-18-crown-6 ether complex is also observed, which is believed to be related to complexation with water in the trap. The 152 m/z peak was further fragmented, displaying the loss of ammonia, indicating a primary amine, along with the loss of two different cyano groups. Since this sample has been studied in prior work, it is known to correspond to either $C_8H_{13}N_3$ or $C_6H_{10}N_5$.[21] From the observed fragments the compound contains a primary amine and a terminal cyano group which also allows for the loss of methyl cyanide. It is very possible that the other compounds within the 110 Da series also allow for the loss methyl cyanide. While these are the same functionalities present within the amino nitrile series, the different binding affinity of the 110 Da suggest fundamental structural differences, likely related to the incorporation of a secondary or tertiary amine.

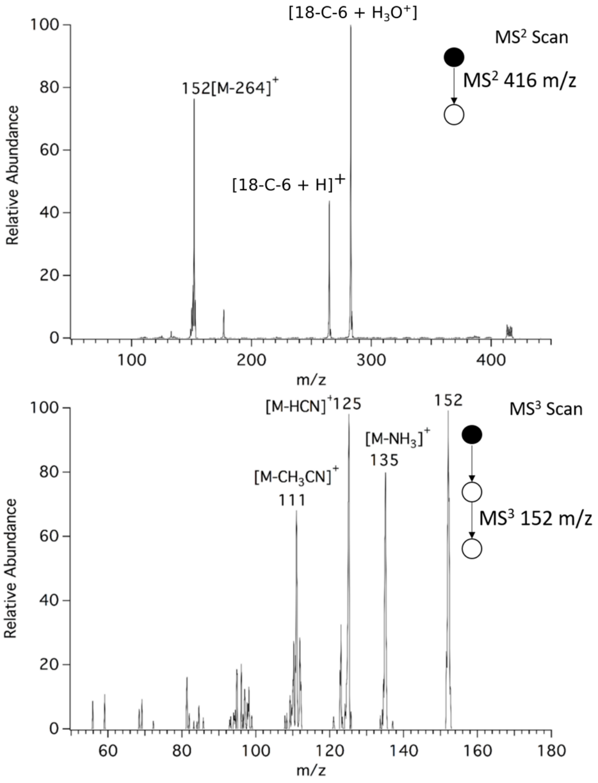

Figure 5.5 CID data for 416 m/z for the new tholin sample. Top: MS/MS spectrum of 416 m/z for the new tholin. Bottom: The MS3 spectrum for 152 m/z form 416 m/z. Reproduced with permission from Hodyss 2006.[64]

This example demonstrates that CID allows for dissociation of the complex, with MS^3 allowing for further fragmentation and an increased structural understanding. Other peaks within figure 5.2 could be identified, but it would require manual selection of each peak to screen for a complex with 18-crown-6 ether. The NL protocol utilized for the aged tholins discussed above allowed for the automation of this selection process, overcoming the limitations from the manual selection of peaks. This NL method allowed not only for the increased identification of peaks, as shown in Table 5.1, but also the identification of multiple species as discussed below.

5.5.2 Aged Tholin

From the NL method data for the aged tholin, shown in Table 5.1, most likely chemical formulae can be proposed, and from these data four different structural series seem to dominate. The amino nitrile series was confirmed from the MS^3 scan, shown in figure 5.6, of the five methylene amino nitrile. There are four major fragments seen corresponding to losses from either the amine end of the molecule or the nitrile end, suggesting that the structure corresponds to an aliphatic amino nitrile with the formula $NH_2(CH_2)_4CN$, identifying the compound as 6-aminohexanenitrile, fitting with the assumption of a linear series discussed for the new tholin amino nitrile series. The loss of methyl and ethyl nitrile indicates that, while the 17 Da (NH_3) loss is expected for primary amines, the nitrile-containing losses will dominate over the loss of alkyl amines. This observation is important to the future interpretation of other peaks not examined in this work. While the other peaks corresponding to this series are not analyzed in detail, they are identified in Table 5.1. The observation of this series in the aged tholin is also encouraging since it is the main series observed in the new tholin sample. When comparing the series between the two samples it can be seen that the two methylene species is missing from the aged tholin, but three additional members of the series corresponding to 7-9 methylenes were newly identified.

The large difference in intensity for the same series in these two tholin samples demonstrates the impact that aging can have, which has been suggested by prior studies.[20]

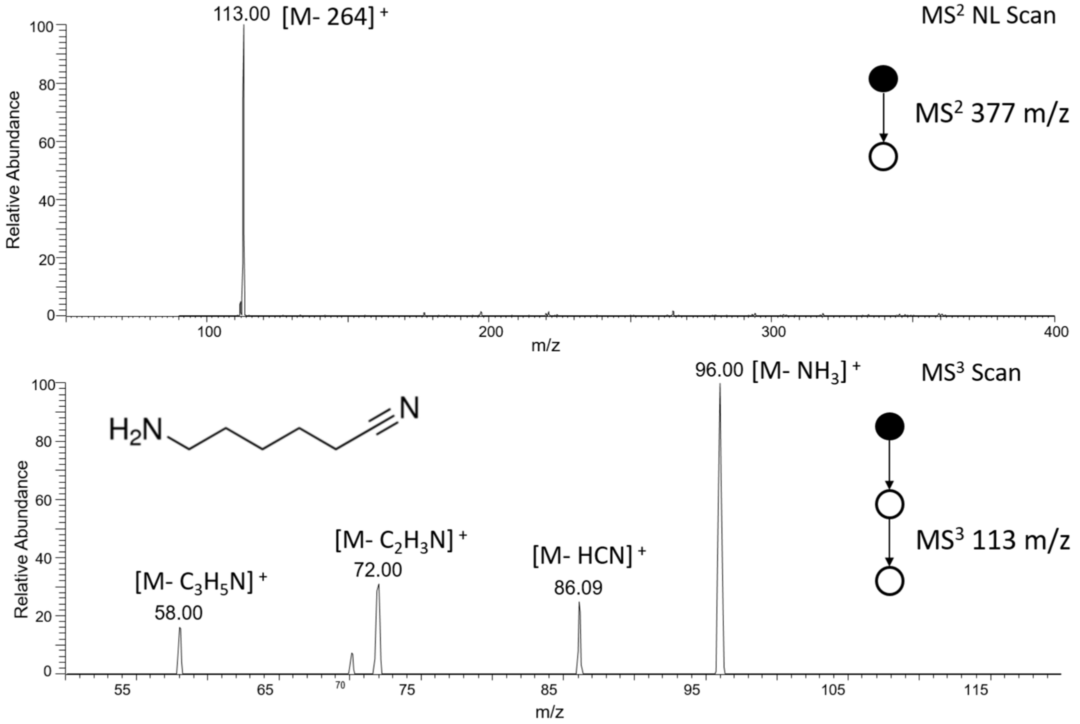

Figure 5.6. CID data for 377 m/z from the aged tholin sample. Top: MS/MS scan for 377 m/z showing the loss of the neutral 18-crown-6 ether (264 Da) as the major peak. Bottom: MS^3 scan for 113 m/z, showing losses indicative of an amino nitrile species.

A major series observed for the aged tholin unseen in the new tholin is the alkyl amine series, for which the smallest observed species corresponds to ethylamine. The seven carbon compound in this series was the smallest isolated for MS^3 (Not shown here), which presents complications. This is due to the large number of possible structural isomers as the number of carbons increase. As such, interpretation of these larger carbon MS^3 scans becomes difficult and outside the scope of the present work. The identification of a 17 Da loss does cement these compounds as primary amines with minimal branching close to the amine. The lack of their explicit identification in this work demonstrates the need for chromatographic methods to identify these large carbon count alkyl amines; future study of these fragments with exact mass resolution could enable better identification of any branching present.[32]

The second newly observed series corresponds to a single degree of unsaturation and does not show a carbon count fewer than five within the suggested chemical formulae. This is suggestive of ring formation contributing to the unsaturation as opposed to a double bond, since no smaller compounds with regular unsaturation are observed and a five carbon ring would be the first stable ring for which a host-guest complex could form and 17 Da loss be possible. The increasing carbon counts likely correspond to additions to a six carbon ring. The seven carbon compound in this series was able to be examined by MS^3, as is shown in figure 5.7. This spectra shows the loss of a primary amine which is expected, but two other losses that are more difficult to interpret. The loss of 29 Da shown by the 85 m/z peak is suggestive of a methylimine loss, while the 41 Da loss from the 73 m/z peak matches best with the loss of acetonitrile. While the methylimine is possible from double bond formation during fragmentation of the ring, the acetonitrile loss is not possible with a single nitrogen structure that still complexes to a primary amine. The nitrile presence suggests more nitrogen incorporation. There are no stable structures with two nitrogen atoms that would allow for the observed losses, indicating that at least three nitrogen atoms are necessary to produce all of the fragments seen.

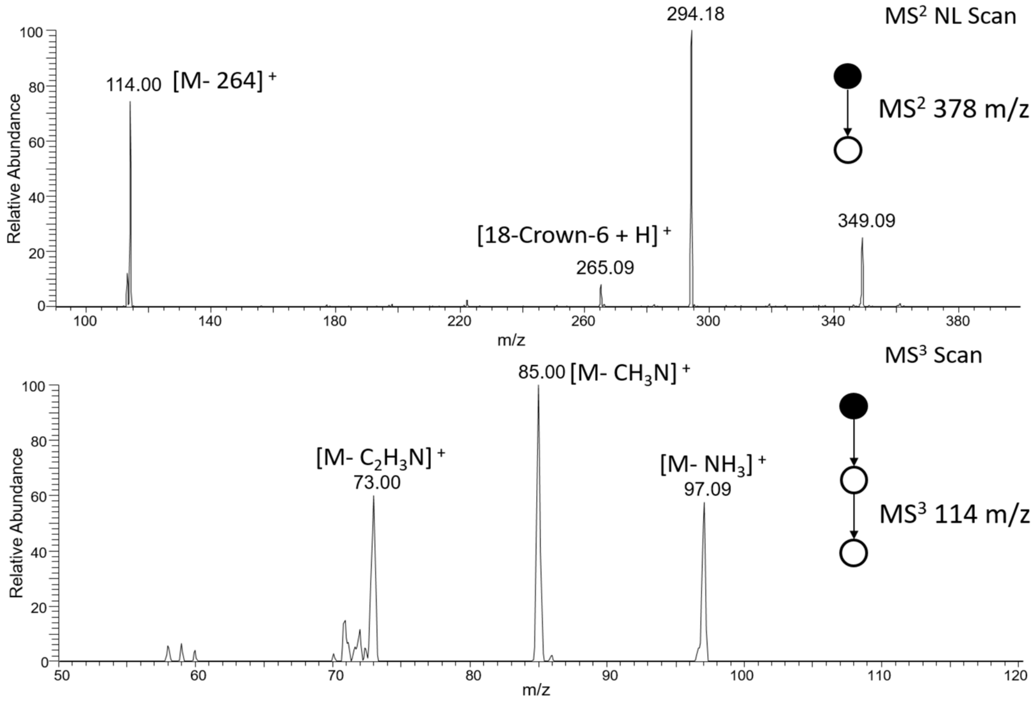

Figure 5.7. CID data for 378 m/z from the aged tholin sample. Top: MS/MS scan for 378 m/z showing the loss of the neutral 18-crown-6 ether (264 Da) as the second most intense peak and the protonated 18-crown-6 ether. Bottom: MS^3 scan for 114 m/z, showing losses of ammonia, methylimine, and acetonitrile. These losses are suggestive of multiple structural isomers.

The loss of both a primary amine and methylimine is suggestive of another possibility: the observation of more than one structural isomer within the same neutral loss scan. This would allow for the complexation of one compound, a cyclic primary amine that readily loses 17 Da and produces the observed 97 m/z and 85 m/z peaks, and a different isomer that contributes to these peaks while also producing the 73 m/z fragment. The second isomer could contain a nitrile and a methyl substituted secondary amine. This would help to explain the methylimine loss being the most intense fragment, since it could be possible from both proposed isomers. The presence of two isomers is further supported by the observation of both the protonated 18-crown-6 ether and the loss of the crown ether in the NL scan, as opposed to the observation of only the NL species seen in the amino nitrile spectrum in figure 5.6. The observation of both peaks suggests that the different isomers seen have different binding affinities to the crown ether. This would follow from one isomer containing a substituted secondary amine, since secondary amines have lower proton affinities compared to primary amines. The large number of different possibilities for these isomers precludes identification but suggests that the unsaturation observed for the primary amine loss could relate to either a ring formation or higher nitrogen inclusion. This higher degree of nitrogen incorporation also helps explain why unsaturation is observed only for higher mass species. The possibility of both isomers being contained in this series is accounted for in Table 5.1 and shows the care necessary in these identifications.

While the possibility of isomers presents difficulties for some identifications, others are simplified by structural possibilities. This is most obvious for the NL and MS^3 scans of 372 and 386 m/z, shown in figure 5.8 a and b respectively. Both MS3 scans show a peak at 91 m/z, which most likely corresponds to a toluene $[M-H]^{\bullet+}$ radical cation, due to its stability and observation in the MS/MS spectra of other substituted benzene molecules. This would make the complex at 372 m/z correspond to benzyl amine by comparison with prior reported MS/MS data. Taking the 91 m/z in the MS^3 scan of 386 m/z to be the same toluene cation, the 105 m/z fragment would also correspond to another substituted benzene molecule. Comparison with other MS/MS data can also provide a most likely identification of phenylethylamine for this second compound. These data show that with distinctive fragments, identifications can be made even if multiple isomers are possible.

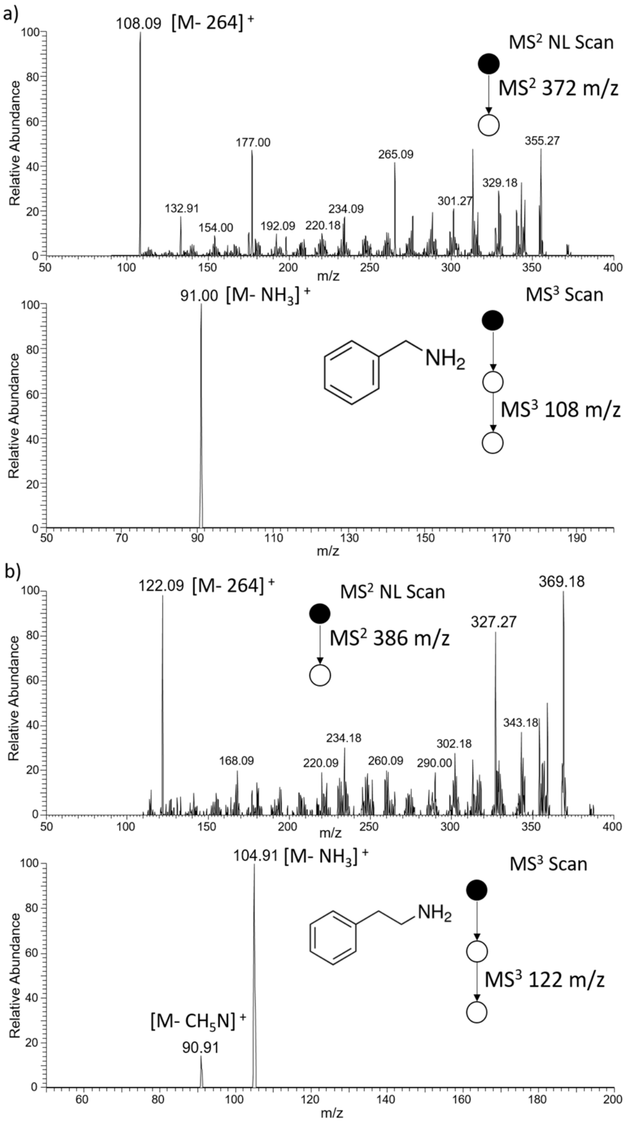

Figure 5.8. CID data for benzene containing species from the aged tholin sample. a) *Top*: MS/MS scan for 372 m/z showing the loss of the neutral 18-crown-6 ether (264 Da) as the most intense peak with multiple other fragments also visible. *Bottom*: MS^3 scan for 108 m/z, showing loss of ammonia and a fragment indicative of a toluene radical cation. b) *Top*: MS/MS scan for 386 m/z showing the loss of the neutral 18-crown-6 ether as the second most intense peaks, with another loss from a non-complexed 386 species as the dominant fragment. *Bottom*: MS^3 scan for 122 m/z, showing loss of ammonia from one fragment and a second fragment from methylamine loss also matching a toluene ion. Both of these fragments are assigned to benzene containing species.

The identification of two substituted benzene molecules is ideal for the characterization of tholins. These types of amines would be expected on Titan due to the prior observation of benzene in Titan's atmosphere.[8, 66] The production of two different substituted benzene molecules with a methylene difference between then suggests more complex chemistry for primary amines is possible and possibly favored. This second possibility is further supported by the lack of aniline, which was expected from ammonia addition to a phenyl radical. Benzyl radicals are more stable than phenyl radical and thus may be more readily synthesized and available for reactions with small amines. Since other substituted benzene molecules were not identified with this method when looking for the 91 m/z fragment, there may be quenching characteristics to the chemistry that truncate subsequent reactions. This could be due to consumption of smaller amines and ammonia in the synthesis of the many other primary amines observed in the material. Benzene is much more complicated than the other subunits observed here, and the longer timescale for its synthesis could be a limiting factor since ammonia may already be consumed in other reactions and not available in a large enough scale. While these observations would need to be confirmed, this does show that the 18-crown-6 ether complex can readily form with more complex primary amines.

The final observation true for both the new and aged tholin samples was the lack of any doubly complexed species. Since both species display the amino nitrile series and the 110 Da series it can be assumed that this is also a fundamental characteristic common between the tholins. This suggests that, contrary to what might be expected from such a complex mixture, compounds with two sterically available primary amines are not readily produced during tholin synthesis. Some of the possible reasons for this observation include increased reactivity of amines within the plasma, or compounds with two primary amines being more volatile and readily lost. The most likely possibility is that the high energy of the plasma contributes to an increased abundance of other functional group which decreases the probability of forming a compound with two sterically available primary amines. These high energy processes may also convert a second primary amine to a secondary or tertiary amine, precluding their detection.

The data presented here show that the 18-crown-6 ether host-guest complex with primary amines is effective for the identification of various primary amines within the tholin sample without the need for extensive preprocessing. The in source CID method combined with the MS^3 NL method allow for the unambiguous identification of primary amines as the favored guest, confirming that the complex is not readily formed with secondary amines or imines. The MS^3 NL method provides much needed structural information. Production of primary amines has prebiotic significance, but the variety of primary amines observed in this experiment demonstrates that they may be a more common substituent than expected.

While the primary amines observed in the aged sample are lower in intensity and thus not present in high quantities compared to the new tholin, they also remained stable under atmospheric storage for two years. This suggests that enough primary amines are produced in stable enough confirmations to allow for detection after atmospheric degradation and evaporative losses. Combined with the observation of two regular series in the new tholin, it can be assumed that primary amines with a range of complexity likely comprise a reasonable amount of molecules within the tholins, making their identification necessary for proper characterization of the material.

Identification of complexes for which two different isomers are possible presents an additional difficultly, since the crown ether complex does not discern beyond a sterically available primary amine. More specific identification would require increased sensitivity or mass resolution. These studies would need to be combined with MS^n data to allow for structural identification, for which these data may provide a starting point upon which to base that future analysis. Another possibility would be the incorporation of the 18-crown-6 ether with high-performance liquid chromatography as a post column reagent. This would allow for the identification of different structural isomers assumed to be present for the more complex MS^3 data in this study. The initial 18-crown-6 either complexation does present a complement to other analytical methods, allowing for the unambiguous identification of a primary amine functionality and the precise identification of some molecules. These data provide interesting insights into the prevalence of primary amines within tholins and the difficulties in their characterization.

5.6 Conclusions

A supramolecular host-guest complex for the detection of primary amines in two tholin samples representative of Titan's atmosphere has been presented using an 18-crown-6 ether host. The complex was observed for various primary amines within each sample without extensive sample processing. The complexes formed were confirmed as primary amines and a MS^3 NL method allowed for additional structural information to be obtained. From the available data possible chemical formulae are proposed and some compounds identified, including a compounds with both amine and nitrile functionalities along with substituted benzene molecules. Both of these have important implications for Titan's atmospheric chemistry due to their expected occurrence on Titan and, in the case of the aminoacetonitrile, possible astrobiological significance. The significant presence of primary amines in the aged tholin show that, while a new tholin sample is necessary for high intensity peaks, primary amines in tholins are produced in high abundance and are relatively stable. These data show that this supramolecular complex presents a complementary analytical method for the identification of primary amines within tholins and establishes a solid foundation for future analyses.

5.7 Acknowledgements

We would like to thank Mark Smith for providing the tholin samples for analysis. The research was funded by NSF award number CHE-1508825. The early part of this work was funded by NASA Astrobiology Institute, Titan as a Prebiotic Chemical System, and the Keck Institute for Space Studies, Future Missions to Titan: Scientific and Engineering Challenges. K.T.U. acknowledges financial support from the Harriett Jenkins Pre-Doctoral Fellowship Program.

5.8 References

1. E. R. Stofan, C. Elachi, J. I. Lunine, R. D. Lorenz, B. Stiles, K. L. Mitchell, S. Ostro, L. Soderblom, C. Wood, H. Zebker, S. Wall, M. Janssen, R. Kirk, R. Lopes, F. Paganelli, J. Radebaugh, L. Wye, Y. Anderson, M. Allison, R. Boehmer, P. Callahan, P. Encrenaz, E. Flamini, G. Francescetti, Y. Gim, G. Hamilton, S. Hensley, W. T. K. Johnson, K.

Kelleher, D. Muhleman, P. Paillou, G. Picardi, F. Posa, L. Roth, R. Seu, S. Shaffer, S. Vetrella and R. West, *Nature*, 2007, **445**, 61-64.

2. J. Radebaugh, R. Lorenz, T. Farr, P. Paillou, C. Savage and C. Spencer, *Geomorphology*, 2010, **121**, 122-132.
3. J. T. Perron, M. P. Lamb, C. D. Koven, I. Y. Fung, E. Yager and M. Ádámkovics, *Journal of Geophysical Research: Planets*, 2006, **111**, E11001.
4. F. M. Flasar, R. K. Achterberg, B. J. Conrath, P. J. Gierasch, V. G. Kunde, C. A. Nixon, G. L. Bjoraker, D. E. Jennings, P. N. Romani, A. A. Simon-Miller, B. Bézard, A. Coustenis, P. G. J. Irwin, N. A. Teanby, J. Brasunas, J. C. Pearl, M. E. Segura, R. C. Carlson, A. Mamoutkine, P. J. Schinder, A. Barucci, R. Courtin, T. Fouchet, D. Gautier, E. Lellouch, A. Marten, R. Prangé, S. Vinatier, D. F. Strobel, S. B. Calcutt, P. L. Read, F. W. Taylor, N. Bowles, R. E. Samuelson, G. S. Orton, L. J. Spilker, T. C. Owen, J. R. Spencer, M. R. Showalter, C. Ferrari, M. M. Abbas, F. Raulin, S. Edgington, P. Ade and E. H. Wishnow, *Science*, 2005, **308**, 975-978.
5. M. Fulchignoni, F. Ferri, F. Angrilli, A. J. Ball, A. Bar-Nun, M. A. Barucci, C. Bettanini, G. Bianchini, W. Borucki, G. Colombatti, M. Coradini, A. Coustenis, S. Debei, P. Falkner, G. Fanti, E. Flamini, V. Gaborit, R. Grard, M. Hamelin, A. M. Harri, B. Hathi, I. Jernej, M. R. Leese, A. Lehto, P. F. Lion Stoppato, J. J. Lopez-Moreno, T. Makinen, J. A. M. McDonnell, C. P. McKay, G. Molina-Cuberos, F. M. Neubauer, V. Pirronello, R. Rodrigo, B. Saggin, K. Schwingenschuh, A. Seiff, F. Simoes, H. Svedhem, T. Tokano, M. C. Towner, R. Trautner, P. Withers and J. C. Zarnecki, *Nature*, 2005, **438**, 785-791.
6. N. Balucani, F. Leonori, R. Petrucci, M. Stazi, D. Skouteris, M. Rosi and P. Casavecchia, *Faraday Discussions*, 2010, **147**, 189-216.

7. H. Imanaka and M. A. Smith, *Geophysical Research Letters*, 2007, **34**, n/a-n/a.
8. V. Vuitton, R. V. Yelle and J. Cui, *Journal of Geophysical Research: Planets*, 2008, **113**, E05007.
9. H. B. Niemann, S. K. Atreya, J. E. Demick, D. Gautier, J. A. Haberman, D. N. Harpold, W. T. Kasprzak, J. I. Lunine, T. C. Owen and F. Raulin, *J Geophys Res-Planet*, 2010, **115**, E12006.
10. M. L. Cable, S. M. Hörst, R. Hodyss, P. M. Beauchamp, M. A. Smith and P. A. Willis, *Chemical Reviews*, 2012, **112**, 1882-1909.
11. N. Carrasco, I. Schmitz-Afonso, J. Y. Bonnet, E. Quirico, R. Thissen, O. Dutuit, A. Bagag, O. Laprévote, A. Buch, A. Giulani, G. Adandé, F. Ouni, E. Hadamcik, C. Szopa and G. Cernogora, *The Journal of Physical Chemistry A*, 2009, **113**, 11195-11203.
12. B. Cunha de Miranda, G. A. Garcia, F. Gaie-Levrel, A. Mahjoub, T. Gautier, B. Fleury, L. Nahon, P. Pernot and N. Carrasco, *The Journal of Physical Chemistry A*, 2016, **120**, 6529-6540.
13. C. He, G. Lin and M. A. Smith, *Icarus*, 2012, **220**, 627-634.
14. C. He, G. Lin, K. T. Upton, H. Imanaka and M. A. Smith, *The Journal of Physical Chemistry A*, 2012, **116**, 4760-4767.
15. H. Imanaka, B. N. Khare, J. E. Elsila, E. L. O. Bakes, C. P. McKay, D. P. Cruikshank, S. Sugita, T. Matsui and R. N. Zare, *Icarus*, 2004, **168**, 344-366.
16. M. Morisson, C. Szopa, N. Carrasco, A. Buch and T. Gautier, *Icarus*, 2016, **277**, 442-454.
17. M. C. Pietrogrande, P. Coll, R. Sternberg, C. Szopa, R. Navarro-Gonzalez, C. Vidal-Madjar and F. Dondi, *Journal of Chromatography A*, 2001, **939**, 69-77.

18. N. Sarker, A. Somogyi, J. I. Lunine and M. A. Smith, *Astrobiology*, 2003, **3**, 719-726.

19. E. Sciamma-O'Brien, N. Carrasco, C. Szopa, A. Buch and G. Cernogora, *Icarus*, 2010, **209**, 704-714.

20. E. Sciamma-O'Brien, K. T. Upton and F. Salama, *Icarus*, 2017, **289**, 214-226.

21. A. Somogyi, C. H. Oh, M. A. Smith and J. I. Lunine, *Journal of the American Society for Mass Spectrometry*, 2005, **16**, 850-859.

22. A. Somogyi, M. A. Smith, V. Vuitton, R. Thissen and I. Komaromi, *Int J Mass Spectrom*, 2012, **316**, 157-163.

23. C. Szopa, G. Cernogora, L. Boufendi, J. J. Correia and P. Coll, *Planetary and Space Science*, 2006, **54**, 394-404.

24. G. Alcouffe, M. Cavarroc, G. Cernogora, F. Ouni, A. Jolly, L. Boufendi and C. Szopa, *Plasma Sources Sci T*, 2010, **19**.

25. S. M. Hörst, *Journal of Geophysical Research: Planets*, 2017, **122**, 432-482.

26. P. Ehrenfreund, J. J. Boon, J. Commandeur, C. Sagan, W. R. Thompson and B. Khare, *Adv Space Res*, 1994, **15**, 335-342.

27. S. M. Horst, R. V. Yelle, A. Buch, N. Carrasco, G. Cernogora, O. Dutuit, E. Quirico, E. Sciamma-O'Brien, M. A. Smith, A. Somogyi, C. Szopa, R. Thissen and V. Vuitton, *Astrobiology*, 2012, **12**, 809-817.

28. M. McGuigan, J. H. Waite, H. Imanaka and R. D. Sacks, *J Chromatogr A*, 2006, **1132**, 280-288.

29. L. Torokova, J. Watson, F. Krcma, V. Mazankova, N. J. Mason, G. Horvath and S. Matejcik, *Contributions to Plasma Physics*, 2015, **55**, 470-480.

30. R. Courtin, R. Wagener, C. P. McKay, J. Caldwell, K.-H. Fricke, F. Raulin and P. Bruston, *Icarus*, 1991, **90**, 43-56.

31. J. M. Bernard, E. Quirico, O. Brissaud, G. Montagnac, B. Reynard, P. McMillan, P. Coll, M. J. Nguyen, F. Raulin and B. Schmitt, *Icarus*, 2006, **185**, 301-307.

32. A. Somogyi, R. Thissen, F. R. Orthous-Daunay and V. Vuitton, *Int J Mol Sci*, 2016, **17**.

33. M. L. Cable, A. M. Stockton, M. F. Mora and P. A. Willis, *Analytical Chemistry*, 2013, **85**, 1124-1131.

34. R. M. Izatt, J. S. Bradshaw and R. L. Bruening, (2007) Ion Separation in Membrane and Solid Phase Extraction Systems. In: *Perspectives in Supramolecular Chemistry*, John Wiley & Sons, Ltd., pp 225-243

35. R. M. Izatt, J. S. Bradshaw, R. L. Bruening, B. J. Tarbet and M. L. Bruening, *Comprehensive Supramolecular Chemistry*, 1996.

36. J. Lehn, *Science*, 1993, **260**, 1762-1763.

37. M. J. Webber, E. A. Appel, E. W. Meijer and R. Langer, *Nat Mater*, 2016, **15**, 13-26.

38. B. Hasenknopf, J.-M. Lehn, B. O. Kneisel, G. Baum and D. Fenske, *Angewandte Chemie International Edition in English*, 1996, **35**, 1838-1840.

39. J.-M. Lehn, *Angewandte Chemie International Edition in English*, 1990, **29**, 1304-1319.

40. B. J. G. E. Pieters, M. B. van Eldijk, R. J. M. Nolte and J. Mecinovic, *Chemical Society Reviews*, 2016, **45**, 24-39.

41. D. S. Lawrence, T. Jiang and M. Levett, *Chemical Reviews*, 1995, **95**, 2229-2260.

42. F. Li, J. K. Clegg, L. F. Lindoy, R. B. Macquart and G. V. Meehan, *Nature Communications*, 2011, **2**, 205.

43. G. V. Oshovsky, D. N. Reinhoudt and W. Verboom, *Angewandte Chemie International Edition*, 2007, **46**, 2366-2393.
44. S. Zhang, *Nat Biotech*, 2003, **21**, 1171-1178.
45. K. D. Daze, T. Pinter, C. S. Beshara, A. Ibraheem, S. A. Minaker, M. C. F. Ma, R. J. M. Courtemanche, R. E. Campbell and F. Hof, *Chemical Science*, 2012, **3**, 2695-2699.
46. A. I. Day, R. J. Blanch, A. P. Arnold, S. Lorenzo, G. R. Lewis and I. Dance, *Angewandte Chemie International Edition*, 2002, **41**, 275-277.
47. H.-J. Schneider, *Angewandte Chemie International Edition*, 2009, **48**, 3924-3977.
48. A. Späth and B. König, *Beilstein Journal of Organic Chemistry*, 2010, **6**, 32.
49. D. J. Harvey, *Journal of Chromatography B*, 2011, **879**, 1196-1225.
50. I. Ilisz, R. Berkecz and A. Péter, *Journal of Pharmaceutical and Biomedical Analysis*, 2008, **47**, 1-15.
51. H. Kataoka, *Journal of Chromatography A*, 1996, **733**, 19-34.
52. J. Laskin, P. A. Eckert, P. J. Roach, B. S. Heath, S. A. Nizkorodov and A. Laskin, *Analytical Chemistry*, 2012, **84**, 7179-7187.
53. A. G. Marshall and R. P. Rodgers, *Proc Natl Acad Sci U S A*, 2008, **105**, 18090-18095.
54. J. M. Purcell, C. L. Hendrickson, R. P. Rodgers and A. G. Marshall, *Analytical Chemistry*, 2006, **78**, 5906-5912.
55. S. Blair, E. Kempen and J. Brodbelt, *Journal of the American Society for Mass Spectrometry*, 1998, **9**, 1049-1059.
56. J. S. Bradshaw and R. M. Izatt, *Accounts of Chemical Research*, 1997, **30**, 338-345.
57. M. Bühl, R. Ludwig, R. Schurhammer and G. Wipff, *The Journal of Physical Chemistry A*, 2004, **108**, 11463-11468.

58. C. J. Pedersen and H. K. Frensdorff, *Angewandte Chemie International Edition in English*, 1972, **11**, 16-25.

59. V. Rüdiger, H.-J. Schneider, V. P. Solov'ev, V. P. Kazachenko and O. A. Raevsky, *European Journal of Organic Chemistry*, 1999, **1999**, 1847-1856.

60. B. L. Williamson and C. S. Creaser, *Int J Mass Spectrom*, 1999, **188**, 53-61.

61. R. R. Julian and J. L. Beauchamp, *Int J Mass Spectrom*, 2001, **210–211**, 613-623.

62. Y. Qi and D. A. Volmer, *Rapid Communications in Mass Spectrometry*, 2015, **29**, 2316-2318.

63. M. G. Schmid and G. Gübitz, in *Chiral Separations: Methods and Protocols*, eds. G. Gübitz and M. G. Schmid, Humana Press, Totowa, NJ, 2004, DOI: 10.1385/1-59259-648-7:317, pp. 317-321.

64. R. Hodyss, Dissertation (Ph.D.), The California Institute of Technology, 2006.

65. B. N. Tran, J. C. Joseph, M. Force, R. G. Briggs, V. Vuitton and J. P. Ferris, *Icarus*, 2005, **177**, 106-115.

66. E. H. Wilson and S. K. Atreya, *Planetary and Space Science*, 2003, **51**, 1017-1033.